



PDHonline Course C552 (7 PDH)

Rock Engineering Series: Rock Mass Classifications and Properties

Instructor: Yun Zhou, Ph.D., PE

2020

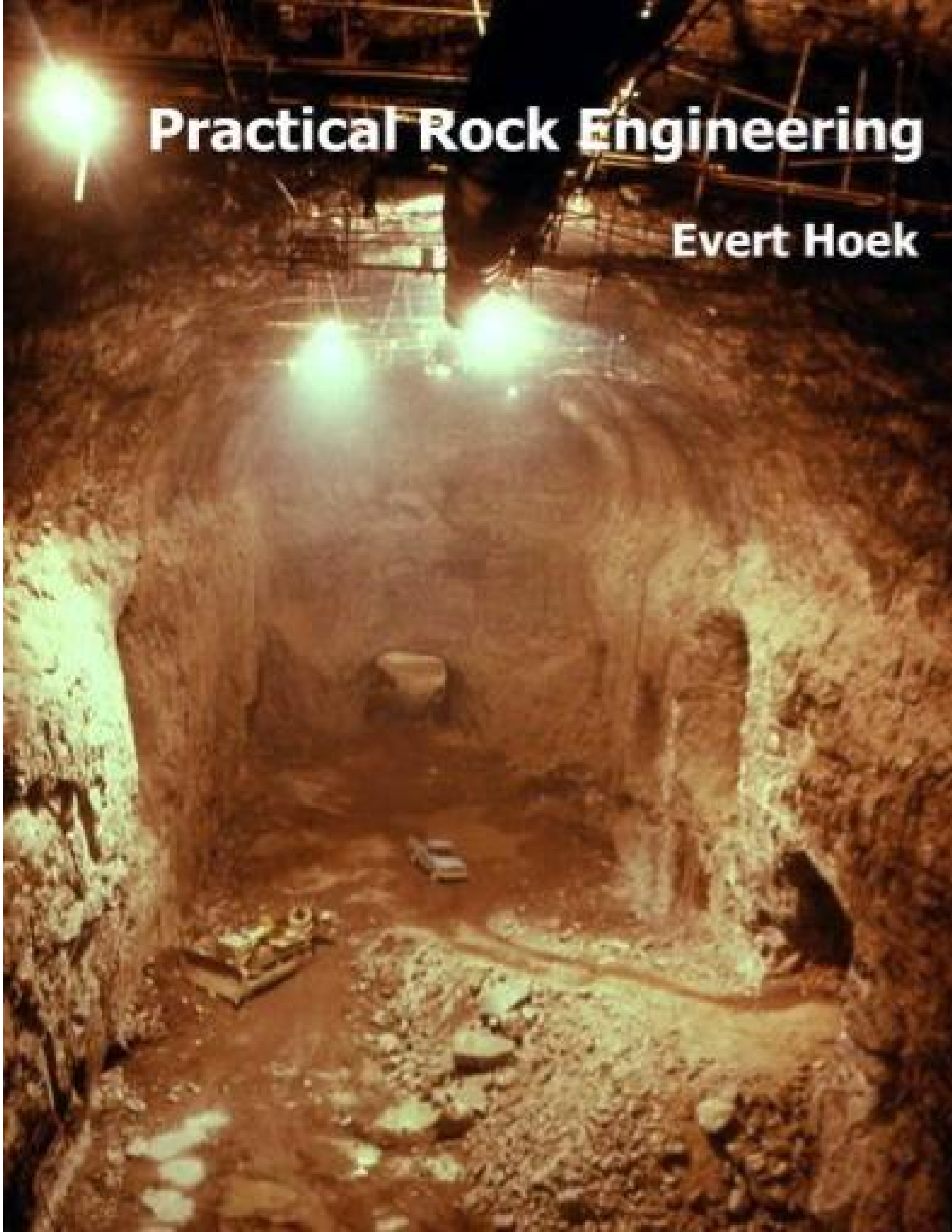
PDH Online | PDH Center

5272 Meadow Estates Drive
Fairfax, VA 22030-6658
Phone: 703-988-0088
www.PDHonline.com

An Approved Continuing Education Provider

Practical Rock Engineering

Evert Hoek



Preface

These notes were originally prepared during the period 1987 to 1993 for undergraduate and graduate courses in rock engineering at the University of Toronto. While some revisions were made in 2000 these were difficult because the notes had been formatted as a book with sequential chapter and page numbering. Any changes required reformatting the entire set of notes and this made it impractical to carry out regular updates.

In 2006 it was decided that a major revision was required in order to incorporate significant developments in rock engineering during the 20 years since the notes were originally written. The existing document was broken into a series of completely self-contained chapters, each with its own page numbering and references. This means that individual chapters can be updated at any time and that new chapters can be inserted as required.

The notes are intended to provide an insight into practical rock engineering to students, geotechnical engineers and engineering geologists. Case histories are used, wherever possible, to illustrate the methods currently used by practicing engineers. No attempt has been made to include recent research findings which have not yet found their way into everyday practical application. These research findings are adequately covered in conference proceedings, journals and on the Internet.

It is emphasised that these are notes are not a formal text. They have not been and will not be published in their present form and the contents will be revised from time to time to meet the needs of particular audiences.

Readers are encouraged to send their comments, corrections, criticisms and suggestions to me at the address given below. These contributions will help me to improve the notes for the future.



Dr Evert Hoek
Evert Hoek Consulting Engineer Inc.
3034 Edgemont Boulevard
P.O. Box 75516
North Vancouver, B.C.
Canada V7R 4X1
Email: ehoek@mailas.com



Dr. Evert Hoek: Experience and Expertise

Evert Hoek was born in Zimbabwe, graduated in mechanical engineering from the University of Cape Town and became involved in the young science of rock mechanics in 1958, when he started working in research on problems of brittle fracture associated with rockbursts in very deep mines in South Africa.

His degrees include a PhD from the University of Cape Town, a DSc (eng) from the University of London, and honorary doctorates from the Universities of Waterloo and Toronto in Canada. He has been elected as a Fellow of the Royal Academy of Engineering (UK), a Foreign Associate of the US National Academy of Engineering and a Fellow of the Canadian Academy of Engineering.

Dr. Hoek has published more than 100 papers and 3 books. He spent 9 years as a Reader and then Professor at the Imperial College of Science and Technology in London, 6 years as a Professor at the University of Toronto, 12 years as a Principal of Golder Associates in Vancouver, and the last 17 years as an independent consulting engineer based in North Vancouver. His consulting work has included major civil and mining projects in 35 countries around the world and has involved rock slopes, dam foundations, hydroelectric projects, underground caverns and tunnels excavated conventionally and by TBM.

Dr. Hoek has now retired from active consulting work but, in 2010, is still a member of consulting boards on three major civil and mining engineering projects in Canada, the USA and Chile.



Rock mass classification

Introduction

During the feasibility and preliminary design stages of a project, when very little detailed information is available on the rock mass and its stress and hydrologic characteristics, the use of a rock mass classification scheme can be of considerable benefit. At its simplest, this may involve using the classification scheme as a check-list to ensure that all relevant information has been considered. At the other end of the spectrum, one or more rock mass classification schemes can be used to build up a picture of the composition and characteristics of a rock mass to provide initial estimates of support requirements, and to provide estimates of the strength and deformation properties of the rock mass.

It is important to understand the limitations of rock mass classification schemes (Palmstrom and Broch, 2006) and that their use does not (and cannot) replace some of the more elaborate design procedures. However, the use of these design procedures requires access to relatively detailed information on in situ stresses, rock mass properties and planned excavation sequence, none of which may be available at an early stage in the project. As this information becomes available, the use of the rock mass classification schemes should be updated and used in conjunction with site specific analyses.

Engineering rock mass classification

Rock mass classification schemes have been developing for over 100 years since Ritter (1879) attempted to formalise an empirical approach to tunnel design, in particular for determining support requirements. While the classification schemes are appropriate for their original application, especially if used within the bounds of the case histories from which they were developed, considerable caution must be exercised in applying rock mass classifications to other rock engineering problems.

Summaries of some important classification systems are presented in this chapter, and although every attempt has been made to present all of the pertinent data from the original texts, there are numerous notes and comments which cannot be included. The interested reader should make every effort to read the cited references for a full appreciation of the use, applicability and limitations of each system.

Most of the multi-parameter classification schemes (Wickham et al (1972) Bieniawski (1973, 1989) and Barton et al (1974)) were developed from civil engineering case histories in which all of the components of the engineering geological character of the rock mass were included. In underground hard rock mining, however, especially at deep levels, rock mass weathering and the influence of water usually are not significant and may be ignored. Different classification systems place different emphases on the various

Rock mass classification

parameters, and it is recommended that at least two methods be used at any site during the early stages of a project.

Terzaghi's rock mass classification

The earliest reference to the use of rock mass classification for the design of tunnel support is in a paper by Terzaghi (1946) in which the rock loads, carried by steel sets, are estimated on the basis of a descriptive classification. While no useful purpose would be served by including details of Terzaghi's classification in this discussion on the design of support, it is interesting to examine the rock mass descriptions included in his original paper, because he draws attention to those characteristics that dominate rock mass behaviour, particularly in situations where gravity constitutes the dominant driving force. The clear and concise definitions and the practical comments included in these descriptions are good examples of the type of engineering geology information, which is most useful for engineering design.

Terzaghi's descriptions (quoted directly from his paper) are:

- *Intact* rock contains neither joints nor hair cracks. Hence, if it breaks, it breaks across sound rock. On account of the injury to the rock due to blasting, spalls may drop off the roof several hours or days after blasting. This is known as a *spalling* condition. Hard, intact rock may also be encountered in the *popping* condition involving the spontaneous and violent detachment of rock slabs from the sides or roof.
- *Stratified* rock consists of individual strata with little or no resistance against separation along the boundaries between the strata. The strata may or may not be weakened by transverse joints. In such rock the spalling condition is quite common.
- *Moderately jointed* rock contains joints and hair cracks, but the blocks between joints are locally grown together or so intimately interlocked that vertical walls do not require lateral support. In rocks of this type, both spalling and popping conditions may be encountered.
- *Blocky and seamy* rock consists of chemically intact or almost intact rock fragments which are entirely separated from each other and imperfectly interlocked. In such rock, vertical walls may require lateral support.
- *Crushed* but chemically intact rock has the character of crusher run. If most or all of the fragments are as small as fine sand grains and no recementation has taken place, crushed rock below the water table exhibits the properties of a water-bearing sand.
- *Squeezing* rock slowly advances into the tunnel without perceptible volume increase. A prerequisite for squeeze is a high percentage of microscopic and sub-microscopic particles of micaceous minerals or clay minerals with a low swelling capacity.
- *Swelling* rock advances into the tunnel chiefly on account of expansion. The capacity to swell seems to be limited to those rocks that contain clay minerals such as montmorillonite, with a high swelling capacity.

Rock mass classification

Classifications involving stand-up time

Lauffer (1958) proposed that the stand-up time for an unsupported span is related to the quality of the rock mass in which the span is excavated. In a tunnel, the unsupported span is defined as the span of the tunnel or the distance between the face and the nearest support, if this is greater than the tunnel span. Lauffer's original classification has since been modified by a number of authors, notably Pacher et al (1974), and now forms part of the general tunnelling approach known as the New Austrian Tunnelling Method.

The significance of the stand-up time concept is that an increase in the span of the tunnel leads to a significant reduction in the time available for the installation of support. For example, a small pilot tunnel may be successfully constructed with minimal support, while a larger span tunnel in the same rock mass may not be stable without the immediate installation of substantial support.

The New Austrian Tunnelling Method includes a number of techniques for safe tunnelling in rock conditions in which the stand-up time is limited before failure occurs. These techniques include the use of smaller headings and benching or the use of multiple drifts to form a reinforced ring inside which the bulk of the tunnel can be excavated. These techniques are applicable in soft rocks such as shales, phyllites and mudstones in which the squeezing and swelling problems, described by Terzaghi (see previous section), are likely to occur. The techniques are also applicable when tunnelling in excessively broken rock, but great care should be taken in attempting to apply these techniques to excavations in hard rocks in which different failure mechanisms occur.

In designing support for hard rock excavations it is prudent to assume that the stability of the rock mass surrounding the excavation is not time-dependent. Hence, if a structurally defined wedge is exposed in the roof of an excavation, it will fall as soon as the rock supporting it is removed. This can occur at the time of the blast or during the subsequent scaling operation. If it is required to keep such a wedge in place, or to enhance the margin of safety, it is essential that the support be installed as early as possible, preferably before the rock supporting the full wedge is removed. On the other hand, in a highly stressed rock, failure will generally be induced by some change in the stress field surrounding the excavation. The failure may occur gradually and manifest itself as spalling or slabbing or it may occur suddenly in the form of a rock burst. In either case, the support design must take into account the change in the stress field rather than the 'stand-up' time of the excavation.

Rock quality designation index (RQD)

The Rock Quality Designation index (*RQD*) was developed by Deere (Deere et al 1967) to provide a quantitative estimate of rock mass quality from drill core logs. *RQD* is defined as the percentage of intact core pieces longer than 100 mm (4 inches) in the total length of core. The core should be at least NW size (54.7 mm or 2.15 inches in diameter) and should be drilled with a double-tube core barrel. The correct procedures for

Rock mass classification

measurement of the length of core pieces and the calculation of *RQD* are summarised in Figure 1.

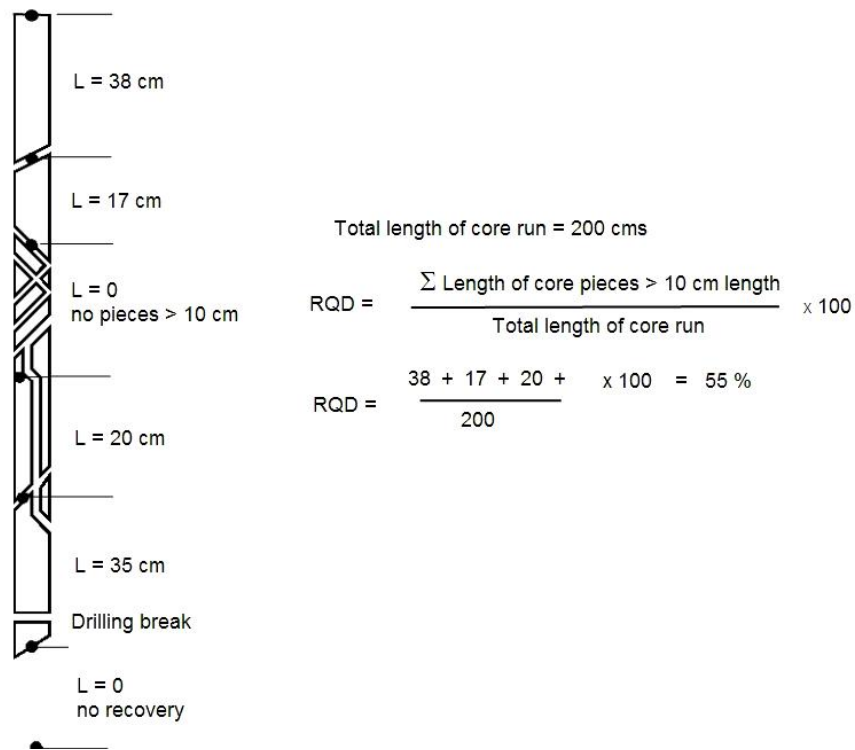


Figure 1: Procedure for measurement and calculation of *RQD* (After Deere, 1989).

Palmström (1982) suggested that, when no core is available but discontinuity traces are visible in surface exposures or exploration adits, the *RQD* may be estimated from the number of discontinuities per unit volume. The suggested relationship for clay-free rock masses is:

$$RQD = 115 - 3.3 J_v \quad (1)$$

where J_v is the sum of the number of joints per unit length for all joint (discontinuity) sets known as the volumetric joint count.

RQD is a directionally dependent parameter and its value may change significantly, depending upon the borehole orientation. The use of the volumetric joint count can be quite useful in reducing this directional dependence.

RQD is intended to represent the rock mass quality in situ. When using diamond drill core, care must be taken to ensure that fractures, which have been caused by handling or the drilling process, are identified and ignored when determining the value of *RQD*.

When using Palmström's relationship for exposure mapping, blast induced fractures should not be included when estimating J_v .

Rock mass classification

Deere's *RQD* was widely used, particularly in North America, after its introduction. Cording and Deere (1972), Merritt (1972) and Deere and Deere (1988) attempted to relate *RQD* to Terzaghi's rock load factors and to rockbolt requirements in tunnels. In the context of this discussion, the most important use of *RQD* is as a component of the *RMR* and *Q* rock mass classifications covered later in this chapter.

Rock Structure Rating (RSR)

Wickham et al (1972) described a quantitative method for describing the quality of a rock mass and for selecting appropriate support on the basis of their Rock Structure Rating (*RSR*) classification. Most of the case histories, used in the development of this system, were for relatively small tunnels supported by means of steel sets, although historically this system was the first to make reference to shotcrete support. In spite of this limitation, it is worth examining the *RSR* system in some detail since it demonstrates the logic involved in developing a quasi-quantitative rock mass classification system.

The significance of the *RSR* system, in the context of this discussion, is that it introduced the concept of rating each of the components listed below to arrive at a numerical value of $RSR = A + B + C$.

1. *Parameter A, Geology*: General appraisal of geological structure on the basis of:
 - a. Rock type origin (igneous, metamorphic, sedimentary).
 - b. Rock hardness (hard, medium, soft, decomposed).
 - c. Geologic structure (massive, slightly faulted/folded, moderately faulted/folded, intensely faulted/folded).
2. *Parameter B, Geometry*: Effect of discontinuity pattern with respect to the direction of the tunnel drive on the basis of:
 - a. Joint spacing.
 - b. Joint orientation (strike and dip).
 - c. Direction of tunnel drive.
3. *Parameter C*: Effect of groundwater inflow and joint condition on the basis of:
 - a. Overall rock mass quality on the basis of A and B combined.
 - b. Joint condition (good, fair, poor).
 - c. Amount of water inflow (in gallons per minute per 1000 feet of tunnel).

Note that the *RSR* classification used Imperial units and that these units have been retained in this discussion.

Three tables from Wickham et al's 1972 paper are reproduced in Tables 1, 2 and 3. These tables can be used to evaluate the rating of each of these parameters to arrive at the *RSR* value (maximum $RSR = 100$).

Rock mass classification

Table 1: Rock Structure Rating: Parameter A: General area geology

	Basic Rock Type				Geological Structure			
	Hard	Medium	Soft	Decomposed	Slightly	Moderately	Intensively	
Igneous	1	2	3	4	Folded or	Folded or	Folded or	
Metamorphic	1	2	3	4	Massive	Faulted	Faulted	Faulted
Sedimentary	2	3	4	4				
Type 1					30	22	15	9
Type 2					27	20	13	8
Type 3					24	18	12	7
Type 4					19	15	10	6

Table 2: Rock Structure Rating: Parameter B: Joint pattern, direction of drive

Average joint spacing	Strike \perp to Axis					Strike \parallel to Axis		
	Direction of Drive					Direction of Drive		
	Both	With Dip		Against Dip		Either direction		
	Dip of Prominent Joints ^a					Dip of Prominent Joints		
	Flat	Dipping	Vertical	Dipping	Vertical	Flat	Dipping	Vertical
1. Very closely jointed, < 2 in	9	11	13	10	12	9	9	7
2. Closely jointed, 2-6 in	13	16	19	15	17	14	14	11
3. Moderately jointed, 6-12 in	23	24	28	19	22	23	23	19
4. Moderate to blocky, 1-2 ft	30	32	36	25	28	30	28	24
5. Blocky to massive, 2-4 ft	36	38	40	33	35	36	24	28
6. Massive, > 4 ft	40	43	45	37	40	40	38	34

Table 3: Rock Structure Rating: Parameter C: Groundwater, joint condition

Anticipated water inflow gpm/1000 ft of tunnel	Sum of Parameters A + B					
	13 - 44			45 - 75		
	Joint Condition ^b					
	Good	Fair	Poor	Good	Fair	Poor
None	22	18	12	25	22	18
Slight, < 200 gpm	19	15	9	23	19	14
Moderate, 200-1000 gpm	15	22	7	21	16	12
Heavy, > 1000 gp	10	8	6	18	14	10

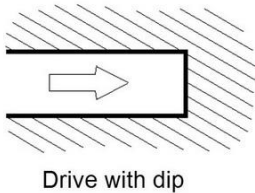
^a Dip: flat: 0-20°; dipping: 20-50°; and vertical: 50-90°

^b Joint condition: good = tight or cemented; fair = slightly weathered or altered; poor = severely weathered, altered or open

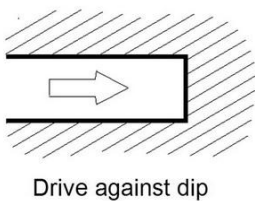
Rock mass classification

For example, a hard metamorphic rock which is slightly folded or faulted has a rating of $A = 22$ (from Table 1). The rock mass is moderately jointed, with joints striking perpendicular to the tunnel axis which is being driven east-west, and dipping at between 20° and 50° .

Table 2 gives the rating for $B = 24$ for driving with dip (defined below).



The value of $A + B = 46$ and this means that, for joints of fair condition (slightly weathered and altered) and a moderate water inflow of between 200 and 1,000 gallons per minute, Table 3 gives the rating for $C = 16$. Hence, the final value of the rock structure rating $RSR = A + B + C = 62$.



A typical set of prediction curves for a 24 foot diameter tunnel are given in Figure 2 which shows that, for the RSR value of 62 derived above, the predicted support would be 2 inches of shotcrete and 1 inch diameter rockbolts spaced at 5 foot centres. As indicated in the figure, steel sets would be spaced at more than 7 feet apart and would not be considered a practical solution for the support of this tunnel.

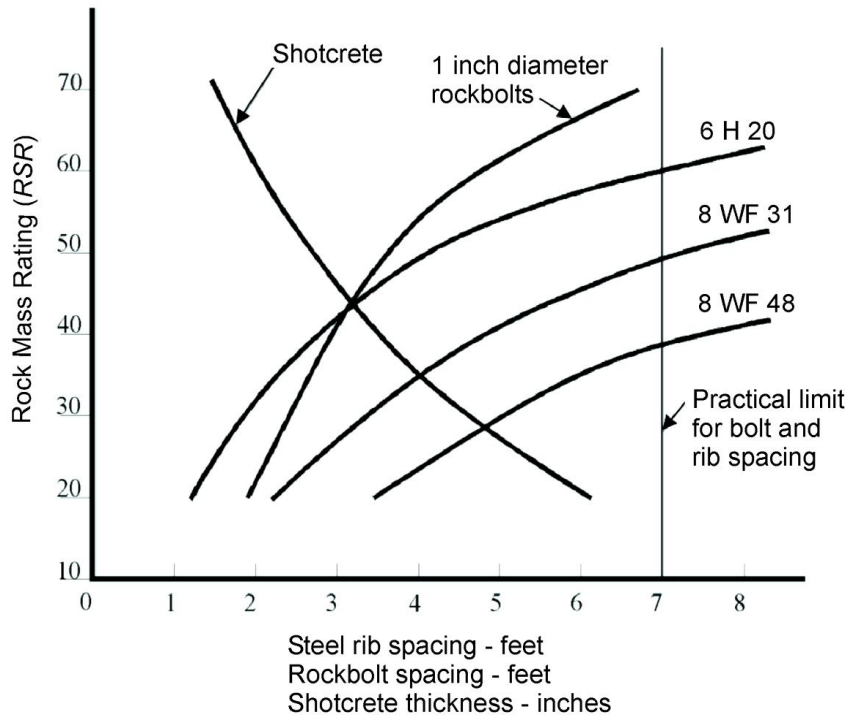


Figure 2: RSR support estimates for a 24 ft. (7.3 m) diameter circular tunnel. Note that rockbolts and shotcrete are generally used together. (After Wickham et al 1972).

Rock mass classification

For the same size tunnel in a rock mass with $RSR = 30$, the support could be provided by 8 WF 31 steel sets (8 inch deep wide flange I section weighing 31 lb per foot) spaced 3 feet apart, or by 5 inches of shotcrete and 1 inch diameter rockbolts spaced at 2.5 feet centres. In this case it is probable that the steel set solution would be cheaper and more effective than the use of rockbolts and shotcrete.

Although the *RSR* classification system is not widely used today, Wickham et al's work played a significant role in the development of the classification schemes discussed in the remaining sections of this chapter.

Geomechanics Classification

Bieniawski (1976) published the details of a rock mass classification called the Geomechanics Classification or the Rock Mass Rating (*RMR*) system. Over the years, this system has been successively refined as more case records have been examined and the reader should be aware that Bieniawski has made significant changes in the ratings assigned to different parameters. The discussion which follows is based upon the 1989 version of the classification (Bieniawski, 1989). Both this version and the 1976 version deal with estimating the strength of rock masses. The following six parameters are used to classify a rock mass using the *RMR* system:

1. Uniaxial compressive strength of rock material.
2. Rock Quality Designation (*RQD*).
3. Spacing of discontinuities.
4. Condition of discontinuities.
5. Groundwater conditions.
6. Orientation of discontinuities.

In applying this classification system, the rock mass is divided into a number of structural regions and each region is classified separately. The boundaries of the structural regions usually coincide with a major structural feature such as a fault or with a change in rock type. In some cases, significant changes in discontinuity spacing or characteristics, within the same rock type, may necessitate the division of the rock mass into a number of small structural regions.

The Rock Mass Rating system is presented in Table 4, giving the ratings for each of the six parameters listed above. These ratings are summed to give a value of *RMR*. The following example illustrates the use of these tables to arrive at an *RMR* value.

A tunnel is to be driven through slightly weathered granite with a dominant joint set dipping at 60° against the direction of the drive. Index testing and logging of diamond drilled core give typical Point-load strength index values of 8 MPa and average *RQD* values of 70%. The slightly rough and slightly weathered joints with a separation of < 1 mm, are spaced at 300 mm. Tunnelling conditions are anticipated to be wet.

Rock mass classification

Table 4: Rock Mass Rating System (After Bieniawski 1989).

A. CLASSIFICATION PARAMETERS AND THEIR RATINGS								
Parameter		Range of values						
1	Strength of intact rock material	Point-load strength index	>10 MPa	4 - 10 MPa	2 - 4 MPa	1 - 2 MPa	For this low range - uniaxial compressive test is preferred	
		Uniaxial comp. strength	>250 MPa	100 - 250 MPa	50 - 100 MPa	25 - 50 MPa	5 - 25 MPa	1 - 5 MPa
	Rating	15	12	7	4	2	1	0
2	Drill core Quality <i>RQD</i>		90% - 100%	75% - 90%	50% - 75%	25% - 50%	< 25%	
	Rating		20	17	13	8	3	
3	Spacing of discontinuities		> 2 m	0.6 - 2 . m	200 - 600 mm	60 - 200 mm	< 60 mm	
	Rating		20	15	10	8	5	
4	Condition of discontinuities (See E)		Very rough surfaces Not continuous No separation Unweathered wall rock	Slightly rough surfaces Separation < 1 mm Slightly weathered walls	Slightly rough surfaces Separation < 1 mm Highly weathered walls	Slickensided surfaces or Gouge < 5 mm thick or Separation 1-5 mm Continuous	Soft gouge >5 mm thick or Separation > 5 mm Continuous	
	Rating		30	25	20	10	0	
5	Groundwater	Inflow per 10 m tunnel length (l/m)	None	< 10	10 - 25	25 - 125	> 125	
		(Joint water press)/ (Major principal σ)	0	< 0.1	0.1, - 0.2	0.2 - 0.5	> 0.5	
	General conditions		Completely dry	Damp	Wet	Dripping	Flowing	
	Rating		15	10	7	4	0	
B. RATING ADJUSTMENT FOR DISCONTINUITY ORIENTATIONS (See F)								
Strike and dip orientations			Very favourable	Favourable	Fair	Unfavourable	Very Unfavourable	
Ratings	Tunnels & mines		0	-2	-5	-10	-12	
	Foundations		0	-2	-7	-15	-25	
	Slopes		0	-5	-25	-50		
C. ROCK MASS CLASSES DETERMINED FROM TOTAL RATINGS								
Rating			100 ← 81	80 ← 61	60 ← 41	40 ← 21	< 21	
Class number			I	II	III	IV	V	
Description			Very good rock	Good rock	Fair rock	Poor rock	Very poor rock	
D. MEANING OF ROCK CLASSES								
Class number			I	II	III	IV	V	
Average stand-up time			20 yrs for 15 m span	1 year for 10 m span	1 week for 5 m span	10 hrs for 2.5 m span	30 min for 1 m span	
Cohesion of rock mass (kPa)			> 400	300 - 400	200 - 300	100 - 200	< 100	
Friction angle of rock mass (deg)			> 45	35 - 45	25 - 35	15 - 25	< 15	
E. GUIDELINES FOR CLASSIFICATION OF DISCONTINUITY conditions								
Discontinuity length (persistence)			< 1 m	1 - 3 m	3 - 10 m	10 - 20 m	> 20 m	
Rating			6	4	2	1	0	
Separation (aperture)			None	< 0.1 mm	0.1 - 1.0 mm	1 - 5 mm	> 5 mm	
Rating			6	5	4	1	0	
Roughness			Very rough	Rough	Slightly rough	Smooth	Slickensided	
Rating			6	5	3	1	0	
Infilling (gouge)			None	Hard filling < 5 mm	Hard filling > 5 mm	Soft filling < 5 mm	Soft filling > 5 mm	
Rating			6	4	2	2	0	
Weathering			Unweathered	Slightly weathered	Moderately weathered	Highly weathered	Decomposed	
Ratings			6	5	3	1	0	
F. EFFECT OF DISCONTINUITY STRIKE AND DIP ORIENTATION IN TUNNELLING**								
Strike perpendicular to tunnel axis				Strike parallel to tunnel axis				
Drive with dip - Dip 45 - 90°		Drive with dip - Dip 20 - 45°		Dip 45 - 90°		Dip 20 - 45°		
Very favourable		Favourable		Very unfavourable		Fair		
Drive against dip - Dip 45-90°		Drive against dip - Dip 20-45°		Dip 0-20 - Irrespective of strike°				
Fair		Unfavourable		Fair				

* Some conditions are mutually exclusive . For example, if infilling is present, the roughness of the surface will be overshadowed by the influence of the gouge. In such cases use A.4 directly.

** Modified after Wickham et al (1972).

Rock mass classification

The *RMR* value for the example under consideration is determined as follows:

<i>Table</i>	<i>Item</i>	<i>Value</i>	<i>Rating</i>
4: A.1	Point load index	8 MPa	12
4: A.2	<i>RQD</i>	70%	13
4: A.3	Spacing of discontinuities	300 mm	10
4: E.4	Condition of discontinuities	Note 1	22
4: A.5	Groundwater	Wet	7
4: B	Adjustment for joint orientation	Note 2	-5
Total			59

Note 1. For slightly rough and altered discontinuity surfaces with a separation of < 1 mm, Table 4.A.4 gives a rating of 25. When more detailed information is available, Table 4.E can be used to obtain a more refined rating. Hence, in this case, the rating is the sum of: 4 (1-3 m discontinuity length), 4 (separation 0.1-1.0 mm), 3 (slightly rough), 6 (no infilling) and 5 (slightly weathered) = 22.

Note 2. Table 4.F gives a description of ‘Fair’ for the conditions assumed where the tunnel is to be driven against the dip of a set of joints dipping at 60° . Using this description for ‘Tunnels and Mines’ in Table 4.B gives an adjustment rating of -5.

Bieniawski (1989) published a set of guidelines for the selection of support in tunnels in rock for which the value of *RMR* has been determined. These guidelines are reproduced in Table 4. Note that these guidelines have been published for a 10 m span horseshoe shaped tunnel, constructed using drill and blast methods, in a rock mass subjected to a vertical stress < 25 MPa (equivalent to a depth below surface of < 900 m).

For the case considered earlier, with $RMR = 59$, Table 4 suggests that a tunnel could be excavated by top heading and bench, with a 1.5 to 3 m advance in the top heading. Support should be installed after each blast and the support should be placed at a maximum distance of 10 m from the face. Systematic rock bolting, using 4 m long 20 mm diameter fully grouted bolts spaced at 1.5 to 2 m in the crown and walls, is recommended. Wire mesh, with 50 to 100 mm of shotcrete for the crown and 30 mm of shotcrete for the walls, is recommended.

The value of *RMR* of 59 indicates that the rock mass is on the boundary between the ‘Fair rock’ and ‘Good rock’ categories. In the initial stages of design and construction, it is advisable to utilise the support suggested for fair rock. If the construction is progressing well with no stability problems, and the support is performing very well, then it should be possible to gradually reduce the support requirements to those indicated for a good rock mass. In addition, if the excavation is required to be stable for a short amount of time, then it is advisable to try the less expensive and extensive support suggested for good rock. However, if the rock mass surrounding the excavation is expected to undergo large mining induced stress changes, then more substantial support appropriate for fair rock should be installed. This example indicates that a great deal of judgement is needed in the application of rock mass classification to support design.

Rock mass classification

Table 5: Guidelines for excavation and support of 10 m span rock tunnels in accordance with the *RMR* system (After Bieniawski 1989).

Rock mass class	Excavation	Rock bolts (20 mm diameter, fully grouted)	Shotcrete	Steel sets
I - Very good rock <i>RMR</i> : 81-100	Full face, 3 m advance.	Generally no support required except spot bolting.		
II - Good rock <i>RMR</i> : 61-80	Full face , 1-1.5 m advance. Complete support 20 m from face.	Locally, bolts in crown 3 m long, spaced 2.5 m with occasional wire mesh.	50 mm in crown where required.	None.
III - Fair rock <i>RMR</i> : 41-60	Top heading and bench 1.5-3 m advance in top heading. Commence support after each blast. Complete support 10 m from face.	Systematic bolts 4 m long, spaced 1.5 - 2 m in crown and walls with wire mesh in crown.	50-100 mm in crown and 30 mm in sides.	None.
IV - Poor rock <i>RMR</i> : 21-40	Top heading and bench 1.0-1.5 m advance in top heading. Install support concurrently with excavation, 10 m from face.	Systematic bolts 4-5 m long, spaced 1-1.5 m in crown and walls with wire mesh.	100-150 mm in crown and 100 mm in sides.	Light to medium ribs spaced 1.5 m where required.
V – Very poor rock <i>RMR</i> : < 20	Multiple drifts 0.5-1.5 m advance in top heading. Install support concurrently with excavation. Shotcrete as soon as possible after blasting.	Systematic bolts 5-6 m long, spaced 1-1.5 m in crown and walls with wire mesh. Bolt invert.	150-200 mm in crown, 150 mm in sides, and 50 mm on face.	Medium to heavy ribs spaced 0.75 m with steel lagging and forepoling if required. Close invert.

It should be noted that Table 5 has not had a major revision since 1973. In many mining and civil engineering applications, steel fibre reinforced shotcrete may be considered in place of wire mesh and shotcrete.

Modifications to *RMR* for mining

Bieniawski's Rock Mass Rating (*RMR*) system was originally based upon case histories drawn from civil engineering. Consequently, the mining industry tended to regard the classification as somewhat conservative and several modifications have been proposed in order to make the classification more relevant to mining applications. A comprehensive summary of these modifications was compiled by Bieniawski (1989).

Laubscher (1977, 1984), Laubscher and Taylor (1976) and Laubscher and Page (1990) have described a Modified Rock Mass Rating system for mining. This *MRMR* system takes the basic *RMR* value, as defined by Bieniawski, and adjusts it to account for in situ and induced stresses, stress changes and the effects of blasting and weathering. A set of support recommendations is associated with the resulting *MRMR* value. In using Laubscher's *MRMR* system it should be borne in mind that many of the case histories upon which it is based are derived from caving operations. Originally, block caving in asbestos mines in Africa formed the basis for the modifications but, subsequently, other case histories from around the world have been added to the database.

Rock mass classification

Cummings et al (1982) and Kendorski et al (1983) have also modified Bieniawski's RMR classification to produce the *MBR* (modified basic *RMR*) system for mining. This system was developed for block caving operations in the USA. It involves the use of different ratings for the original parameters used to determine the value of *RMR* and the subsequent adjustment of the resulting *MBR* value to allow for blast damage, induced stresses, structural features, distance from the cave front and size of the caving block. Support recommendations are presented for isolated or development drifts as well as for the final support of intersections and drifts.

Rock Tunnelling Quality Index, Q

On the basis of an evaluation of a large number of case histories of underground excavations, Barton et al (1974) of the Norwegian Geotechnical Institute proposed a Tunnelling Quality Index (Q) for the determination of rock mass characteristics and tunnel support requirements. The numerical value of the index Q varies on a logarithmic scale from 0.001 to a maximum of 1,000 and is defined by:

$$Q = \frac{RQD}{J_n} \times \frac{J_r}{J_a} \times \frac{J_w}{SRF} \quad (2)$$

where RQD is the Rock Quality Designation

J_n is the joint set number

J_r is the joint roughness number

J_a is the joint alteration number

J_w is the joint water reduction factor

SRF is the stress reduction factor

In explaining the meaning of the parameters used to determine the value of Q , Barton et al (1974) offer the following comments:

The first quotient (RQD/J_n), representing the structure of the rock mass, is a crude measure of the block or particle size, with the two extreme values (100/0.5 and 10/20) differing by a factor of 400. If the quotient is interpreted in units of centimetres, the extreme 'particle sizes' of 200 to 0.5 cm are seen to be crude but fairly realistic approximations. Probably the largest blocks should be several times this size and the smallest fragments less than half the size. (Clay particles are of course excluded).

The second quotient (J_r/J_a) represents the roughness and frictional characteristics of the joint walls or filling materials. This quotient is weighted in favour of rough, unaltered joints in direct contact. It is to be expected that such surfaces will be close to peak strength, that they will dilate strongly when sheared, and they will therefore be especially favourable to tunnel stability.

When rock joints have thin clay mineral coatings and fillings, the strength is reduced significantly. Nevertheless, rock wall contact after small shear displacements have occurred may be a very important factor for preserving the excavation from ultimate failure.

Rock mass classification

Where no rock wall contact exists, the conditions are extremely unfavourable to tunnel stability. The 'friction angles' (given in Table 6) are a little below the residual strength values for most clays, and are possibly down-graded by the fact that these clay bands or fillings may tend to consolidate during shear, at least if normal consolidation or if softening and swelling has occurred. The swelling pressure of montmorillonite may also be a factor here.

The third quotient (J_w/SRF) consists of two stress parameters. SRF is a measure of: 1) loosening load in the case of an excavation through shear zones and clay bearing rock, 2) rock stress in competent rock, and 3) squeezing loads in plastic incompetent rocks. It can be regarded as a total stress parameter. The parameter J_w is a measure of water pressure, which has an adverse effect on the shear strength of joints due to a reduction in effective normal stress. Water may, in addition, cause softening and possible out-wash in the case of clay-filled joints. It has proved impossible to combine these two parameters in terms of inter-block effective stress, because paradoxically a high value of effective normal stress may sometimes signify less stable conditions than a low value, despite the higher shear strength. The quotient (J_w/SRF) is a complicated empirical factor describing the 'active stress'.

It appears that the rock tunnelling quality Q can now be considered to be a function of only three parameters which are crude measures of:

- | | |
|-------------------------------|-------------|
| 1. Block size | (RQD/J_n) |
| 2. Inter-block shear strength | (J_r/J_a) |
| 3. Active stress | (J_w/SRF) |

Undoubtedly, there are several other parameters which could be added to improve the accuracy of the classification system. One of these would be the joint orientation. Although many case records include the necessary information on structural orientation in relation to excavation axis, it was not found to be the important general parameter that might be expected. Part of the reason for this may be that the orientations of many types of excavations can be, and normally are, adjusted to avoid the maximum effect of unfavourably oriented major joints. However, this choice is not available in the case of tunnels, and more than half the case records were in this category. The parameters J_n , J_r and J_a appear to play a more important role than orientation, because the number of joint sets determines the degree of freedom for block movement (if any), and the frictional and dilational characteristics can vary more than the down-dip gravitational component of unfavourably oriented joints. If joint orientations had been included the classification would have been less general, and its essential simplicity lost.

Table 6 (After Barton et al 1974) gives the classification of individual parameters used to obtain the Tunnelling Quality Index Q for a rock mass.

The use of Table 6 is illustrated in the following example. A 15 m span crusher chamber for an underground mine is to be excavated in a norite at a depth of 2,100 m below surface. The rock mass contains two sets of joints controlling stability. These joints are

Rock mass classification

undulating, rough and unweathered with very minor surface staining. *RQD* values range from 85% to 95% and laboratory tests on core samples of intact rock give an average uniaxial compressive strength of 170 MPa. The principal stress directions are approximately vertical and horizontal and the magnitude of the horizontal principal stress is approximately 1.5 times that of the vertical principal stress. The rock mass is locally damp but there is no evidence of flowing water.

The numerical value of *RQD* is used directly in the calculation of *Q* and, for this rock mass, an average value of 90 will be used. Table 6.2 shows that, for two joint sets, the joint set number, $J_n = 4$. For rough or irregular joints which are undulating, Table 6.3 gives a joint roughness number of $J_r = 3$. Table 6.4 gives the joint alteration number, $J_a = 1.0$, for unaltered joint walls with surface staining only. Table 6.5 shows that, for an excavation with minor inflow, the joint water reduction factor, $J_w = 1.0$. For a depth below surface of 2,100 m the overburden stress will be approximately 57 MPa and, in this case, the major principal stress $\sigma_I = 85$ MPa. Since the uniaxial compressive strength of the norite is approximately 170 MPa, this gives a ratio of $\sigma_c / \sigma_I = 2$. Table 6.6 shows that, for competent rock with rock stress problems, this value of σ_c / σ_I can be expected to produce heavy rock burst conditions and that the value of *SRF* should lie between 10 and 20. A value of $SRF = 15$ will be assumed for this calculation. Using these values gives:

$$Q = \frac{90}{4} \times \frac{3}{1} \times \frac{1}{15} = 4.5$$

In relating the value of the index *Q* to the stability and support requirements of underground excavations, Barton et al (1974) defined an additional parameter which they called the Equivalent Dimension, *De*, of the excavation. This dimension is obtained by dividing the span, diameter or wall height of the excavation by a quantity called the Excavation Support Ratio, *ESR*. Hence:

$$D_e = \frac{\text{Excavation span, diameter or height (m)}}{\text{Excavation Support Ratio } ESR}$$

The value of *ESR* is related to the intended use of the excavation and to the degree of security which is demanded of the support system installed to maintain the stability of the excavation. Barton et al (1974) suggest the following values:

Excavation category	<i>ESR</i>
A Temporary mine openings.	3-5
B Permanent mine openings, water tunnels for hydro power (excluding high pressure penstocks), pilot tunnels, drifts and headings for large excavations.	1.6
C Storage rooms, water treatment plants, minor road and railway tunnels, surge chambers, access tunnels.	1.3
D Power stations, major road and railway tunnels, civil defence chambers, portal intersections.	1.0
E Underground nuclear power stations, railway stations, sports and public facilities, factories.	0.8

Rock mass classification

Table 6: Classification of individual parameters used in the Tunnelling Quality Index Q

DESCRIPTION	VALUE	NOTES
1. ROCK QUALITY DESIGNATION	RQD	
A. Very poor	0 - 25	1. Where RQD is reported or measured as ≤ 10 (including 0), a nominal value of 10 is used to evaluate Q .
B. Poor	25 - 50	
C. Fair	50 - 75	2. RQD intervals of 5, i.e. 100, 95, 90 etc. are sufficiently accurate.
D. Good	75 - 90	
E. Excellent	90 - 100	
2. JOINT SET NUMBER	J_n	
A. Massive, no or few joints	0.5 - 1.0	
B. One joint set	2	
C. One joint set plus random	3	
D. Two joint sets	4	
E. Two joint sets plus random	6	
F. Three joint sets	9	1. For intersections use $(3.0 \times J_n)$
G. Three joint sets plus random	12	
H. Four or more joint sets, random, heavily jointed, 'sugar cube', etc.	15	2. For portals use $(2.0 \times J_n)$
J. Crushed rock, earthlike	20	
3. JOINT ROUGHNESS NUMBER	J_r	
a. Rock wall contact		
b. Rock wall contact before 10 cm shear		
A. Discontinuous joints	4	
B. Rough and irregular, undulating	3	
C. Smooth undulating	2	
D. Slickensided undulating	1.5	1. Add 1.0 if the mean spacing of the relevant joint set is greater than 3 m.
E. Rough or irregular, planar	1.5	
F. Smooth, planar	1.0	2. $J_r = 0.5$ can be used for planar, slickensided joints having lineations, provided that the lineations are oriented for minimum strength.
G. Slickensided, planar	0.5	
c. No rock wall contact when sheared		
H. Zones containing clay minerals thick enough to prevent rock wall contact	1.0 (nominal)	
J. Sandy, gravely or crushed zone thick enough to prevent rock wall contact	1.0 (nominal)	
4. JOINT ALTERATION NUMBER	J_a	ϕ_r degrees (approx.)
a. Rock wall contact		
A. Tightly healed, hard, non-softening, impermeable filling	0.75	1. Values of ϕ_r , the residual friction angle, are intended as an approximate guide to the mineralogical properties of the alteration products, if present.
B. Unaltered joint walls, surface staining only	1.0	
C. Slightly altered joint walls, non-softening mineral coatings, sandy particles, clay-free disintegrated rock, etc.	2.0	25 - 30
D. Silty-, or sandy-clay coatings, small clay-fraction (non-softening)	3.0	20 - 25
E. Softening or low-friction clay mineral coatings, i.e. kaolinite, mica. Also chlorite, talc, gypsum and graphite etc., and small quantities of swelling clays. (Discontinuous coatings, 1 - 2 mm or less)	4.0	8 - 16

Rock mass classification

Table 6: (cont'd.) Classification of individual parameters used in the Tunnelling Quality Index Q (After Barton et al 1974).

4. JOINT ALTERATION NUMBER	J_a	ϕ_r degrees (approx.)	
b. Rock wall contact before 10 cm shear			
F. Sandy particles, clay-free, disintegrating rock etc.	4.0	25 - 30	
G. Strongly over-consolidated, non-softening clay mineral fillings (continuous < 5 mm thick)	6.0	16 - 24	
H. Medium or low over-consolidation, softening clay mineral fillings (continuous < 5 mm thick)	8.0	12 - 16	
J. Swelling clay fillings, i.e. montmorillonite, (continuous < 5 mm thick). Values of J_a depend on percent of swelling clay-size particles, and access to water.	8.0 - 12.0	6 - 12	
c. No rock wall contact when sheared			
K. Zones or bands of disintegrated or crushed	6.0		
L. rock and clay (see G, H and J for clay	8.0		
M. conditions)	8.0 - 12.0	6 - 24	
N. Zones or bands of silty- or sandy-clay, small clay fraction, non-softening	5.0		
O. Thick continuous zones or bands of clay	10.0 - 13.0		
P. & R. (see G.H and J for clay conditions)	6.0 - 24.0		
5. JOINT WATER REDUCTION	J_w	approx. water pressure (kgf/cm ²)	
A. Dry excavation or minor inflow i.e. < 5 l/m locally	1.0	< 1.0	
B. Medium inflow or pressure, occasional outwash of joint fillings	0.66	1.0 - 2.5	
C. Large inflow or high pressure in competent rock with unfilled joints	0.5	2.5 - 10.0	1. Factors C to F are crude estimates; increase J_w if drainage installed.
D. Large inflow or high pressure	0.33	2.5 - 10.0	
E. Exceptionally high inflow or pressure at blasting, decaying with time	0.2 - 0.1	> 10	2. Special problems caused by ice formation are not considered.
F. Exceptionally high inflow or pressure	0.1 - 0.05	> 10	
6. STRESS REDUCTION FACTOR		SRF	
a. Weakness zones intersecting excavation, which may cause loosening of rock mass when tunnel is excavated			
A. Multiple occurrences of weakness zones containing clay or chemically disintegrated rock, very loose surrounding rock (any depth)	10.0		1. Reduce these values of SRF by 25 - 50% but only if the relevant shear zones influence do not intersect the excavation
B. Single weakness zones containing clay, or chemically disintegrated rock (excavation depth < 50 m)	5.0		
C. Single weakness zones containing clay, or chemically disintegrated rock (excavation depth > 50 m)	2.5		
D. Multiple shear zones in competent rock (clay free), loose surrounding rock (any depth)	7.5		
E. Single shear zone in competent rock (clay free). (depth of excavation < 50 m)	5.0		
F. Single shear zone in competent rock (clay free). (depth of excavation > 50 m)	2.5		
G. Loose open joints, heavily jointed or 'sugar cube', (any depth)	5.0		

Rock mass classification

Table 6: (cont'd.) Classification of individual parameters in the Tunnelling Quality Index Q (After Barton et al 1974).

DESCRIPTION	VALUE		NOTES
6. STRESS REDUCTION FACTOR			SRF
b. Competent rock, rock stress problems			
	σ_c/σ_1	σ_t/σ_1	
H. Low stress, near surface	> 200	> 13	2.5
J. Medium stress	200 - 10	13 - 0.66	1.0
K. High stress, very tight structure (usually favourable to stability, may be unfavourable to wall stability)	10 - 5	0.66 - 0.33	0.5 - 2
L. Mild rockburst (massive rock)	5 - 2.5	0.33 - 0.16	5 - 10
M. Heavy rockburst (massive rock)	< 2.5	< 0.16	10 - 20
c. Squeezing rock, plastic flow of incompetent rock under influence of high rock pressure			
N. Mild squeezing rock pressure			5 - 10
O. Heavy squeezing rock pressure			10 - 20
d. Swelling rock, chemical swelling activity depending on presence of water			
P. Mild swelling rock pressure			5 - 10
R. Heavy swelling rock pressure			10 - 15
ADDITIONAL NOTES ON THE USE OF THESE TABLES			
When making estimates of the rock mass Quality (Q), the following guidelines should be followed in addition to the notes listed in the tables:			
1. When borehole core is unavailable, RQD can be estimated from the number of joints per unit volume, in which the number of joints per metre for each joint set are added. A simple relationship can be used to convert this number to RQD for the case of clay free rock masses: $RQD = 115 - 3.3 J_v$ (approx.), where J_v = total number of joints per m^3 ($0 < RQD < 100$ for $35 > J_v > 4.5$).			
2. The parameter J_n representing the number of joint sets will often be affected by foliation, schistosity, slaty cleavage or bedding etc. If strongly developed, these parallel 'joints' should obviously be counted as a complete joint set. However, if there are few 'joints' visible, or if only occasional breaks in the core are due to these features, then it will be more appropriate to count them as 'random' joints when evaluating J_n .			
3. The parameters J_r and J_a (representing shear strength) should be relevant to the weakest significant joint set or clay filled discontinuity in the given zone. However, if the joint set or discontinuity with the minimum value of J_r/J_a is favourably oriented for stability, then a second, less favourably oriented joint set or discontinuity may sometimes be more significant, and its higher value of J_r/J_a should be used when evaluating Q . The value of J_r/J_a should in fact relate to the surface most likely to allow failure to initiate.			
4. When a rock mass contains clay, the factor SRF appropriate to loosening loads should be evaluated. In such cases the strength of the intact rock is of little interest. However, when jointing is minimal and clay is completely absent, the strength of the intact rock may become the weakest link, and the stability will then depend on the ratio rock-stress/rock-strength. A strongly anisotropic stress field is unfavourable for stability and is roughly accounted for as in note 2 in the table for stress reduction factor evaluation.			
5. The compressive and tensile strengths (σ_c and σ_t) of the intact rock should be evaluated in the saturated condition if this is appropriate to the present and future in situ conditions. A very conservative estimate of the strength should be made for those rocks that deteriorate when exposed to moist or saturated conditions.			

Rock mass classification

The crusher station discussed earlier falls into the category of permanent mine openings and is assigned an excavation support ratio $ESR = 1.6$. Hence, for an excavation span of 15 m, the equivalent dimension, $De = 15/1.6 = 9.4$.

The equivalent dimension, De , plotted against the value of Q , is used to define a number of support categories in a chart published in the original paper by Barton et al (1974). This chart has recently been updated by Grimstad and Barton (1993) to reflect the increasing use of steel fibre reinforced shotcrete in underground excavation support. Figure 3 is reproduced from this updated chart.

From Figure 3, a value of De of 9.4 and a value of Q of 4.5 places this crusher excavation in category (4) which requires a pattern of rockbolts (spaced at 2.3 m) and 40 to 50 mm of unreinforced shotcrete.

Because of the mild to heavy rock burst conditions which are anticipated, it may be prudent to destress the rock in the walls of this crusher chamber. This is achieved by using relatively heavy production blasting to excavate the chamber and omitting the smooth blasting usually used to trim the final walls of an excavation such as an underground powerhouse at shallower depth. Caution is recommended in the use of destress blasting and, for critical applications, it may be advisable to seek the advice of a blasting specialist before embarking on this course of action.

Løset (1992) suggests that, for rocks with $4 < Q < 30$, blasting damage will result in the creation of new 'joints' with a consequent local reduction in the value of Q for the rock surrounding the excavation. He suggests that this can be accounted for by reducing the RQD value for the blast damaged zone.

Assuming that the RQD value for the destressed rock around the crusher chamber drops to 50 %, the resulting value of $Q = 2.9$. From Figure 3, this value of Q , for an equivalent dimension, De of 9.4, places the excavation just inside category (5) which requires rockbolts, at approximately 2 m spacing, and a 50 mm thick layer of steel fibre reinforced shotcrete.

Barton et al (1980) provide additional information on rockbolt length, maximum unsupported spans and roof support pressures to supplement the support recommendations published in the original 1974 paper.

The length L of rockbolts can be estimated from the excavation width B and the Excavation Support Ratio ESR :

$$L = 2 + \frac{0.15B}{ESR} \quad (3)$$

The maximum unsupported span can be estimated from:

$$\text{Maximum span (unsupported)} = 2 ESR Q^{0.4} \quad (4)$$

Rock mass classification

Based upon analyses of case records, Grimstad and Barton (1993) suggest that the relationship between the value of Q and the permanent roof support pressure P_{roof} is estimated from:

$$P_{roof} = \frac{2\sqrt{J_n} Q^{\frac{1}{3}}}{3J_r} \quad (5)$$

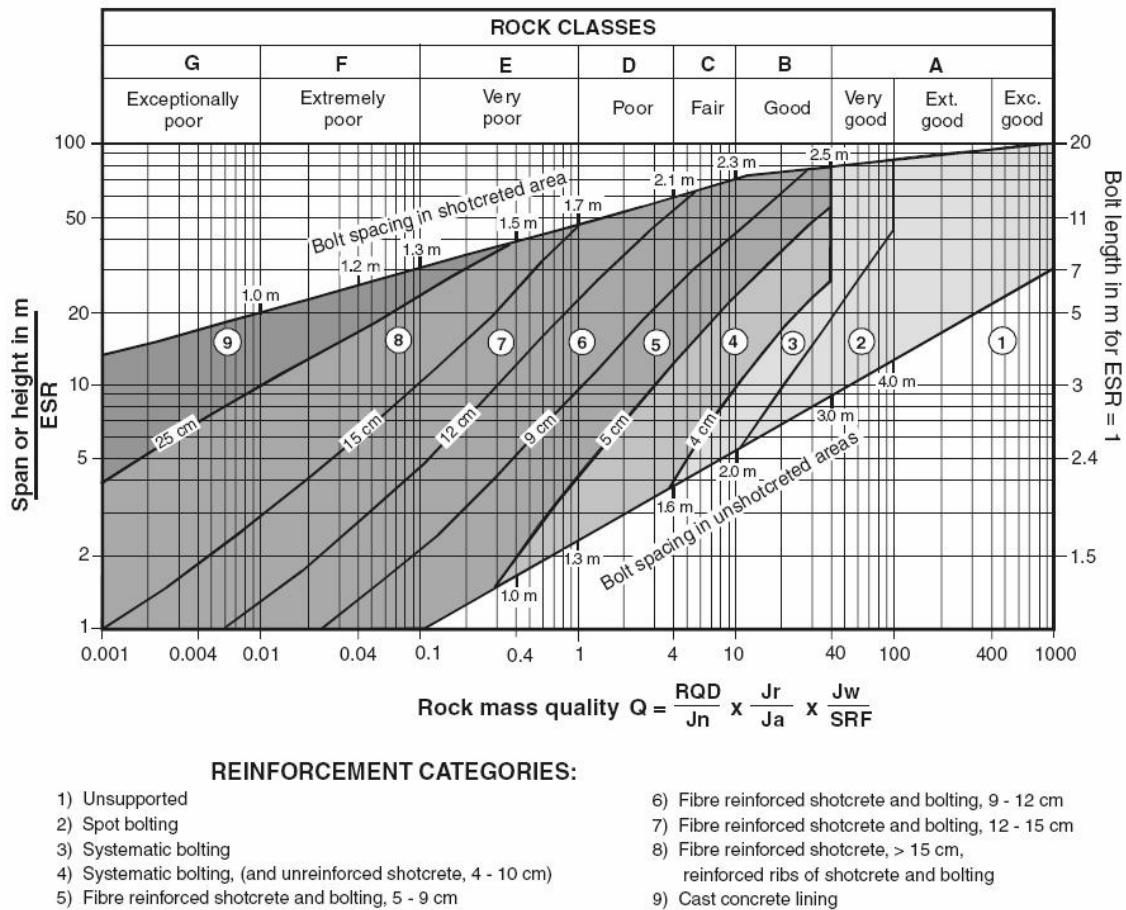


Figure 3: Estimated support categories based on the tunnelling quality index Q (After Grimstad and Barton, 1993, reproduced from Palmstrom and Broch, 2006).

Using rock mass classification systems

The two most widely used rock mass classifications are Bieniawski's RMR (1976, 1989) and Barton et al's Q (1974). Both methods incorporate geological, geometric and design/engineering parameters in arriving at a quantitative value of their rock mass quality. The similarities between RMR and Q stem from the use of identical, or very

Rock mass classification

similar, parameters in calculating the final rock mass quality rating. The differences between the systems lie in the different weightings given to similar parameters and in the use of distinct parameters in one or the other scheme.

RMR uses compressive strength directly while *Q* only considers strength as it relates to in situ stress in competent rock. Both schemes deal with the geology and geometry of the rock mass, but in slightly different ways. Both consider groundwater, and both include some component of rock material strength. Some estimate of orientation can be incorporated into *Q* using a guideline presented by Barton et al (1974): 'the parameters *Jr* and *Ja* should ... relate to the surface most likely to allow failure to initiate.' The greatest difference between the two systems is the lack of a stress parameter in the *RMR* system.

When using either of these methods, two approaches can be taken. One is to evaluate the rock mass specifically for the parameters included in the classification methods; the other is to accurately characterise the rock mass and then attribute parameter ratings at a later time. The latter method is recommended since it gives a full and complete description of the rock mass which can easily be translated into either classification index. If rating values alone had been recorded during mapping, it would be almost impossible to carry out verification studies.

In many cases, it is appropriate to give a range of values to each parameter in a rock mass classification and to evaluate the significance of the final result. An example of this approach is given in Figure 4 which is reproduced from field notes prepared by Dr. N. Barton on a project. In this particular case, the rock mass is dry and is subjected to 'medium' stress conditions (Table 6.6.K) and hence $J_w = 1.0$ and $SRF = 1.0$. Histograms showing the variations in *RQD*, *Jn*, *Jr* and *Ja*, along the exploration adit mapped, are presented in this figure. The average value of *Q* = 8.9 and the approximate range of *Q* is $1.7 < Q < 20$. The average value of *Q* can be used in choosing a basic support system while the range gives an indication of the possible adjustments which will be required to meet different conditions encountered during construction.

A further example of this approach is given in a paper by Barton et al (1992) concerned with the design of a 62 m span underground sports hall in jointed gneiss. Histograms of all the input parameters for the *Q* system are presented and analysed in order to determine the weighted average value of *Q*.

Carter (1992) has adopted a similar approach, but extended his analysis to include the derivation of a probability distribution function and the calculation of a probability of failure in a discussion on the stability of surface crown pillars in abandoned metal mines.

Throughout this chapter it has been suggested that the user of a rock mass classification scheme should check that the latest version is being used. It is also worth repeating that the use of two rock mass classification schemes side by side is advisable.

Rock mass classification

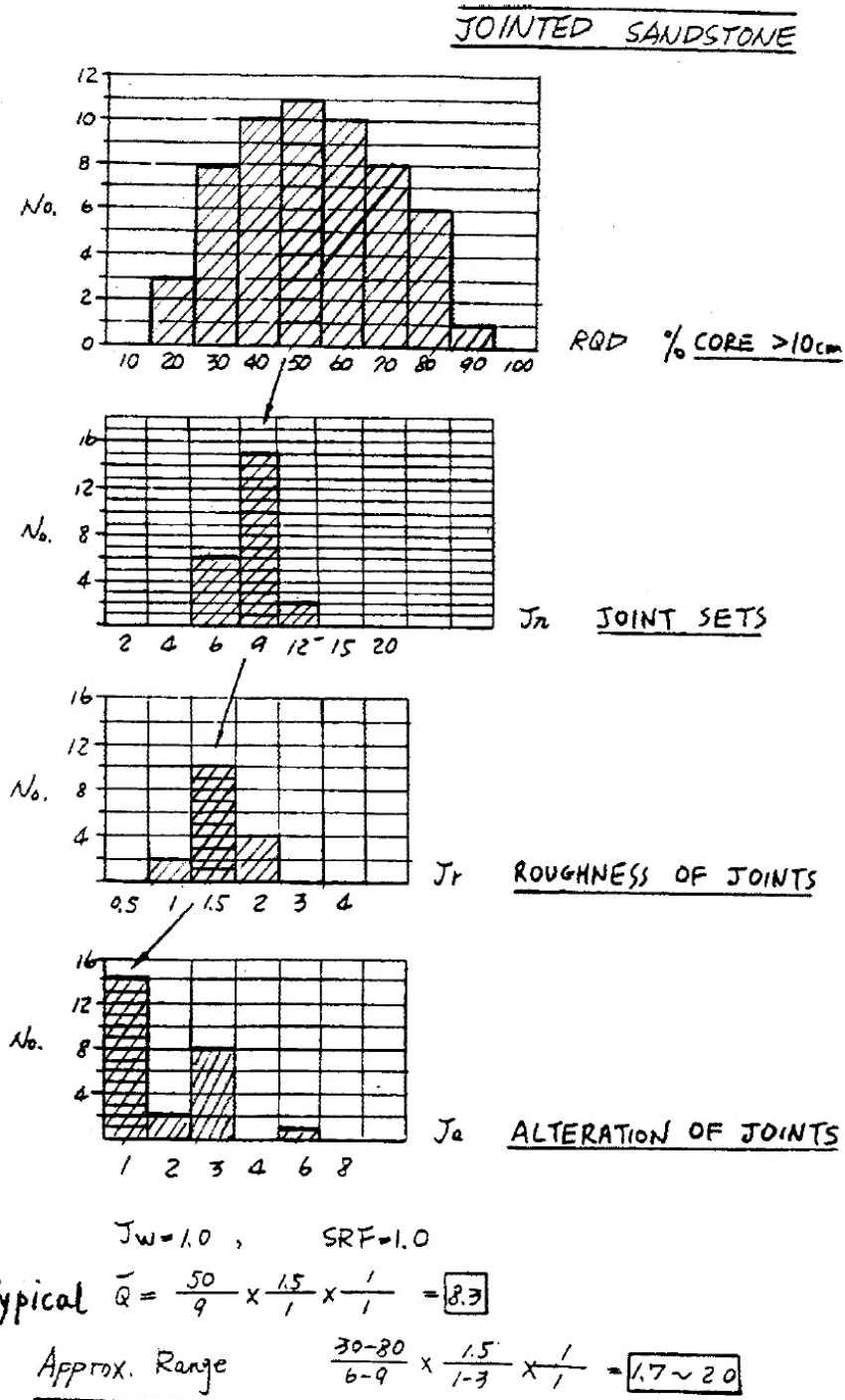


Figure 4: Histograms showing variations in RQD, J_n, J_r and J_a for a dry jointed sandstone under 'medium' stress conditions, reproduced from field notes prepared by Dr. N. Barton.

References

- Barton, N., By, T.L., Chryssanthakis, L., Tunbridge, L., Kristiansen, J., Løset, F., Bhasin, R.K., Westerdahl, H. and Vik, G. 1992. Comparison of prediction and performance for a 62 m span sports hall in jointed gneiss. *Proc. 4th. int. rock mechanics and rock engineering conf.*, Torino. Paper 17.
- Barton, N., Løset, F., Lien, R. and Lunde, J. 1980. Application of the Q-system in design decisions. In *Subsurface space*, (ed. M. Bergman) **2**, 553-561. New York: Pergamon.
- Barton, N.R., Lien, R. and Lunde, J. 1974. Engineering classification of rock masses for the design of tunnel support. *Rock Mech.* **6**(4), 189-239.
- Bieniawski, Z.T. 1973. Engineering classification of jointed rock masses. *Trans S. Afr. Inst. Civ. Engrs* **15**, 335-344.
- Bieniawski, Z.T. 1976. Rock mass classification in rock engineering. In *Exploration for rock engineering, proc. of the symp.*, (ed. Z.T. Bieniawski) **1**, 97-106. Cape Town: Balkema.
- Bieniawski, Z.T. 1989. *Engineering rock mass classifications*. New York: Wiley.
- Carter, T.G. 1992. A new approach to surface crown pillar design. *Proc. 16th. Canadian Rock Mechanics Symposium, Sudbury*, 75-83.
- Carter, T.G. 1992. Prediction and uncertainties in geological engineering and rock mass characterization assessments. *Proc. 4th. int. rock mechanics and rock engineering conf.*, Torino. Paper 1.
- Cording, E.J. and Deere, D.U. 1972. Rock tunnel supports and field measurements. *Proc. North American rapid excav. tunneling conf.*, Chicago, (eds. K.S. Lane and L.A. Garfield) **1**, 601-622. New York: Soc. Min. Engrs, Am. Inst. Min. Metall. Petrolm Engrs.
- Cummings, R.A., Kendorski, F.S. and Bieniawski, Z.T. 1982. *Caving rock mass classification and support estimation*. U.S. Bureau of Mines Contract Report #J0100103. Chicago: Engineers International Inc.
- Deere, D.U. 1989. *Rock quality designation (RQD) after 20 years*. U.S. Army Corps Engrs Contract Report GL-89-1. Vicksburg, MS: Waterways Experimental Station.
- Deere, D.U. and Deere, D.W. 1988. The rock quality designation (RQD) index in practice. In *Rock classification systems for engineering purposes*, (ed. L. Kirkaldie), ASTM Special Publication 984, 91-101. Philadelphia: Am. Soc. Test. Mat.
- Deere, D.U., Hendron, A.J., Patton, F.D. and Cording, E.J. 1967. Design of surface and near surface construction in rock. In *Failure and breakage of rock, proc. 8th U.S. symp. rock mech.*, (ed. C. Fairhurst), 237-302. New York: Soc. Min. Engrs, Am. Inst. Min. Metall. Petrolm Engrs.

Rock mass classification

- Grimstad, E. and Barton, N. 1993. Updating the Q-System for NMT. *Proc. int. symp. on sprayed concrete - modern use of wet mix sprayed concrete for underground support*, Fagernes. 46-66. Oslo: Norwegian Concrete Assn.
- Kendorski, F., Cummings, R., Bieniawski, Z.T. and Skinner, E. 1983. Rock mass classification for block caving mine drift support. *Proc. 5th Congr. Int. Soc. Rock Mech.*, Melbourne, B51-B63. Rotterdam: Balkema.
- Laubscher, D.H. 1977. Geomechanics classification of jointed rock masses - mining applications. *Trans. Instn Min. Metall.* **86**, A1-8.
- Laubscher, D.H. 1984. Design aspects and effectiveness of support systems in different mining conditions. *Trans Instn Min. Metall.* **93**, A70 - A82.
- Laubscher, D.H. and Taylor, H.W. 1976. The importance of geomechanics classification of jointed rock masses in mining operations. In *Exploration for rock engineering*, (ed. Z.T. Bieniawski) **1**, 119-128. Cape Town: Balkema.
- Laubscher, D.M. and Page, C.H. 1990. The design of rock support in high stress or weak rock environments. *Proc. 92nd Can. Inst. Min. Metall. AGM*, Ottawa, Paper # 91.
- Lauffer, H. 1958. Gebirgsklassifizierung für den Stollenbau. *Geol. Bauwesen* **24**(1), 46-51.
- Løset, F. 1992. Support needs compared at the Svartisen Road Tunnel. *Tunnels and Tunnelling*, June.
- Merritt, A.H. 1972. Geologic prediction for underground excavations. *Proc. North American rapid excav. tunneling conf.*, Chicago, (eds K.S. Lane and L.A. Garfield) **1**, 115-132. New York: Soc. Min. Engrs, Am. Inst. Min. Metall. Petrolm Engrs.
- Pacher, F., Rabcewicz, L. and Golser, J. 1974. Zum der seitigen Stand der Gebirgsklassifizierung in Stollen-und Tunnelbau. *Proc. XXII Geomech. colloq.*, Salzburg, 51-58.
- Palmström, A. 1982. The volumetric joint count - a useful and simple measure of the degree of rock jointing. *Proc. 4th Congr. Int. Assn Engng Geol.*, Delhi **5**, 221-228.
- Palmstrom, A. and Broch, E. 2006. Use and misuse of rock mass classification systems with particular reference to the Q-system. *Tunnels and Underground Space Technology*, **21**, 575-593.
- Ritter, W. 1879. *Die Statik der Tunnelgewölbe*. Berlin: Springer.
- Terzaghi, K. 1946. Rock defects and loads on tunnel supports. In *Rock tunneling with steel supports*, (eds R. V. Proctor and T. L. White) **1**, 17-99. Youngstown, OH: Commercial Shearing and Stamping Company.
- Wickham, G.E., Tiedemann, H.R. and Skinner, E.H. 1972. Support determination based on geologic predictions. In *Proc. North American rapid excav. tunneling conf.*, Chicago, (eds K.S. Lane and L.A. Garfield), 43-64. New York: Soc. Min. Engrs, Am. Inst. Min. Metall. Petrolm Engrs.

Rock mass properties

Introduction

Reliable estimates of the strength and deformation characteristics of rock masses are required for almost any form of analysis used for the design of slopes, foundations and underground excavations. Hoek and Brown (1980a, 1980b) proposed a method for obtaining estimates of the strength of jointed rock masses, based upon an assessment of the interlocking of rock blocks and the condition of the surfaces between these blocks. This method was modified over the years in order to meet the needs of users who were applying it to problems that were not considered when the original criterion was developed (Hoek 1983, Hoek and Brown 1988). The application of the method to very poor quality rock masses required further changes (Hoek, Wood and Shah 1992) and, eventually, the development of a new classification called the Geological Strength Index (Hoek, Kaiser and Bawden 1995, Hoek 1994, Hoek and Brown 1997, Hoek, Marinos and Benissi, 1998, Marinos and Hoek, 2001). A major revision was carried out in 2002 in order to smooth out the curves, necessary for the application of the criterion in numerical models, and to update the methods for estimating Mohr Coulomb parameters (Hoek, Carranza-Torres and Corkum, 2002). A related modification for estimating the deformation modulus of rock masses was made by Hoek and Diederichs (2006).

This chapter presents the most recent version of the Hoek-Brown criterion in a form that has been found practical in the field and that appears to provide the most reliable set of results for use as input for methods of analysis in current use in rock engineering.

Generalised Hoek-Brown criterion

The Generalised Hoek-Brown failure criterion for jointed rock masses is defined by:

$$\sigma_1' = \sigma_3' + \sigma_{ci} \left(m_b \frac{\sigma_3'}{\sigma_{ci}} + s \right)^a \quad (1)$$

where σ_1' and σ_3' are the maximum and minimum effective principal stresses at failure, m_b is the value of the Hoek-Brown constant m for the rock mass, s and a are constants which depend upon the rock mass characteristics, and σ_{ci} is the uniaxial compressive strength of the intact rock pieces.

Rock mass properties

Normal and shear stresses are related to principal stresses by the equations published by Balmer¹ (1952).

$$\sigma'_n = \frac{\sigma'_1 + \sigma'_3}{2} - \frac{\sigma'_1 - \sigma'_3}{2} \cdot \frac{d\sigma'_1/d\sigma'_3 - 1}{d\sigma'_1/d\sigma'_3 + 1} \quad (2)$$

$$\tau = (\sigma'_1 - \sigma'_3) \frac{\sqrt{d\sigma'_1/d\sigma'_3}}{d\sigma'_1/d\sigma'_3 + 1} \quad (3)$$

where

$$d\sigma'_1/d\sigma'_3 = 1 + am_b \left(m_b \sigma'_3 / \sigma_{ci} + s \right)^{a-1} \quad (4)$$

In order to use the Hoek-Brown criterion for estimating the strength and deformability of jointed rock masses, three ‘properties’ of the rock mass have to be estimated. These are:

- uniaxial compressive strength σ_{ci} of the intact rock pieces,
- value of the Hoek-Brown constant m_i for these intact rock pieces, and
- value of the Geological Strength Index GSI for the rock mass.

Intact rock properties

For the intact rock pieces that make up the rock mass, equation (1) simplifies to:

$$\sigma'_1 = \sigma'_3 + \sigma_{ci} \left(m_i \frac{\sigma'_3}{\sigma_{ci}} + 1 \right)^{0.5} \quad (5)$$

The relationship between the principal stresses at failure for a given rock is defined by two constants, the uniaxial compressive strength σ_{ci} and a constant m_i . Wherever possible the values of these constants should be determined by statistical analysis of the results of a set of triaxial tests on carefully prepared core samples.

Note that the range of minor principal stress (σ'_3) values over which these tests are carried out is critical in determining reliable values for the two constants. In deriving the original values of σ_{ci} and m_i , Hoek and Brown (1980a) used a range of $0 < \sigma'_3 < 0.5 \sigma_{ci}$ and, in order to be consistent, it is essential that the same range be used in any laboratory triaxial tests on intact rock specimens. At least five well spaced data points should be included in the analysis.

¹ The original equations derived by Balmer contained errors that have been corrected in equations 2 and 3.

One type of triaxial cell that can be used for these tests is illustrated in Figure 1. This cell, described by Franklin and Hoek (1970), does not require draining between tests and is convenient for the rapid testing on a large number of specimens. More sophisticated cells are available for research purposes but the results obtained from the cell illustrated in Figure 1 are adequate for the rock strength estimates required for estimating σ_{ci} and m_i . This cell has the additional advantage that it can be used in the field when testing materials such as coals or mudstones that are extremely difficult to preserve during transportation and normal specimen preparation for laboratory testing.

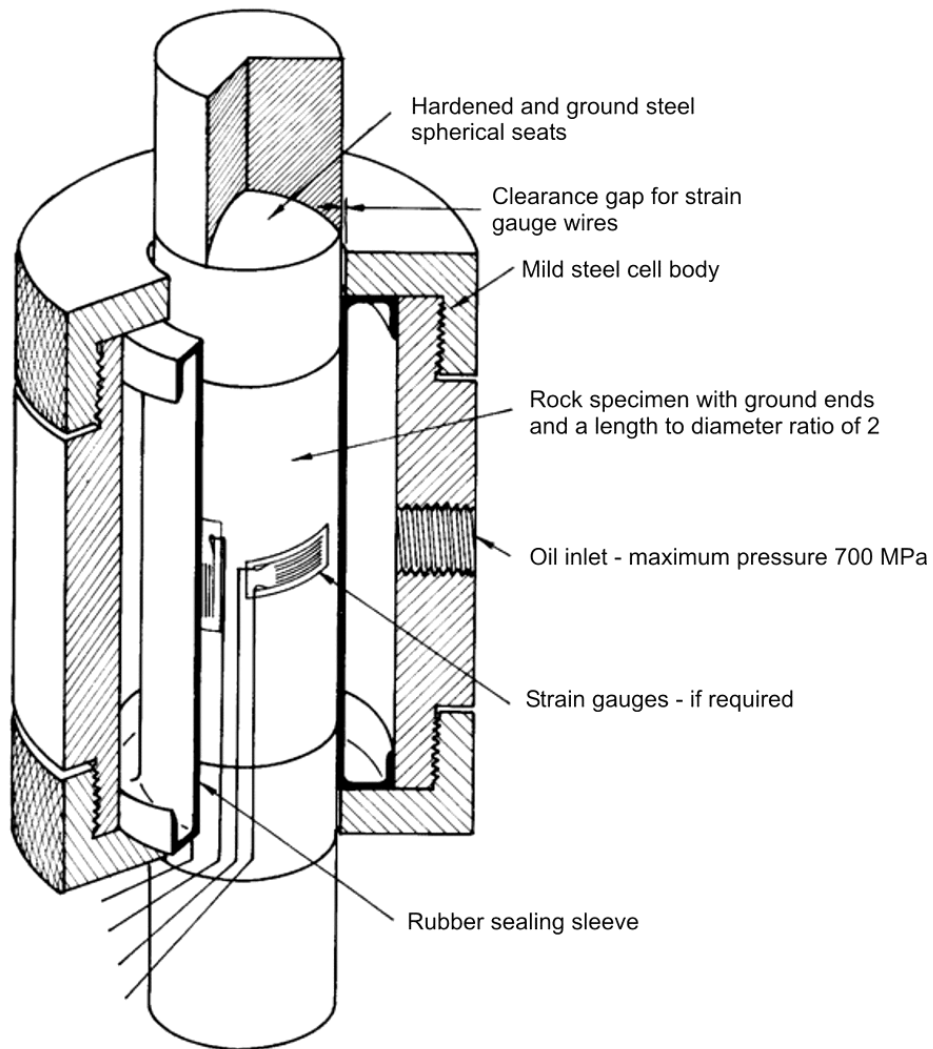


Figure 1: Cut-away view of a triaxial cell for testing rock specimens.

Rock mass properties

Laboratory tests should be carried out at moisture contents as close as possible to those which occur in the field. Many rocks show a significant strength decrease with increasing moisture content and tests on samples, which have been left to dry in a core shed for several months, can give a misleading impression of the intact rock strength.

Once the five or more triaxial test results have been obtained, they can be analysed to determine the uniaxial compressive strength σ_{ci} and the Hoek-Brown constant m_i as described by Hoek and Brown (1980a). In this analysis, equation (5) is re-written in the form:

$$y = m\sigma_{ci}x + s\sigma_{ci} \quad (6)$$

where $x = \sigma_3'$ and $y = (\sigma_1' - \sigma_3')^2$

For n specimens the uniaxial compressive strength σ_{ci} , the constant and m_i the coefficient of determination r^2 are calculated from:

$$\sigma_{ci}^2 = \frac{\sum y}{n} - \left[\frac{\sum xy - (\sum x \sum y/n)}{\sum x^2 - ((\sum x)^2/n)} \right] \frac{\sum x}{n} \quad (7)$$

$$m_i = \frac{1}{\sigma_{ci}} \left[\frac{\sum xy - (\sum x \sum y/n)}{\sum x^2 - ((\sum x)^2/n)} \right] \quad (8)$$

$$r^2 = \frac{[\sum xy - (\sum x \sum y/n)]^2}{[\sum x^2 - (\sum x)^2/n][\sum y^2 - (\sum y)^2/n]} \quad (9)$$

A spreadsheet for the analysis of triaxial test data is given in Table 1. Note that high quality triaxial test data will usually give a coefficient of determination r^2 of greater than 0.9. These calculations, together with many more related to the Hoek-Brown criterion can also be performed by the program RocLab that can be downloaded (free) from www.roscience.com.

When laboratory tests are not possible, Table 2 and Table 3 can be used to obtain estimates of σ_{ci} and m_i .

Rock mass properties

Table 1: Spreadsheet for the calculation of σ_{ci} and m_i from triaxial test data

Triaxial test data

x	y	xy	xsq	ysq
sig3	sig1			
0	38.3	1466.89	0.0	2151766
5	72.4	4542.76	25.0	20636668
7.5	80.5	5329.00	56.3	28398241
15	115.6	10120.36	225.0	102421687
20	134.3	13064.49	400.0	170680899
47.5	441.1	34523.50	706.3	324289261
sumx	sumy	sumxy	sumxsq	sumysq

Calculation results

Number of tests	n =	5
Uniaxial strength	sigci =	37.4
Hoek-Brown constant	mi =	15.50
Hoek-Brown constant	s =	1.00
Coefficient of determination	r2 =	0.997

Cell formulae

$$y = (\text{sig1} - \text{sig3})^2$$

$$\text{sigci} = \text{SQRT}(\text{sumy}/n - (\text{sumxy} - \text{sumx} * \text{sumy}/n) / (\text{sumxsq} - (\text{sumx}^2)/n) * \text{sumx}/n)$$

$$mi = (1/\text{sigci}) * ((\text{sumxy} - \text{sumx} * \text{sumy}/n) / (\text{sumxsq} - (\text{sumx}^2)/n))$$

$$r2 = ((\text{sumxy} - (\text{sumx} * \text{sumy}/n))^2) / ((\text{sumxsq} - (\text{sumx}^2)/n) * (\text{sumysq} - (\text{sumy}^2)/n))$$

Note: These calculations, together with many other calculations related to the Hoek-Brown criterion, can also be carried out using the program RocLab that can be downloaded (free) from www.rocscience.com.

Rock mass properties

Table 2: Field estimates of uniaxial compressive strength.

Grade*	Term	Uniaxial Comp. Strength (MPa)	Point Load Index (MPa)	Field estimate of strength	Examples
R6	Extremely Strong	> 250	>10	Specimen can only be chipped with a geological hammer	Fresh basalt, chert, diabase, gneiss, granite, quartzite
R5	Very strong	100 - 250	4 - 10	Specimen requires many blows of a geological hammer to fracture it	Amphibolite, sandstone, basalt, gabbro, gneiss, granodiorite, limestone, marble, rhyolite, tuff
R4	Strong	50 - 100	2 - 4	Specimen requires more than one blow of a geological hammer to fracture it	Limestone, marble, phyllite, sandstone, schist, shale
R3	Medium strong	25 - 50	1 - 2	Cannot be scraped or peeled with a pocket knife, specimen can be fractured with a single blow from a geological hammer	Claystone, coal, concrete, schist, shale, siltstone
R2	Weak	5 - 25	**	Can be peeled with a pocket knife with difficulty, shallow indentation made by firm blow with point of a geological hammer	Chalk, rocksalt, potash
R1	Very weak	1 - 5	**	Crumbles under firm blows with point of a geological hammer, can be peeled by a pocket knife	Highly weathered or altered rock
R0	Extremely weak	0.25 - 1	**	Indented by thumbnail	Stiff fault gouge

* Grade according to Brown (1981).

** Point load tests on rocks with a uniaxial compressive strength below 25 MPa are likely to yield highly ambiguous results.

Rock mass properties

Table 3: Values of the constant m_i for intact rock, by rock group. Note that values in parenthesis are estimates.

Rock type	Class	Group	Texture			
			Coarse	Medium	Fine	Very fine
SEDIMENTARY	Clastic		Conglomerates* (21 ± 3)	Sandstones 17 ± 4	Siltstones 7 ± 2	Claystones 4 ± 2
			Breccias (19 ± 5)		Greywackes (18 ± 3)	Shales (6 ± 2) Marls (7 ± 2)
	Non-Clastic	Carbonates	Crystalline Limestone (12 ± 3)	Sparitic Limestones (10 ± 2)	Micritic Limestones (9 ± 2)	Dolomites (9 ± 3)
		Evaporites		Gypsum 8 ± 2	Anhydrite 12 ± 2	
	Organic				Chalk 7 ± 2	
METAMORPHIC	Non Foliated		Marble 9 ± 3	Hornfels (19 ± 4) Metasandstone (19 ± 3)	Quartzites 20 ± 3	
	Slightly foliated		Migmatite (29 ± 3)	Amphibolites 26 ± 6		
	Foliated**		Gneiss 28 ± 5	Schists 12 ± 3	Phyllites (7 ± 3)	Slates 7 ± 4
IGNEOUS	Plutonic	Light	Granite 32 ± 3	Diorite 25 ± 5		
			Granodiorite (29 ± 3)			
	Dark	Gabbro 27 ± 3	Dolerite (16 ± 5)			
		Norite 20 ± 5				
	Hypabyssal		Porphyries (20 ± 5)		Diabase (15 ± 5)	Peridotite (25 ± 5)
Volcanic	Lava		Rhyolite (25 ± 5)	Dacite (25 ± 3)	Obsidian (19 ± 3)	
			Andesite 25 ± 5	Basalt (25 ± 5)		
	Pyroclastic	Agglomerate (19 ± 3)	Breccia (19 ± 5)	Tuff (13 ± 5)		

* Conglomerates and breccias may present a wide range of m_i values depending on the nature of the cementing material and the degree of cementation, so they may range from values similar to sandstone to values used for fine grained sediments.

** These values are for intact rock specimens tested normal to bedding or foliation. The value of m_i will be significantly different if failure occurs along a weakness plane.

Anisotropic and foliated rocks such as slates, schists and phyllites, the behaviour of which is dominated by closely spaced planes of weakness, cleavage or schistosity, present particular difficulties in the determination of the uniaxial compressive strengths.

Salcedo (1983) has published the results of a set of directional uniaxial compressive tests on a graphitic phyllite from Venezuela. These results are summarised in Figure 2. It will be noted that the uniaxial compressive strength of this material varies by a factor of about 5, depending upon the direction of loading.

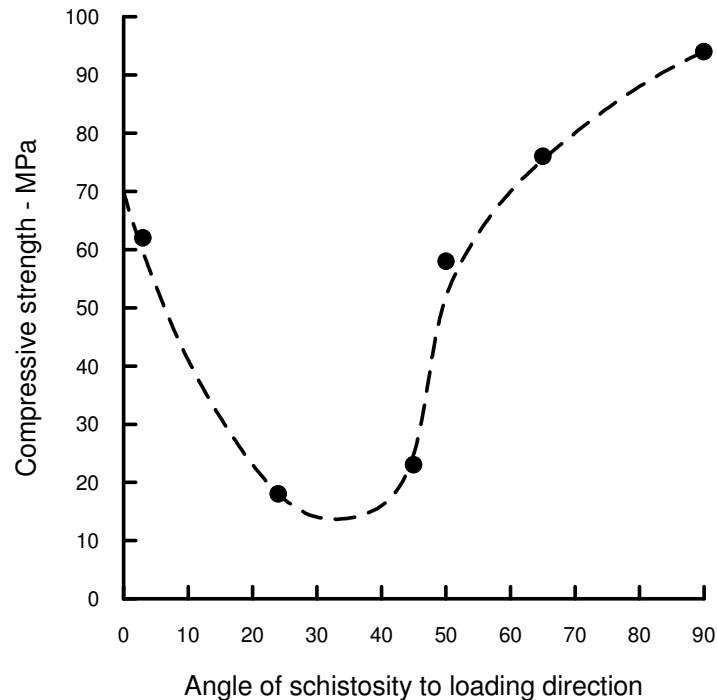


Figure 2: Influence of loading direction on the strength of graphitic phyllite tested by Salcedo (1983).

In deciding upon the value of σ_{ci} for foliated rocks, a decision has to be made on whether to use the highest or the lowest uniaxial compressive strength obtained from results such as those given in Figure 2. Mineral composition, grain size, grade of metamorphism and tectonic history all play a role in determining the characteristics of the rock mass. The author cannot offer any precise guidance on the choice of σ_{ci} but some insight into the role of schistosity in rock masses can be obtained by considering the case of the Yacambú-Quibor tunnel in Venezuela.

This tunnel has been excavated in graphitic phyllite, similar to that tested by Salcedo, at depths of up to 1200 m through the Andes mountains. The appearance of the rock mass at

the tunnel face is shown in Figure 3 and a back analysis of the behaviour of this material suggests that an appropriate value for σ_{ci} is approximately 50 MPa. In other words, on the scale of the 5.5 m diameter tunnel, the rock mass properties are “averaged” and there is no sign of anisotropic behaviour in the deformations measured in the tunnel.



Figure 3: Tectonically deformed and sheared graphitic phyllite in the face of the Yacambú-Quibor tunnel at a depth of 1200 m below surface.

Influence of sample size

The influence of sample size upon rock strength has been widely discussed in geotechnical literature and it is generally assumed that there is a significant reduction in strength with increasing sample size. Based upon an analysis of published data, Hoek and Brown (1980a) have suggested that the uniaxial compressive strength σ_{cd} of a rock specimen with a diameter of d mm is related to the uniaxial compressive strength σ_{c50} of a 50 mm diameter sample by the following relationship:

$$\sigma_{cd} = \sigma_{c50} \left(\frac{50}{d} \right)^{0.18} \quad (10)$$

This relationship, together with the data upon which it was based, is shown in Figure 4.

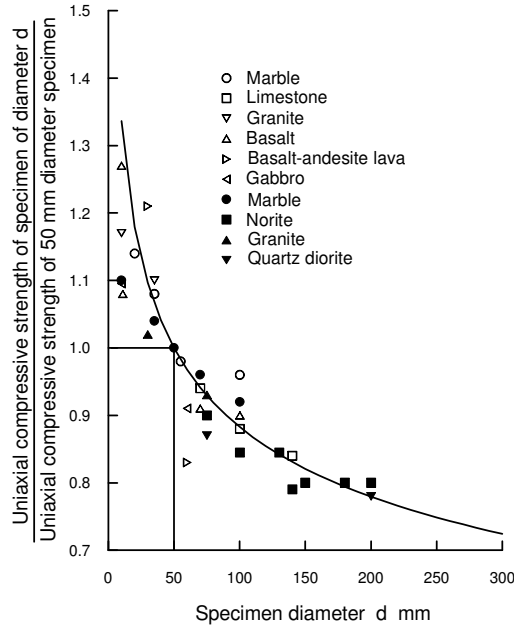


Figure 4: Influence of specimen size on the strength of intact rock. After Hoek and Brown (1980a).

It is suggested that the reduction in strength is due to the greater opportunity for failure through and around grains, the ‘building blocks’ of the intact rock, as more and more of these grains are included in the test sample. Eventually, when a sufficiently large number of grains are included in the sample, the strength reaches a constant value.

The Hoek-Brown failure criterion, which assumes isotropic rock and rock mass behaviour, should only be applied to those rock masses in which there are a sufficient number of closely spaced discontinuities, with similar surface characteristics, that isotropic behaviour involving failure on discontinuities can be assumed. When the structure being analysed is large and the block size small in comparison, the rock mass can be treated as a Hoek-Brown material.

Where the block size is of the same order as that of the structure being analysed or when one of the discontinuity sets is significantly weaker than the others, the Hoek-Brown criterion should not be used. In these cases, the stability of the structure should be analysed by considering failure mechanisms involving the sliding or rotation of blocks and wedges defined by intersecting structural features.

It is reasonable to extend this argument further and to suggest that, when dealing with large scale rock masses, the strength will reach a constant value when the size of individual rock pieces is sufficiently small in relation to the overall size of the structure being considered. This suggestion is embodied in Figure 5 which shows the transition

Rock mass properties

from an isotropic intact rock specimen, through a highly anisotropic rock mass in which failure is controlled by one or two discontinuities, to an isotropic heavily jointed rock mass.

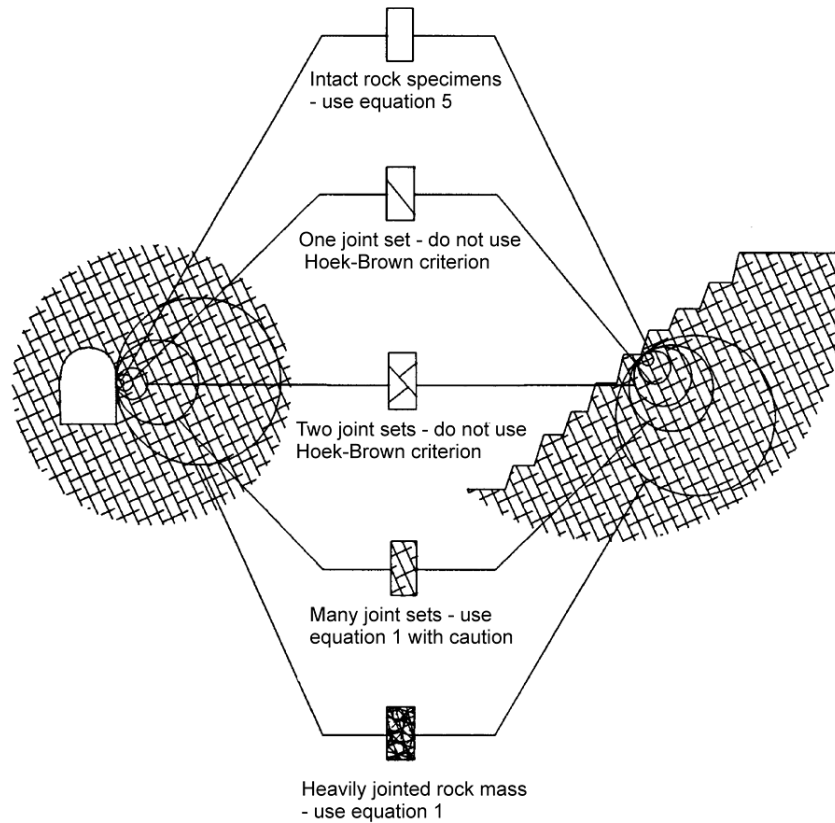


Figure 5: Idealised diagram showing the transition from intact to a heavily jointed rock mass with increasing sample size.

Geological strength Index

The strength of a jointed rock mass depends on the properties of the intact rock pieces and also upon the freedom of these pieces to slide and rotate under different stress conditions. This freedom is controlled by the geometrical shape of the intact rock pieces as well as the condition of the surfaces separating the pieces. Angular rock pieces with clean, rough discontinuity surfaces will result in a much stronger rock mass than one which contains rounded particles surrounded by weathered and altered material.

The Geological Strength Index (GSI), introduced by Hoek (1994) and Hoek, Kaiser and Bawden (1995) provides a number which, when combined with the intact rock properties, can be used for estimating the reduction in rock mass strength for different geological

Rock mass properties

conditions. This system is presented in Table 5, for blocky rock masses, and Table 6 for heterogeneous rock masses such as flysch. Table 6 has also been extended to deal with molassic rocks (Hoek et al 2006) and ophiolites (Marinos et al, 2005).

Before the introduction of the GSI system in 1994, the application of the Hoek-Brown criterion in the field was based on a correlation with the 1976 version of Bieniawski's Rock Mass Rating, with the Groundwater rating set to 10 (dry) and the Adjustment for Joint Orientation set to 0 (very favourable) (Bieniawski, 1976). If the 1989 version of Bieniawski's RMR classification (Bieniawski, 1989) is used, then the Groundwater rating set to 15 and the Adjustment for Joint Orientation set to zero.

During the early years of the application of the GSI system the value of GSI was estimated directly from RMR. However, this correlation has proved to be unreliable, particularly for poor quality rock masses and for rocks with lithological peculiarities that cannot be accommodated in the RMR classification. Consequently, it is recommended that GSI should be estimated directly by means of the charts presented in Tables 5 and 6 and not from the RMR classification.

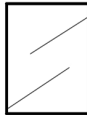





Experience shows that most geologists and engineering geologists are comfortable with the descriptive and largely qualitative nature of the GSI tables and generally have little difficulty in arriving at an estimated value. On the other hand, many engineers feel the need for a more quantitative system in which they can "measure" some physical dimension. Conversely, these engineers have little difficulty understanding the importance of the intact rock strength σ_{ci} and its incorporation in the assessment of the rock mass properties. Many geologists tend to confuse intact and rock mass strength and consistently underestimate the intact strength.

An additional practical question is whether borehole cores can be used to estimate the GSI value behind the visible faces? Borehole cores are the best source of data at depth but it has to be recognized that it is necessary to extrapolate the one dimensional information provided by core to the three-dimensional rock mass. However, this is a common problem in borehole investigation and most experienced engineering geologists are comfortable with this extrapolation process. Multiple boreholes and inclined boreholes are of great help the interpretation of rock mass characteristics at depth.

The most important decision to be made in using the GSI system is whether or not it should be used. If the discontinuity spacing is large compared with the dimensions of the tunnel or slope under consideration then, as shown in Figure 5, the GSI tables and the Hoek-Brown criterion should not be used and the discontinuities should be treated individually. Where the discontinuity spacing is small compared with the size of the structure (Figure 5) then the GSI tables can be used with confidence.

Rock mass properties

Table 5: Characterisation of blocky rock masses on the basis of interlocking and joint conditions.

<p>GEOLOGICAL STRENGTH INDEX FOR JOINTED ROCKS (Hoek and Marinos, 2000)</p> <p>From the lithology, structure and surface conditions of the discontinuities, estimate the average value of GSI. Do not try to be too precise. Quoting a range from 33 to 37 is more realistic than stating that GSI = 35. Note that the table does not apply to structurally controlled failures. Where weak planar structural planes are present in an unfavourable orientation with respect to the excavation face, these will dominate the rock mass behaviour. The shear strength of surfaces in rocks that are prone to deterioration as a result of changes in moisture content will be reduced is water is present. When working with rocks in the fair to very poor categories, a shift to the right may be made for wet conditions. Water pressure is dealt with by effective stress analysis.</p>		<p>SURFACE CONDITIONS</p> <p>VERY GOOD Very rough, fresh unweathered surfaces</p> <p>GOOD Rough, slightly weathered, iron stained surfaces</p> <p>FAIR Smooth, moderately weathered and altered surfaces</p> <p>POOR Slickensided, highly weathered surfaces with compact coatings or fillings or angular fragments</p> <p>VERY POOR Slickensided, highly weathered surfaces with soft clay coatings or fillings</p> <p>DECREASING SURFACE QUALITY →</p>				
<p>STRUCTURE</p>						
 <p>INTACT OR MASSIVE - intact rock specimens or massive in situ rock with few widely spaced discontinuities</p>	90	80	70	60	N/A	
 <p>BLOCKY - well interlocked undisturbed rock mass consisting of cubical blocks formed by three intersecting discontinuity sets</p>	80	70	60	50	40	
 <p>VERY BLOCKY- interlocked, partially disturbed mass with multi-faceted angular blocks formed by 4 or more joint sets</p>	70	60	50	40	30	
 <p>BLOCKY/DISTURBED/SEAMY - folded with angular blocks formed by many intersecting discontinuity sets. Persistence of bedding planes or schistosity</p>	60	50	40	30	20	
 <p>DISINTEGRATED - poorly interlocked, heavily broken rock mass with mixture of angular and rounded rock pieces</p>	50	40	30	20	10	
 <p>LAMINATED/SHEARED - Lack of blockiness due to close spacing of weak schistosity or shear planes</p>	N/A	N/A	N/A	N/A	N/A	

Rock mass properties

One of the practical problems that arises when assessing the value of GSI in the field is related to blast damage. As illustrated in Figure 6, there is a considerable difference in the appearance of a rock face which has been excavated by controlled blasting and a face which has been damaged by bulk blasting. Wherever possible, the undamaged face should be used to estimate the value of GSI since the overall aim is to determine the properties of the undisturbed rock mass.



Figure 6: Comparison between the results achieved using controlled blasting (on the left) and normal bulk blasting for a surface excavation in gneiss.

The influence of blast damage on the near surface rock mass properties has been taken into account in the 2002 version of the Hoek-Brown criterion (Hoek, Carranza-Torres and Corkum, 2002) as follows:

$$m_b = m_i \exp\left(\frac{GSI - 100}{28 - 14D}\right) \quad (11)$$

Rock mass properties

$$s = \exp\left(\frac{GSI-100}{9-3D}\right) \quad (12)$$

and

$$a = \frac{1}{2} + \frac{1}{6} \left(e^{-GSI/15} - e^{-20/3} \right) \quad (13)$$

D is a factor which depends upon the degree of disturbance due to blast damage and stress relaxation. It varies from 0 for undisturbed in situ rock masses to 1 for very disturbed rock masses. Guidelines for the selection of D are presented in Table 7.

Note that the factor D applies only to the blast damaged zone and it should not be applied to the entire rock mass. For example, in tunnels the blast damage is generally limited to a 1 to 2 m thick zone around the tunnel and this should be incorporated into numerical models as a different and weaker material than the surrounding rock mass. Applying the blast damage factor D to the entire rock mass is inappropriate and can result in misleading and unnecessarily pessimistic results.

The uniaxial compressive strength of the rock mass is obtained by setting $\sigma_3' = 0$ in equation 1, giving:

$$\sigma_c = \sigma_{ci} \cdot s^a \quad (14)$$

and, the tensile strength of the rock mass is:






$$\sigma_t = -\frac{s\sigma_{ci}}{m_b} \quad (15)$$

Equation 15 is obtained by setting $\sigma_1' = \sigma_3' = \sigma_t$ in equation 1. This represents a condition of biaxial tension. Hoek (1983) showed that, for brittle materials, the uniaxial tensile strength is equal to the biaxial tensile strength.

Note that the “switch” at GSI = 25 for the coefficients s and a (Hoek and Brown, 1997) has been eliminated in equations 11 and 12 which give smooth continuous transitions for the entire range of GSI values. The numerical values of s and a , given by these equations, are very close to those given by the previous equations and it is not necessary for readers to revisit and make corrections to old calculations.

Rock mass properties

Table 7: Guidelines for estimating disturbance factor D

Appearance of rock mass	Description of rock mass	Suggested value of D
	Excellent quality controlled blasting or excavation by Tunnel Boring Machine results in minimal disturbance to the confined rock mass surrounding a tunnel.	D = 0
	Mechanical or hand excavation in poor quality rock masses (no blasting) results in minimal disturbance to the surrounding rock mass. Where squeezing problems result in significant floor heave, disturbance can be severe unless a temporary invert, as shown in the photograph, is placed.	D = 0 D = 0.5 No invert
	Very poor quality blasting in a hard rock tunnel results in severe local damage, extending 2 or 3 m, in the surrounding rock mass.	D = 0.8
	Small scale blasting in civil engineering slopes results in modest rock mass damage, particularly if controlled blasting is used as shown on the left hand side of the photograph. However, stress relief results in some disturbance.	D = 0.7 Good blasting D = 1.0 Poor blasting
	Very large open pit mine slopes suffer significant disturbance due to heavy production blasting and also due to stress relief from overburden removal. In some softer rocks excavation can be carried out by ripping and dozing and the degree of damage to the slopes is less.	D = 1.0 Production blasting D = 0.7 Mechanical excavation

Mohr-Coulomb parameters

Since many geotechnical software programs are written in terms of the Mohr-Coulomb failure criterion, it is sometimes necessary to determine equivalent angles of friction and cohesive strengths for each rock mass and stress range. This is done by fitting an average linear relationship to the curve generated by solving equation 1 for a range of minor principal stress values defined by $\sigma_1 < \sigma_3 < \sigma_{3max}$, as illustrated in Figure 7. The fitting process involves balancing the areas above and below the Mohr-Coulomb plot. This results in the following equations for the angle of friction ϕ' and cohesive strength c' :

$$\phi' = \sin^{-1} \left[\frac{6am_b (s + m_b \sigma'_{3n})^{a-1}}{2(1+a)(2+a) + 6am_b (s + m_b \sigma'_{3n})^{a-1}} \right] \quad (16)$$

$$c' = \frac{\sigma_{ci} \left[(1+2a)s + (1-a)m_b \sigma'_{3n} \right] (s + m_b \sigma'_{3n})^{a-1}}{(1+a)(2+a) \sqrt{1 + \left(6am_b (s + m_b \sigma'_{3n})^{a-1} \right) / ((1+a)(2+a))}} \quad (17)$$

where $\sigma_{3n} = \sigma'_{3max} / \sigma_{ci}$

Note that the value of σ'_{3max} , the upper limit of confining stress over which the relationship between the Hoek-Brown and the Mohr-Coulomb criteria is considered, has to be determined for each individual case. Guidelines for selecting these values for slopes as well as shallow and deep tunnels are presented later.

The Mohr-Coulomb shear strength τ , for a given normal stress σ , is found by substitution of these values of c' and ϕ' in to the equation:

$$\tau = c' + \sigma \tan \phi' \quad (18)$$

The equivalent plot, in terms of the major and minor principal stresses, is defined by:

$$\sigma'_1 = \frac{2c' \cos \phi'}{1 - \sin \phi'} + \frac{1 + \sin \phi'}{1 - \sin \phi'} \sigma'_3 \quad (19)$$

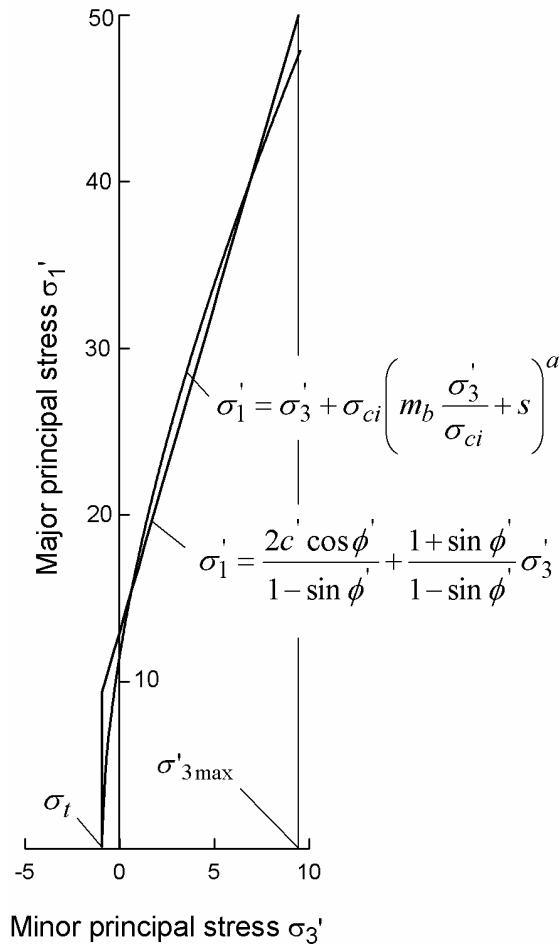


Figure 7: Relationships between major and minor principal stresses for Hoek-Brown and equivalent Mohr-Coulomb criteria.

Rock mass strength

The uniaxial compressive strength of the rock mass σ_c is given by equation 14. Failure initiates at the boundary of an excavation when σ_c is exceeded by the stress induced on that boundary. The failure propagates from this initiation point into a biaxial stress field and it eventually stabilizes when the local strength, defined by equation 1, is higher than the induced stresses σ_1' and σ_3' . Most numerical models can follow this process of fracture propagation and this level of detailed analysis is very important when considering the stability of excavations in rock and when designing support systems.

However, there are times when it is useful to consider the overall behaviour of a rock mass rather than the detailed failure propagation process described above. For example, when considering the strength of a pillar, it is useful to have an estimate of the overall strength of the pillar rather than a detailed knowledge of the extent of fracture propagation in the pillar. This leads to the concept of a global “rock mass strength” and Hoek and Brown (1997) proposed that this could be estimated from the Mohr-Coulomb relationship:

$$\sigma'_{cm} = \frac{2c' \cos \phi'}{1 - \sin \phi'} \quad (20)$$

with c' and ϕ' determined for the stress range $\sigma_t < \sigma'_3 < \sigma_{ci} / 4$ giving

$$\sigma'_{cm} = \sigma_{ci} \cdot \frac{(m_b + 4s - a(m_b - 8s))(m_b/4 + s)^{a-1}}{2(1+a)(2+a)} \quad (21)$$

Determination of $\sigma'_{3\max}$

The issue of determining the appropriate value of $\sigma'_{3\max}$ for use in equations 16 and 17 depends upon the specific application. Two cases will be investigated:

Tunnels – where the value of $\sigma'_{3\max}$ is that which gives equivalent characteristic curves for the two failure criteria for deep tunnels or equivalent subsidence profiles for shallow tunnels.

Slopes – here the calculated factor of safety and the shape and location of the failure surface have to be equivalent.

For the case of deep tunnels, closed form solutions for both the Generalized Hoek-Brown and the Mohr-Coulomb criteria have been used to generate hundreds of solutions and to find the value of $\sigma'_{3\max}$ that gives equivalent characteristic curves.

For shallow tunnels, where the depth below surface is less than 3 tunnel diameters, comparative numerical studies of the extent of failure and the magnitude of surface subsidence gave an identical relationship to that obtained for deep tunnels, provided that caving to surface is avoided.

The results of the studies for deep tunnels are plotted in Figure 8 and the fitted equation for both deep and shallow tunnels is:

Rock mass properties

$$\frac{\sigma'_{3\max}}{\sigma'_{cm}} = 0.47 \left(\frac{\sigma'_{cm}}{\gamma H} \right)^{-0.94} \quad (22)$$

where σ'_{cm} is the rock mass strength, defined by equation 21, γ is the unit weight of the rock mass and H is the depth of the tunnel below surface. In cases where the horizontal stress is higher than the vertical stress, the horizontal stress value should be used in place of γH .

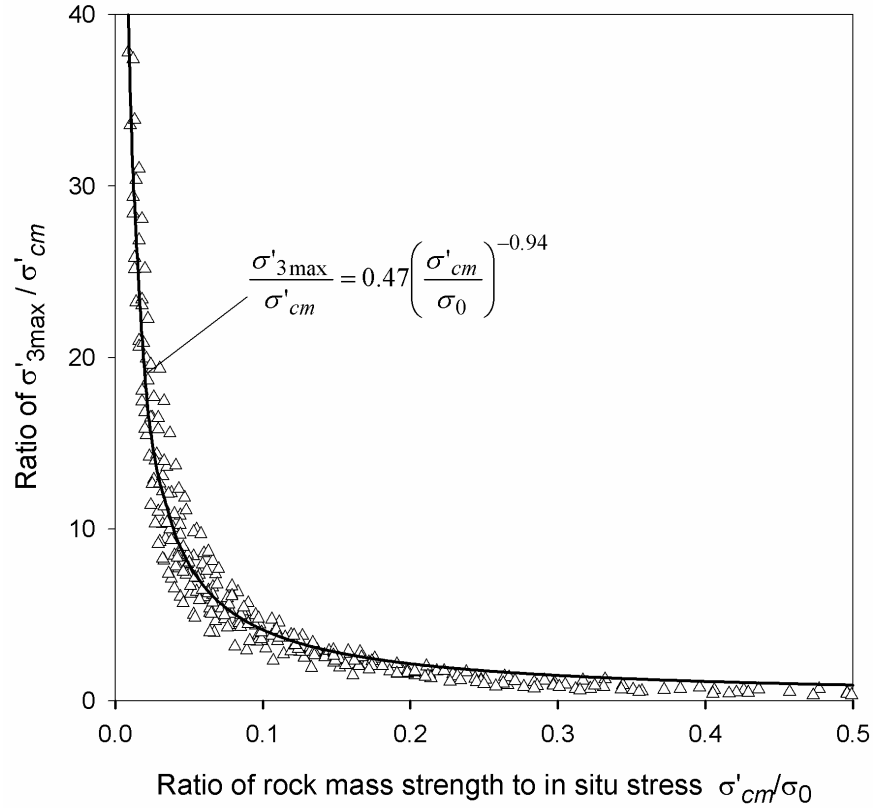


Figure 8: Relationship for the calculation of $\sigma'_{3\max}$ for equivalent Mohr-Coulomb and Hoek-Brown parameters for tunnels.

Equation 22 applies to all underground excavations, which are surrounded by a zone of failure that does not extend to surface. For studies of problems such as block caving in mines it is recommended that no attempt should be made to relate the Hoek-Brown and Mohr-Coulomb parameters and that the determination of material properties and subsequent analysis should be based on only one of these criteria.

Similar studies for slopes, using Bishop's circular failure analysis for a wide range of slope geometries and rock mass properties, gave:

$$\frac{\sigma'_{3\max}}{\sigma'_{cm}} = 0.72 \left(\frac{\sigma'_{cm}}{\gamma H} \right)^{-0.91} \quad (23)$$

where H is the height of the slope.

Deformation modulus

Hoek and Diederichs (2005) re-examined existing empirical methods for estimating rock mass deformation modulus and concluded that none of these methods provided reliable estimates over the whole range of rock mass conditions encountered. In particular, large errors were found for very poor rock masses and, at the other end of the spectrum, for massive strong rock masses. Fortunately, a new set of reliable measured data from China and Taiwan was available for analyses and it was found that the equation which gave the best fit to this data is a sigmoid function having the form:

$$y = c + \frac{a}{1 + e^{-((x-x_0)/b)}} \quad (24)$$

Using commercial curve fitting software, Equation 24 was fitted to the Chinese and Taiwanese data and the constants a and b in the fitted equation were then replaced by expressions incorporating GSI and the disturbance factor D . These were adjusted to give the equivalent average curve and the upper and lower bounds into which > 90% of the data points fitted. Note that the constant $a = 100\,000$ in Equation 25 is a scaling factor and it is not directly related to the physical properties of the rock mass.

The following best-fit equation was derived:

$$E_{rm} (MPa) = 100\,000 \left(\frac{1 - D/2}{1 + e^{((75+25D-GSI)/11)}} \right) \quad (25)$$

The rock mass deformation modulus data from China and Taiwan includes information on the geology as well as the uniaxial compressive strength (σ_{ci}) of the intact rock. This information permits a more detailed analysis in which the ratio of mass to intact modulus (E_{rm}/E_i) can be included. Using the modulus ratio MR proposed by Deere (1968) (modified by the authors based in part on this data set and also on additional correlations from Palmstrom and Singh (2001)) it is possible to estimate the intact modulus from:

Rock mass properties

$$E_i = MR \cdot \sigma_{ci} \quad (26)$$

This relationship is useful when no direct values of the intact modulus (E_i) are available or where completely undisturbed sampling for measurement of E_i is difficult. A detailed analysis of the Chinese and Taiwanese data, using Equation (26) to estimate E_i resulted in the following equation:

$$E_{rm} = E_i \left(0.02 + \frac{1 - D/2}{1 + e^{((60 + 15D - GSI)/11)}} \right) \quad (27)$$

This equation incorporates a finite value for the parameter c (Equation 24) to account for the modulus of broken rock (transported rock, aggregate or soil) described by $GSI = 0$. This equation is plotted against the average normalized field data from China and Taiwan in Figure 9.

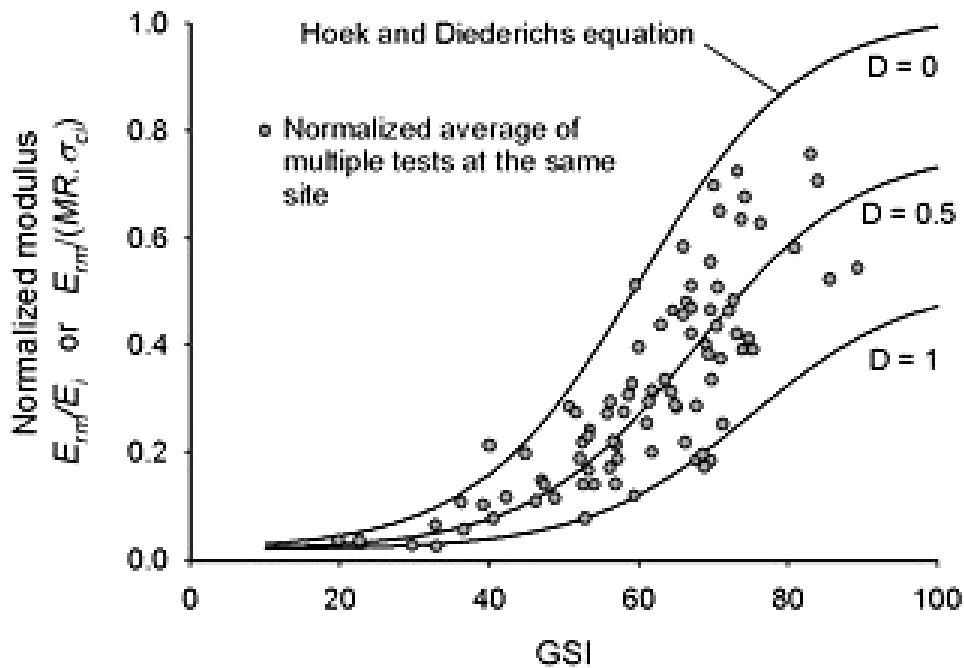


Figure 9: Plot of normalized in situ rock mass deformation modulus from China and Taiwan against Hoek and Diederichs Equation (27). Each data point represents the average of multiple tests at the same site in the same rock mass.

Rock mass properties

Table 8: Guidelines for the selection of modulus ratio (MR) values in Equation (26) - based on Deere (1968) and Palmstrom and Singh (2001)

	Class	Group	Texture			
			Coarse	Medium	Fine	Very fine
SEDIMENTARY	Clastic		Conglomerates 300-400	Sandstones 200-350	Siltstones 350-400	Claystones 200-300
			Breccias 230-350		Greywackes 350	Shales 150-250 * Marls 150-200
	Non-Clastic	Carbonates	Crystalline Limestone 400-600	Sparitic Limestones 600-800	Micritic Limestones 800-1000	Dolomites 350-500
		Evaporites		Gypsum (350)**	Anhydrite (350)**	
		Organic			Chalk 1000+	
METAMORPHIC	Non Foliated		Marble 700-1000	Hornfels 400-700 Metasandstone 200-300	Quartzites 300-450	
	Slightly foliated		Migmatite 350-400	Amphibolites 400-500	Gneiss 300-750*	
	Foliated*			Schists 250-1100*	Phyllites /Mica Schist 300-800*	Slates 400-600*
IGNEOUS	Plutonic	Light	Granite+ 300-550 Granodiorite+ 400-450	Diorite+ 300-350		
		Dark	Gabbro 400-500 Nonte 350-400	Dolerite 300-400		
	Hypabyssal		Porphyries (400)**		Diabase 300-350	Peridotite 250-300
	Volcanic	Lava		Rhyolite 300-500 Andesite 300-500	Dacite 350-450 Basalt 250-450	
		Pyroclastic	Agglomerate 400-600	Volcanic breccia (500)**	Tuff 200-400	

* Highly anisotropic rocks: the value of MR will be significantly different if normal strain and/or loading occurs parallel (high MR) or perpendicular (low MR) to a weakness plane. Uniaxial test loading direction should be equivalent to field application.

+ Felsic Granitoids: Coarse Grained or Altered (high MR), fined grained (low MR).

** No data available, estimated on the basis of geological logic.

Table 8, based on the modulus ratio (MR) values proposed by Deere (1968) can be used for calculating the intact rock modulus E_i . In general, measured values of E_i are seldom available and, even when they are, their reliability is suspect because of specimen damage. This specimen damage has a greater impact on modulus than on strength and, hence, the intact rock strength, when available, can usually be considered more reliable.

Post-failure behaviour

When using numerical models to study the progressive failure of rock masses, estimates of the post-peak or post-failure characteristics of the rock mass are required. In some of these models, the Hoek-Brown failure criterion is treated as a yield criterion and the analysis is carried out using plasticity theory. No definite rules for dealing with this problem can be given but, based upon experience in numerical analysis of a variety of practical problems, the post-failure characteristics, illustrated in Figure 10, are suggested as a starting point.

Reliability of rock mass strength estimates

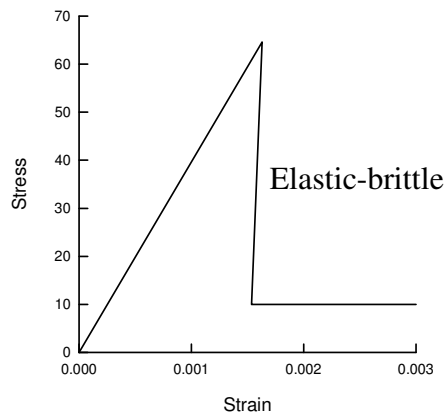
The techniques described in the preceding sections of this chapter can be used to estimate the strength and deformation characteristics of isotropic jointed rock masses. When applying this procedure to rock engineering design problems, most users consider only the 'average' or mean properties. In fact, all of these properties exhibit a distribution about the mean, even under the most ideal conditions, and these distributions can have a significant impact upon the design calculations.

In the text that follows, a slope stability calculation and a tunnel support design calculation are carried out in order to evaluate the influence of these distributions. In each case the strength and deformation characteristics of the rock mass are estimated by means of the Hoek-Brown procedure, assuming that the three input parameters are defined by normal distributions.

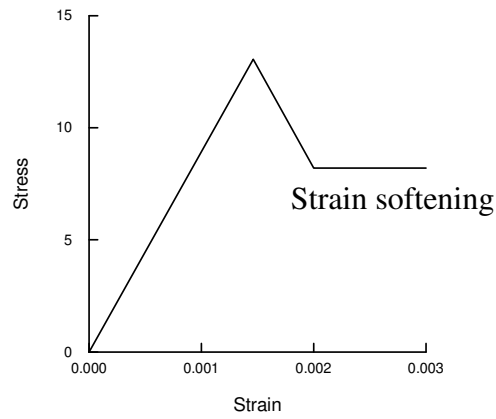
Input parameters

Figure 11 has been used to estimate the value of the value of GSI from field observations of blockiness and discontinuity surface conditions. Included in this figure is a crosshatched circle representing the 90% confidence limits of a GSI value of 25 ± 5 (equivalent to a standard deviation of approximately 2.5). This represents the range of values that an experienced geologist would assign to a rock mass described as BLOCKY/DISTURBED or DISINTEGRATED and POOR. Typically, rocks such as flysch, schist and some phyllites may fall within this range of rock mass descriptions.

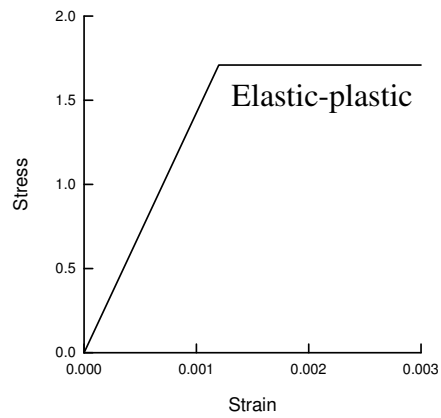
Rock mass properties



(a) Very good quality hard rock mass



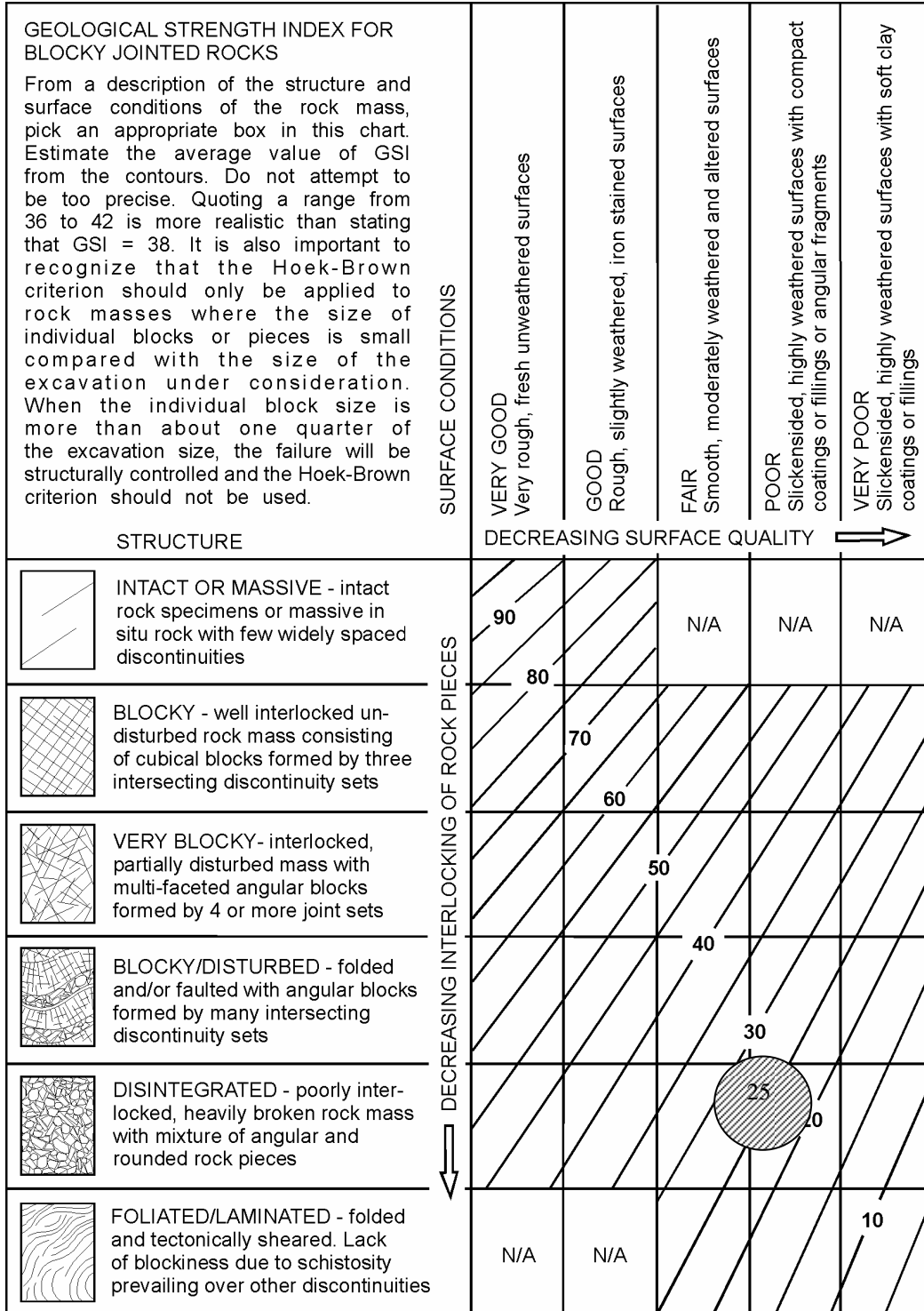
(b) Average quality rock mass



(c) Very poor quality soft rock mass

Figure 10: Suggested post failure characteristics for different quality rock masses.

Figure 11: Estimate of Geological Strength Index GSI based on geological descriptions.



In the author's experience, some geologists go to extraordinary lengths to try to determine an 'exact' value of GSI. Geology does not lend itself to such precision and it is simply not realistic to assign a single value. A range of values, such as that illustrated in Figure 11 is more appropriate. In fact, in some complex geological environments, the range indicated by the crosshatched circle may be too optimistic.

The two laboratory properties required for the application of the Hoek-Brown criterion are the uniaxial compressive strength of the intact rock (σ_{ci}) and the intact rock material constant m_i . Ideally these two parameters should be determined by triaxial tests on carefully prepared specimens as described by Hoek and Brown (1997).

It is assumed that all three input parameters (GSI, σ_{ci} and m_i) can be represented by normal distributions as illustrated in Figure 12. The standard deviations assigned to these three distributions are based upon the author's experience of geotechnical programs for major civil and mining projects where adequate funds are available for high quality investigations. For preliminary field investigations or 'low budget' projects, it is prudent to assume larger standard deviations for the input parameters.

Note that where software programs will accept input in terms of the Hoek-Brown criterion directly, it is preferable to use this input rather than estimates of Mohr Coulomb parameters c and ϕ given by equations 16 and 17. This eliminates the uncertainty associated with estimating equivalent Mohr-Coulomb parameters, as described above and allows the program to compute the conditions for failure at each point directly from the curvilinear Hoek-Brown relationship. In addition, the input parameters for the Hoek-Brown criterion (m_i , s and a) are independent variables and can be treated as such in any probabilistic analysis. On the other hand the Mohr Coulomb c and ϕ parameters are correlated and this results in an additional complication in probabilistic analyses.

Based on the three normal distributions for GSI, σ_{ci} and m_i given in Figure 12, distributions for the rock mass parameters m_b , s and a can be determined by a variety of methods. One of the simplest is to use a Monte Carlo simulation in which the distributions given in Figure 12 are used as input for equations 11, 12 and 13 to determine distributions for m_i , s and a . The results of such an analysis, using the Excel add-in @RISK², are given in Figure 13.

Slope stability calculation

In order to assess the impact of the variation in rock mass parameters, illustrated in Figure 12 and 13, a calculation of the factor of safety for a homogeneous slope was

² Available from www.palisade.com

Rock mass properties

carried out using Bishop's circular failure analysis in the program SLIDE³. The geometry of the slope and the phreatic surface are shown in Figure 14. The probabilistic option offered by the program was used and the rock mass properties were input as follows:

Property	Distribution	Mean	Std. dev.	Min*	Max*
m_b	Normal	0.6894	0.1832	0.0086	1.44
s	Lognormal	0.0002498	0.0000707	0.0000886	0.000704
a	Normal	0.5317	0.00535	0.5171	0.5579
σ_{ci}	Normal	10000 kPa	2500 kPa	1000 kPa	20000 kPa
Unit weight γ		23 kN/m ³			

* Note that, in SLIDE, these values are input as values relative to the mean value and not as the absolute values shown here.

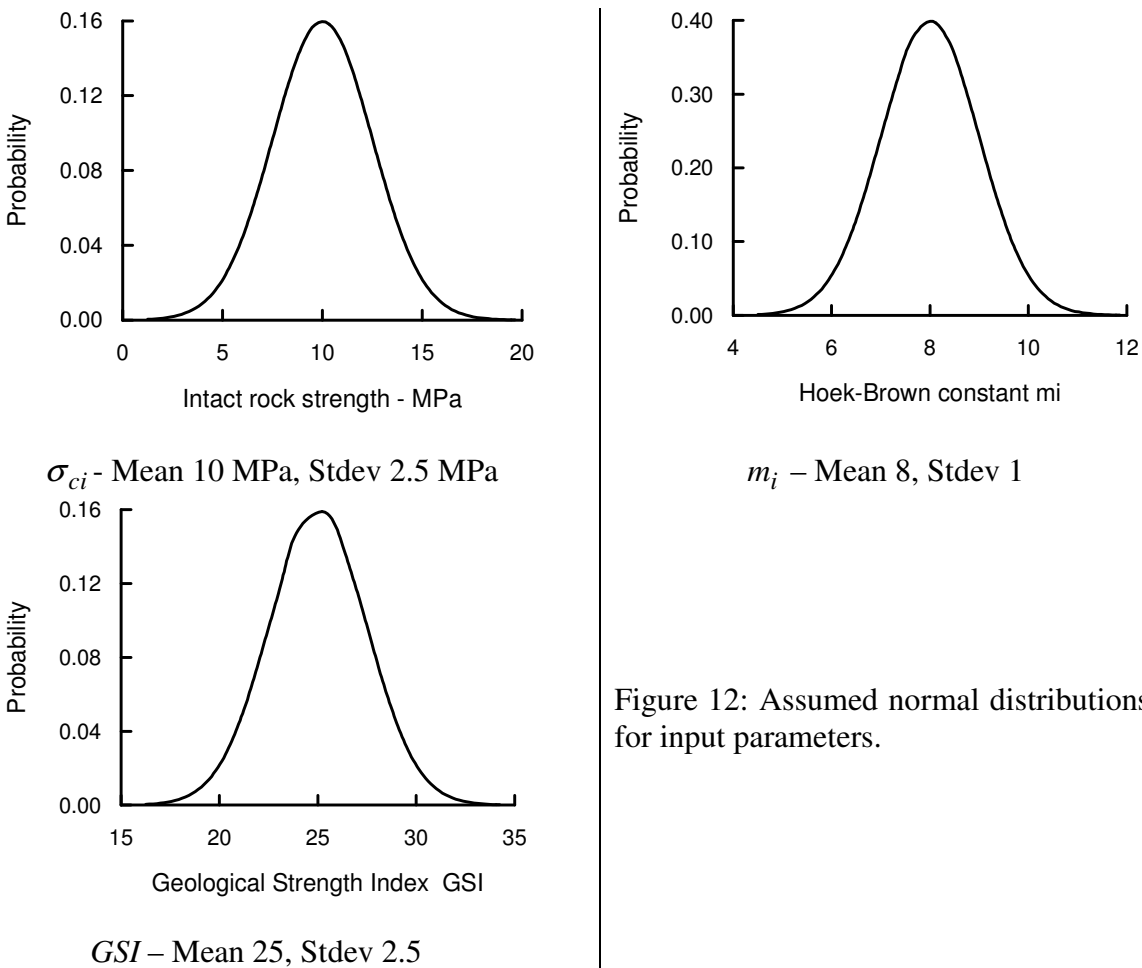
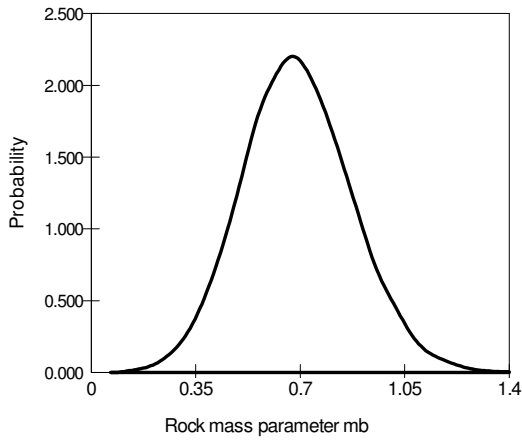


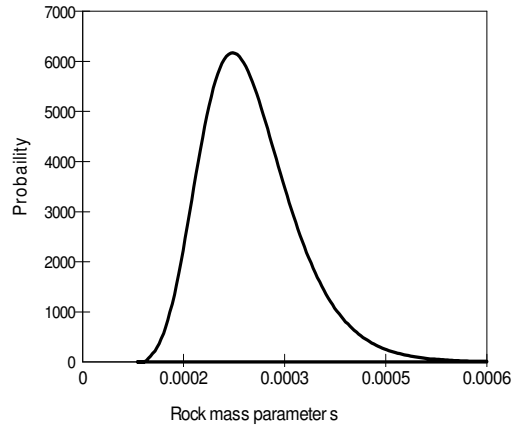
Figure 12: Assumed normal distributions for input parameters.

³ available from www.rocscience.com

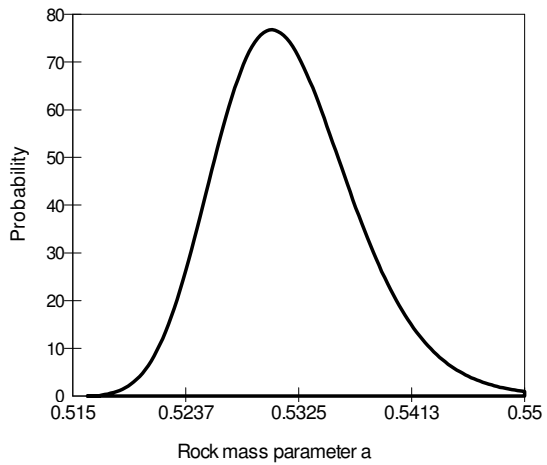
Rock mass properties



m_b - Mean 0.689, Stdev 0.183



s - Mean 0.00025, Stdev 0.00007



a - Mean 0.532, Stdev 0.00535

Figure 13: Calculated distributions for rock mass parameters.

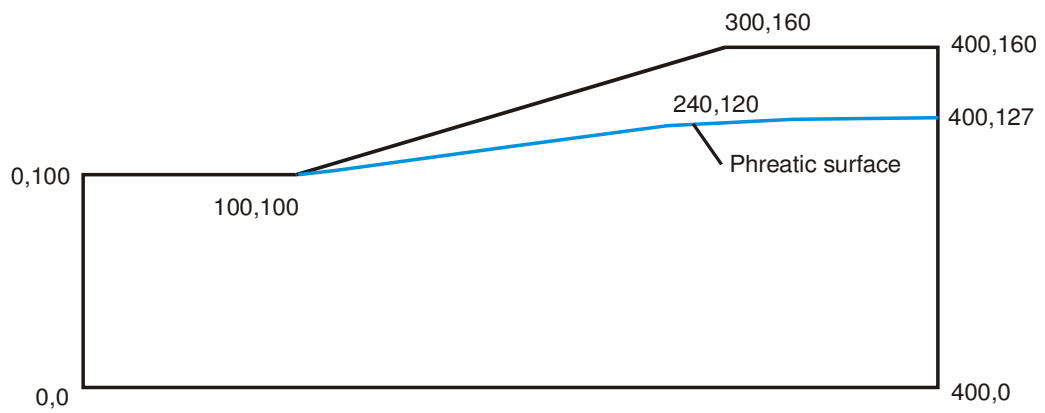


Figure 14: Slope and phreatic surface geometry for a homogeneous slope.

Rock mass properties

The distribution of the factor of safety is shown in Figure 15 and it was found that this is best represented by a beta distribution with a mean value of 2.998, a standard deviation of 0.385, a minimum value of 1.207 and a maximum value of 4.107. There is zero probability of failure for this slope as indicated by the minimum factor of safety of 1.207. All critical failure surface exit at the toe of the slope.

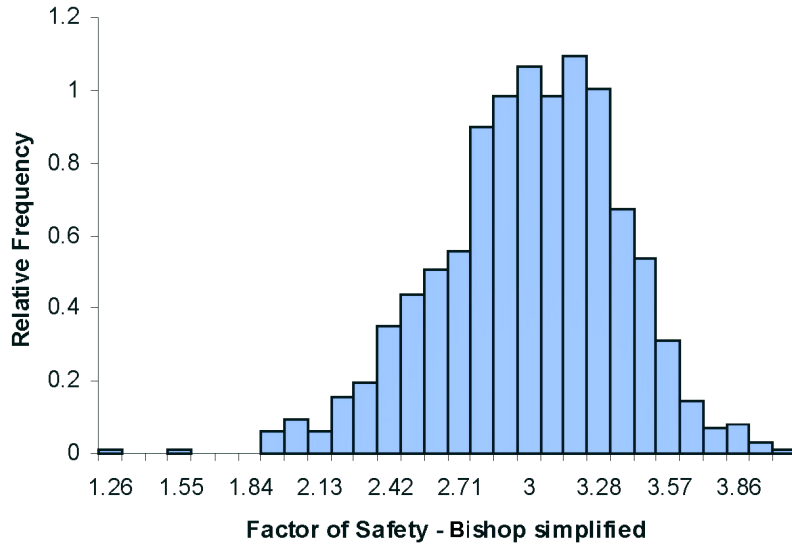


Figure 15: Distribution of factors of safety for the slope shown in Figure 14 from a probabilistic analysis using the program SLIDE.

Tunnel stability calculations

Consider a circular tunnel, illustrated in Figure 16, with a radius r_o in a stress field in which the horizontal and vertical stresses are both p_o . If the stresses are high enough, a ‘plastic’ zone of damaged rock of radius r_p surrounds the tunnel. A uniform support pressure p_i is provided around the perimeter of the tunnel.

A probabilistic analysis of the behaviour of this tunnel was carried out using the program RocSupport (available from www.rocscience.com) with the following input parameters:

Property	Distribution	Mean	Std. dev.	Min*	Max*
Tunnel radius r_o		5 m			
In situ stress p_o		2.5 MPa			
m_b	Normal	0.6894	0.1832	0.0086	1.44
s	Lognormal	0.0002498	0.0000707	0.0000886	0.000704
a	Normal	0.5317	0.00535	0.5171	0.5579
σ_{ci}	Normal	10 MPa	2.5 MPa	1 MPa	20 MPa
E		1050 MPa			

* Note that, in RocSupport, these values are input as values relative to the mean value and not as the absolute values shown here.

Rock mass properties

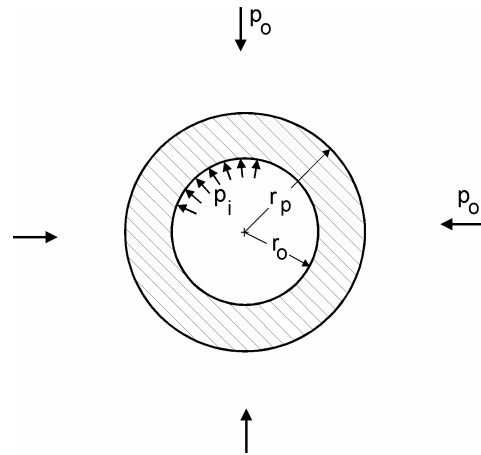


Figure 16: Development of a plastic zone around a circular tunnel in a hydrostatic stress field.

The resulting characteristic curve or support interaction diagram is presented in Figure 17. This diagram shows the tunnel wall displacements induced by progressive failure of the rock mass surrounding the tunnel as the face advances. The support is provided by a 5 cm shotcrete layer with 15 cm wide flange steel ribs spaced 1 m apart. The support is assumed to be installed 2 m behind the face after a wall displacement of 25 mm or a tunnel convergence of 50 mm has occurred. At this stage the shotcrete is assigned a 3 day compressive strength of 11 MPa.

The Factor of Safety of the support system is defined by the ratio of support capacity to demand as defined in Figure 17. The capacity of the shotcrete and steel set support is 0.4 MPa and it can accommodate a tunnel convergence of approximately 30 mm. As can be seen from Figure 17, the mobilised support pressure at equilibrium (where the characteristic curve and the support reaction curves cross) is approximately 0.15 MPa. This gives a first deterministic estimate of the Factor of Safety as 2.7.

The probabilistic analysis of the factor of safety yields the histogram shown in Figure 18. A Beta distribution is found to give the best fit to this histogram and the mean Factor of Safety is 2.73, the standard deviation is 0.46, the minimum is 2.23 and the maximum is 9.57.

This analysis is based on the assumption that the tunnel is circular, the rock mass is homogeneous and isotropic, the in situ stresses are equal in all directions and the support is placed as a closed circular ring. These assumptions are seldom valid for actual tunnelling conditions and hence the analysis described above should only be used as a first rough approximation in design. Where the analysis indicates that tunnel stability is likely to be a problem, it is essential that a more detailed numerical analysis, taking into account actual tunnel geometry and rock mass conditions, should be carried out.

Rock mass properties

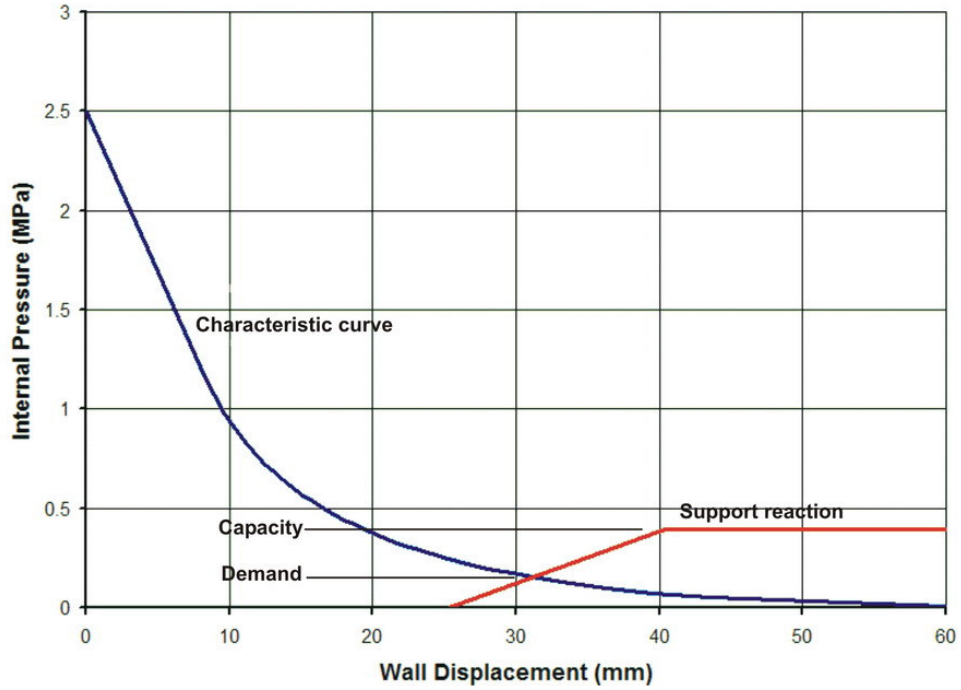


Figure 17: Rock support interaction diagram for a 10 m diameter tunnel subjected to a uniform in situ stress of 2.5 MPa.

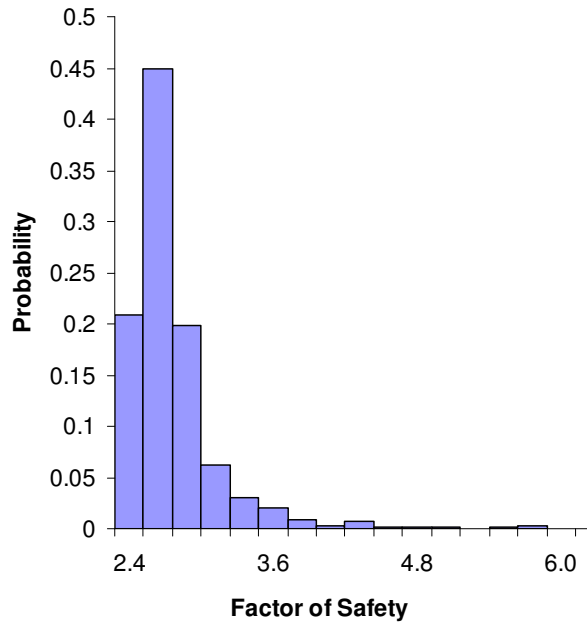


Figure 18: Distribution of the Factor of Safety for the tunnel discussed above.

Conclusions

The uncertainty associated with estimating the properties of in situ rock masses has a significant impact on the design of slopes and excavations in rock. The examples that have been explored in this section show that, even when using the ‘best’ estimates currently available, the range of calculated factors of safety are uncomfortably large. These ranges become alarmingly large when poor site investigation techniques and inadequate laboratory procedures are used.

Given the inherent difficulty of assigning reliable numerical values to rock mass characteristics, it is unlikely that ‘accurate’ methods for estimating rock mass properties will be developed in the foreseeable future. Consequently, the user of the Hoek-Brown procedure or of any other equivalent procedure for estimating rock mass properties should not assume that the calculations produce unique reliable numbers. The simple techniques described in this section can be used to explore the possible range of values and the impact of these variations on engineering design.

Practical examples of rock mass property estimates

The following examples are presented in order to illustrate the range of rock mass properties that can be encountered in the field and to give the reader some insight of how the estimation of rock mass properties was tackled in a number of actual projects.

Massive weak rock

Karzulovic and Diaz (1994) have described the results of a program of triaxial tests on a cemented breccia known as Braden Breccia from the El Teniente mine in Chile. In order to design underground openings in this rock, attempts were made to classify the rock mass in accordance with Bieniawski’s RMR system. However, as illustrated in Figure 19, this rock mass has very few discontinuities and so assigning realistic numbers to terms depending upon joint spacing and condition proved to be very difficult. Finally, it was decided to treat the rock mass as a weak but homogeneous ‘almost intact’ rock, similar to a weak concrete, and to determine its properties by means of triaxial tests on large diameter specimens.

A series of triaxial tests was carried out on 100 mm diameter core samples, illustrated in Figure 20. The results of these tests were analysed by means of the regression analysis using the program RocLab⁴. Back analysis of the behaviour of underground openings in this rock indicate that the in-situ GSI value is approximately 75. From RocLab the following parameters were obtained:

⁴ Available from www.rocscience.com as a free download

Rock mass properties

Intact rock strength	σ_{ci}	51 MPa	Hoek-Brown constant	m_b	6.675
Hoek-Brown constant	m_i	16.3	Hoek-Brown constant	s	0.062
Geological Strength Index	GSI	75	Hoek-Brown constant	a	0.501
			Deformation modulus	E_m	15000 MPa



Figure 19: Braden Breccia at El Teniente Mine in Chile. This rock is a cemented breccia with practically no joints. It was dealt with in a manner similar to weak concrete and tests were carried out on 100 mm diameter specimens illustrated in Figure 20.



Fig. 20. 100 mm diameter by 200 mm long specimens of Braden Breccia from the El Teniente mine in Chile

Massive strong rock masses

The Rio Grande Pumped Storage Project in Argentina includes a large underground powerhouse and surge control complex and a 6 km long tailrace tunnel. The rock mass surrounding these excavations is massive gneiss with very few joints. A typical core from this rock mass is illustrated in Figure 21. The appearance of the rock at the surface was illustrated earlier in Figure 6, which shows a cutting for the dam spillway.



Figure 21: Excellent quality core with very few discontinuities from the massive gneiss of the Rio Grande project in Argentina.

Figure 21: Top heading of the 12 m span, 18 m high tailrace tunnel for the Rio Grande Pumped Storage Project.



Rock mass properties

The rock mass can be described as BLOCKY/VERY GOOD and the GSI value, from Table 5, is 75. Typical characteristics for the rock mass are as follows:

Intact rock strength	σ_{ci}	110 MPa	Hoek-Brown constant	m_b	11.46
Hoek-Brown constant	m_i	28	Hoek-Brown constant	s	0.062
Geological Strength Index	GSI	75	Constant	a	0.501
			Deformation modulus	E_m	45000 MPa

Figure 21 illustrates the 8 m high 12 m span top heading for the tailrace tunnel. The final tunnel height of 18 m was achieved by blasting two 5 m benches. The top heading was excavated by full-face drill and blast and, because of the excellent quality of the rock mass and the tight control on blasting quality, most of the top heading did not require any support.

Details of this project are to be found in Moretto et al (1993). Hammett and Hoek (1981) have described the design of the support system for the 25 m span underground powerhouse in which a few structurally controlled wedges were identified and stabilised during excavation.

Average quality rock mass

The partially excavated powerhouse cavern in the Nathpa Jhakri Hydroelectric project in Himachel Pradesh, India is illustrated in Figure 22. The rock is a jointed quartz mica schist, which has been extensively evaluated by the Geological Survey of India as described by Jalote et al (1996). An average GSI value of 65 was chosen to estimate the rock mass properties which were used for the cavern support design. Additional support, installed on the instructions of the Engineers, was placed in weaker rock zones.

The assumed rock mass properties are as follows:

Intact rock strength	σ_{ci}	30 MPa	Hoek-Brown constant	m_b	4.3
Hoek-Brown constant	m_i	15	Hoek-Brown constant	s	0.02
Geological Strength Index	GSI	65	Constant	a	0.5
			Deformation modulus	E_m	10000 MPa

Two and three dimensional stress analyses of the nine stages used to excavate the cavern were carried out to determine the extent of potential rock mass failure and to provide guidance in the design of the support system. An isometric view of one of the three dimensional models is given in Figure 23.



Figure 22: Partially completed 20 m span, 42.5 m high underground powerhouse cavern of the Nathpa Jhakri Hydroelectric Project in Himachel Pradesh, India. The cavern is approximately 300 m below the surface.

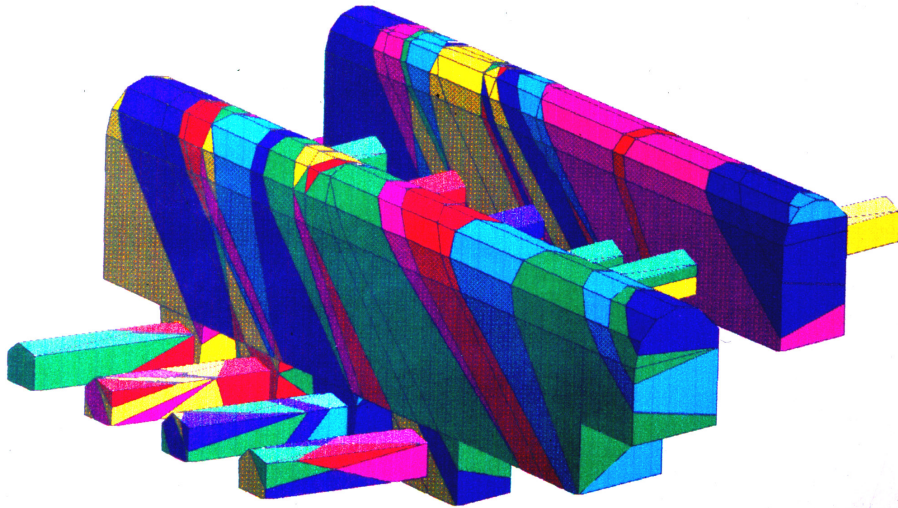


Figure 23: Isometric view of the 3DEC5 model of the underground powerhouse cavern and transformer gallery of the Nathpa Jhakri Hydroelectric Project, analysed by Dr. B. Dasgupta⁶.

⁵ Available from ITASCA Consulting Group Inc, 111 Third Ave. South, Minneapolis, Minnesota 55401, USA.

⁶ Formerly at the Institute of Rock Mechanics (Kolar), Kolar Gold Fields, Karnataka.

Rock mass properties

The support for the powerhouse cavern consists of rockbolts and mesh reinforced shotcrete. Alternating 6 and 8 m long 32 mm diameter bolts on 1 x 1 m and 1.5 x 1.5 m centres are used in the arch. Alternating 9 and 7.5 m long 32 mm diameter bolts were used in the upper and lower sidewalls with alternating 9 and 11 m long 32 mm rockbolts in the centre of the sidewalls, all at a grid spacing of 1.5 m. Shotcrete consists of two 50 mm thick layers of plain shotcrete with an interbedded layer of weldmesh. The support provided by the shotcrete was not included in the support design analysis, which relies upon the rockbolts to provide all the support required.

In the headrace tunnel, some zones of sheared quartz mica schist have been encountered and these have resulted in large displacements as illustrated in Figure 24. This is a common problem in hard rock tunnelling where the excavation sequence and support system have been designed for 'average' rock mass conditions. Unless very rapid changes in the length of blast rounds and the installed support are made when an abrupt change to poor rock conditions occurs, for example when a fault is encountered, problems with controlling tunnel deformation can arise.



Figure 24: Large displacements in the top heading of the headrace tunnel of the Nathpa Jhakri Hydroelectric project. These displacements are the result of deteriorating rock mass quality when tunnelling through a fault zone.

The only effective way to anticipate this type of problem is to keep a probe hole ahead of the advancing face at all times. Typically, a long probe hole is percussion drilled during a maintenance shift and the penetration rate, return water flow and chippings are constantly monitored during drilling. Where significant problems are indicated by this percussion drilling, one or two diamond-drilled holes may be required to investigate these problems in more detail. In some special cases, the use of a pilot tunnel may be more effective in that it permits the ground properties to be defined more accurately than is possible with probe hole drilling. In addition, pilot tunnels allow pre-drainage and pre-reinforcement of the rock ahead of the development of the full excavation profile.

Poor quality rock mass at shallow depth

Kavvadas et al (1996) have described some of the geotechnical issues associated with the construction of 18 km of tunnels and the 21 underground stations of the Athens Metro. These excavations are all shallow with typical depths to tunnel crown of between 15 and 20 m. The principal problem is one of surface subsidence rather than failure of the rock mass surrounding the openings.

The rock mass is locally known as Athenian schist which is a term used to describe a sequence of Upper Cretaceous flysch-type sediments including thinly bedded clayey and calcareous sandstones, siltstones (greywackes), slates, shales and limestones. During the Eocene, the Athenian schist formations were subjected to intense folding and thrusting. Later extensive faulting caused extensional fracturing and widespread weathering and alteration of the deposits.

The GSI values range from about 15 to about 45. The higher values correspond to the intercalated layers of sandstones and limestones, which can be described as BLOCKY/DISTURBED and POOR (Table 5). The completely decomposed schist can be described as DISINTEGRATED and VERY POOR and has GSI values ranging from 15 to 20. Rock mass properties for the completely decomposed schist, using a GSI value of 20, are as follows:

Intact rock strength - MPa	σ_{ci}	5-10	Hoek-Brown constant	m_b	0.55
Hoek-Brown constant	m_i	9.6	Hoek-Brown constant	s	0.0001
Geological Strength Index	GSI	20	Hoek-Brown constant	a	0.544
			Deformation modulus MPa	E_m	600

The Academia, Syntagma, Omonia and Olympion stations were constructed using the New Austrian Tunnelling Method twin side drift and central pillar method as illustrated in Figure 25. The more conventional top heading and bench method, illustrated in Figure 26, was used for the excavation of the Ambelokipi station. These stations are all 16.5 m wide and 12.7 m high. The appearance of the rock mass in one of the Olympion station side drift excavations is illustrated in Figures 27 and 28.

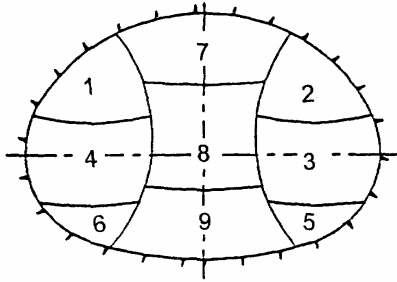


Figure 25: Twin side drift and central pillar excavation method. Temporary support consists of double wire mesh reinforced 250 - 300 mm thick shotcrete shells with embedded lattice girders or HEB 160 steel sets at 0.75 - 1 m spacing.

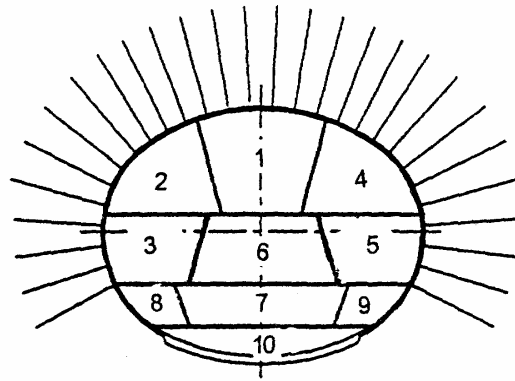


Figure 26: Top heading and bench method of excavation. Temporary support consists of a 200 mm thick shotcrete shell with 4 and 6 m long untensioned grouted rockbolts at 1.0 - 1.5 m spacing



Figure 27: Side drift in the Athens Metro Olympion station excavation that was excavated by the method illustrated in Figure 25. The station has a cover depth of approximately 10 m over the crown.



Figure 28: Appearance of the very poor quality Athenian Schist at the face of the side heading illustrated in Figure 27.

Numerical analyses of the two excavation methods showed that the twin side drift method resulted in slightly less rock mass failure in the crown of the excavation. However, the final surface displacements induced by the two excavation methods were practically identical.

Maximum vertical displacements of the surface above the centre-line of the Omonia station amounted to 51 mm. Of this, 28 mm occurred during the excavation of the side drifts, 14 mm during the removal of the central pillar and a further 9 mm occurred as a time dependent settlement after completion of the excavation. According to Kavvadas et al (1996), this time dependent settlement is due to the dissipation of excess pore water pressures which were built up during excavation. In the case of the Omonia station, the excavation of recesses towards the eastern end of the station, after completion of the station excavation, added a further 10 to 12 mm of vertical surface displacement at this end of the station.

Poor quality rock mass under high stress

The Yacambú Quibor tunnel in Venezuela is considered to be one of the most difficult tunnels in the world. This 25 km long water supply tunnel through the Andes is being excavated in sandstones and phyllites at depths of up to 1200 m below surface. The

graphitic phyllite is a very poor quality rock and gives rise to serious squeezing problems which, without adequate support, result in complete closure of the tunnel. A full-face tunnel-boring machine was completely destroyed in 1979 when trapped by squeezing ground conditions.

The graphitic phyllite has an average unconfined compressive strength of about 50 MPa and the estimated GSI value is about 25 (see Figures 2 and 3). Typical rock mass properties are as follows:

Intact rock strength MPa	σ_{ci}	50	Hoek-Brown constant	m_b	0.481
Hoek-Brown constant	m_i	10	Hoek-Brown constant	s	0.0002
Geological Strength Index	GSI	25	Hoek-Brown constant	a	0.53
			Deformation modulus MPa	E_m	1000

Various support methods have been used on this tunnel and only one will be considered here. This was a trial section of tunnel, at a depth of about 600 m, constructed in 1989. The support of the 5.5 m span tunnel was by means of a complete ring of 5 m long, 32 mm diameter untensioned grouted dowels with a 200 mm thick shell of reinforced shotcrete. This support system proved to be very effective but was later abandoned in favour of yielding steel sets (steel sets with sliding joints) because of construction schedule considerations. In fact, at a depth of 1200 m below surface (2004-2006) it is doubtful if the rockbolts would have been effective because of the very large deformations that could only be accommodated by steel sets with sliding joints.

Examples of the results of a typical numerical stress analysis of this trial section, carried out using the program PHASE2⁷, are given in Figures 29 and 30. Figure 29 shows the extent of failure, with and without support, while Figure 30 shows the displacements in the rock mass surrounding the tunnel. Note that the criteria used to judge the effectiveness of the support design are that the zone of failure surrounding the tunnel should lie within the envelope of the rockbolt support, the rockbolts should not be stressed to failure and the displacements should be of reasonable magnitude and should be uniformly distributed around the tunnel. All of these objectives were achieved by the support system described earlier.

Slope stability considerations

When dealing with slope stability problems in rock masses, great care has to be taken in attempting to apply the Hoek-Brown failure criterion, particularly for small steep slopes. As illustrated in Figure 31, even rock masses that appear to be good candidates for the application of the criterion can suffer shallow structurally controlled failures under the very low stress conditions which exist in such slopes.

⁷ Available from www.rocscience.com.

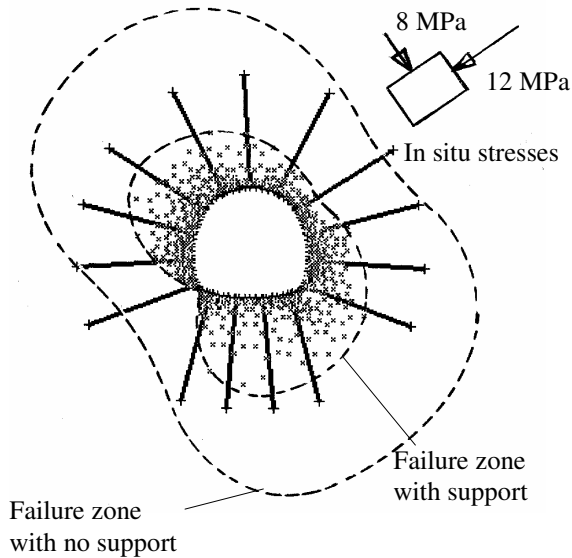


Figure 29: Results of a numerical analysis of the failure of the rock mass surrounding the Yacambu-Quibor tunnel when excavated in graphitic phyllite at a depth of about 600 m below surface.

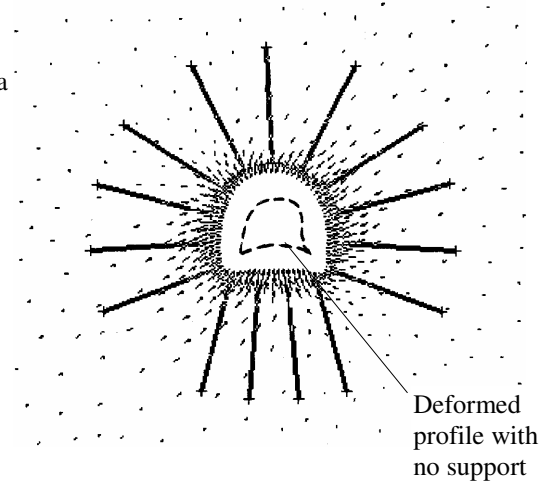


Figure 30: Displacements in the rock mass surrounding the Yacambu-Quibor tunnel. The maximum calculated displacement is 258 mm with no support and 106 mm with support.

As a general rule, when designing slopes in rock, the initial approach should always be to search for potential failures controlled by adverse structural conditions. These may take the form of planar failures on outward dipping features, wedge failures on intersecting features, toppling failures on inward dipping failures or complex failure modes involving all of these processes. Only when the potential for structurally controlled failures has been eliminated should consideration be given to treating the rock mass as an isotropic material as required by the Hoek-Brown failure criterion.

Figure 32 illustrates a case in which the base of a slope failure is defined by an outward dipping fault that does not daylight at the toe of the slope. Circular failure through the poor quality rock mass overlying the fault allows failure of the toe of the slope. Analysis of this problem was carried out by assigning the rock mass at the toe properties that had been determined by application of the Hoek-Brown criterion. A search for the critical failure surface was carried out utilising the program SLIDE which allows complex failure surfaces to be analysed and which includes facilities for the input of the Hoek-Brown failure criterion.



Figure 31: Structurally controlled failure in the face of a steep bench in a heavily jointed rock mass.

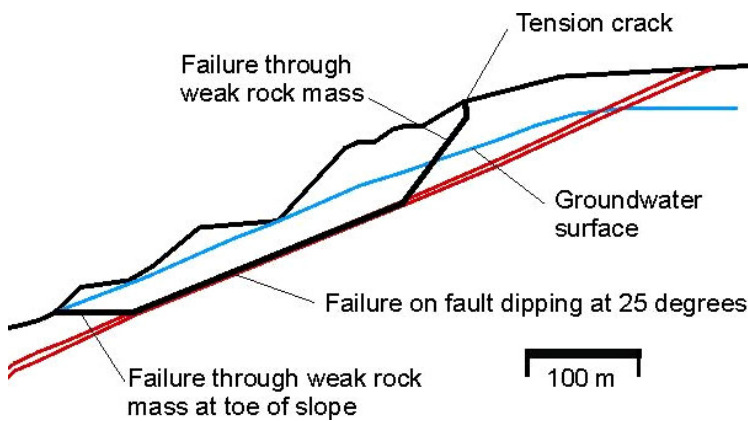


Figure 32: Complex slope failure controlled by an outward dipping basal fault and circular failure through the poor quality rock mass overlying the toe of the slope.

References

- Balmer, G. 1952. A general analytical solution for Mohr's envelope. *Am. Soc. Test. Mat.* **52**, 1260-1271.
- Bieniawski, Z.T. 1976. Rock mass classification in rock engineering. In *Exploration for rock engineering, proc. of the symp.*, (ed. Z.T. Bieniawski) **1**, 97-106. Cape Town: Balkema.
- Bieniawski, Z.T. 1989. *Engineering rock mass classifications*. New York: Wiley.
- Deere D.U. 1968. Chapter 1: Geological considerations. In *Rock Mechanics in Engineering Practice* (eds. Stagg K.G. and Zienkiewicz, O.C.), 1-20. London: John Wiley and Sons.
- Franklin, J.A. and Hoek, E. 1970. Developments in triaxial testing equipment. *Rock Mech.* **2**, 223-228. Berlin: Springer-Verlag.
- Hammett, R.D. and Hoek, E. 1981. Design of large underground caverns for hydroelectric projects, with reference to structurally controlled failure mechanisms. *Proc. American Soc. Civil Engrs. Int. Conf. on recent developments in geotechnical engineering for hydro projects*. 192-206. New York: ASCE
- Hoek, E. 1983. Strength of jointed rock masses, 23rd. Rankine Lecture. *Géotechnique* **33**(3), 187-223.
- Hoek, E. 1994. Strength of rock and rock masses, *ISRM News J*, **2**(2), 4-16.
- Hoek, E. and Brown, E.T. 1980a. *Underground excavations in rock*. London: Instn Min. Metall.
- Hoek, E. and Brown, E.T. 1980b. Empirical strength criterion for rock masses. *J. Geotech. Engng Div., ASCE* **106**(GT9), 1013-1035.
- Hoek, E. and Brown, E.T. 1988. The Hoek-Brown failure criterion - a 1988 update. In *Rock engineering for underground excavations, proc. 15th Canadian rock mech. symp.*, (ed. J.C. Curran), 31-38. Toronto: Dept. Civ. Engineering, University of Toronto.
- Hoek, E., Marinos, P. and Benissi, M. 1998. Applicability of the Geological Strength Index (GSI) classification for very weak and sheared rock masses. The case of the Athens Schist Formation. *Bull. Engng. Geol. Env.* **57**(2), 151-160.
- Hoek, E. and Brown, E.T. 1997. Practical estimates of rock mass strength. *Int. J. Rock Mech. Min.g Sci. & Geomech. Abstr.* **34**(8), 1165-1186.
- Hoek, E., Kaiser, P.K. and Bawden. W.F. 1995. *Support of underground excavations in hard rock*. Rotterdam: Balkema.

- Hoek, E., Wood, D. and Shah, S. 1992. A modified Hoek-Brown criterion for jointed rock masses. *Proc. rock characterization, symp. Int. Soc. Rock Mech.: Eurock '92*, (ed. J.A. Hudson), 209-214. London: Brit. Geol. Soc.
- Hoek E, Carranza-Torres CT, Corkum B. Hoek-Brown failure criterion-2002 edition. In: *Proceedings of the 5th North American Rock Mechanics Symp.*, Toronto, Canada, 2002: **1**: 267-73.
- Hoek, E., Marinos, P., Marinos, V. 2005. Characterization and engineering properties of tectonically undisturbed but lithologically varied sedimentary rock masses. *Int. J. Rock Mech. Min. Sci.*, **42/2**, 277-285
- Hoek, E and Diederichs, M. 2006. Empirical estimates of rock mass modulus. *Int. J Rock Mech. Min. Sci.*, **43**, 203-215
- Karzulovic A. and Díaz, A.1994. Evaluación de las Propiedades Geomacánicas de la Brecha Braden en Mina El Teniente. *Proc. IV Congreso Sudamericano de Mecánica de Rocas, Santiago* **1**, 39-47.
- Kavvadas M., Hewison L.R., Lastaratos P.G., Seferoglou, C. and Michalis, I. 1996. Experience in the construction of the Athens Metro. *Proc. Int. symp. geotechnical aspects of underground construction in soft ground*. (Eds Mair R.J. and Taylor R.N.), 277-282. London: City University.
- Jalote, P.M., Kumar A. and Kumar V. 1996. Geotechniques applied in the design of the machine hall cavern, Nathpa Jhakri Hydel Project, N.W. Himalaya, India. *J. Engng Geol. (India)* XXV(1-4), 181-192.
- Marinos, P, and Hoek, E. 2001 – Estimating the geotechnical properties of heterogeneous rock masses such as flysch. *Bull. Enginng Geol. & the Environment (IAEG)*, **60**, 85-92
- Marinos, P., Hoek, E., Marinos, V. 2006. Variability of the engineering properties of rock masses quantified by the geological strength index: the case of ophiolites with special emphasis on tunnelling. *Bull. Eng. Geol. Env.*, **65/2**, 129-142.
- Moretto O., Sarra Pistone R.E. and Del Rio J.C. 1993. A case history in Argentina - Rock mechanics for underground works in the pumping storage development of Rio Grande No 1. *In Comprehensive Rock Engineering*. (Ed. Hudson, J.A.) **5**, 159-192. Oxford: Pergamon.
- Palmstrom A. and Singh R. 2001. The deformation modulus of rock masses: comparisons between in situ tests and indirect estimates. *Tunnelling and Underground Space Technology*. **16**: 115-131.
- Salcedo D.A.1983. Macizos Rocosos: Caracterización, Resistencia al Corte y Mecanismos de Rotura. *Proc. 25 Aniversario Conferencia Soc. Venezolana de Mecánica del Suelo e Ingeniería de Fundaciones*, Caracas. 143-172.

Shear strength of discontinuities

Introduction

All rock masses contain discontinuities such as bedding planes, joints, shear zones and faults. At shallow depth, where stresses are low, failure of the intact rock material is minimal and the behaviour of the rock mass is controlled by sliding on the discontinuities. In order to analyse the stability of this system of individual rock blocks, it is necessary to understand the factors that control the shear strength of the discontinuities which separate the blocks. These questions are addressed in the discussion that follows.

Shear strength of planar surfaces

Suppose that a number of samples of a rock are obtained for shear testing. Each sample contains a through-going bedding plane that is cemented; in other words, a tensile force would have to be applied to the two halves of the specimen in order to separate them. The bedding plane is absolutely planar, having no surface irregularities or undulations. As illustrated in Figure 1, in a shear test each specimen is subjected to a stress σ_n normal to the bedding plane, and the shear stress τ , required to cause a displacement δ , is measured.

The shear stress will increase rapidly until the peak strength is reached. This corresponds to the sum of the strength of the cementing material bonding the two halves of the bedding plane together and the frictional resistance of the matching surfaces. As the displacement continues, the shear stress will fall to some residual value that will then remain constant, even for large shear displacements.

Plotting the peak and residual shear strengths for different normal stresses results in the two lines illustrated in Figure 1. For planar discontinuity surfaces the experimental points will generally fall along straight lines. The peak strength line has a slope of ϕ and an intercept of c on the shear strength axis. The residual strength line has a slope of ϕ_r .

The relationship between the peak shear strength τ_p and the normal stress σ_n can be represented by the Mohr-Coulomb equation:

$$\tau_p = c + \sigma_n \tan \phi \quad (1)$$

where c is the cohesive strength of the cemented surface and ϕ is the angle of friction.

Shear strength of rock discontinuities

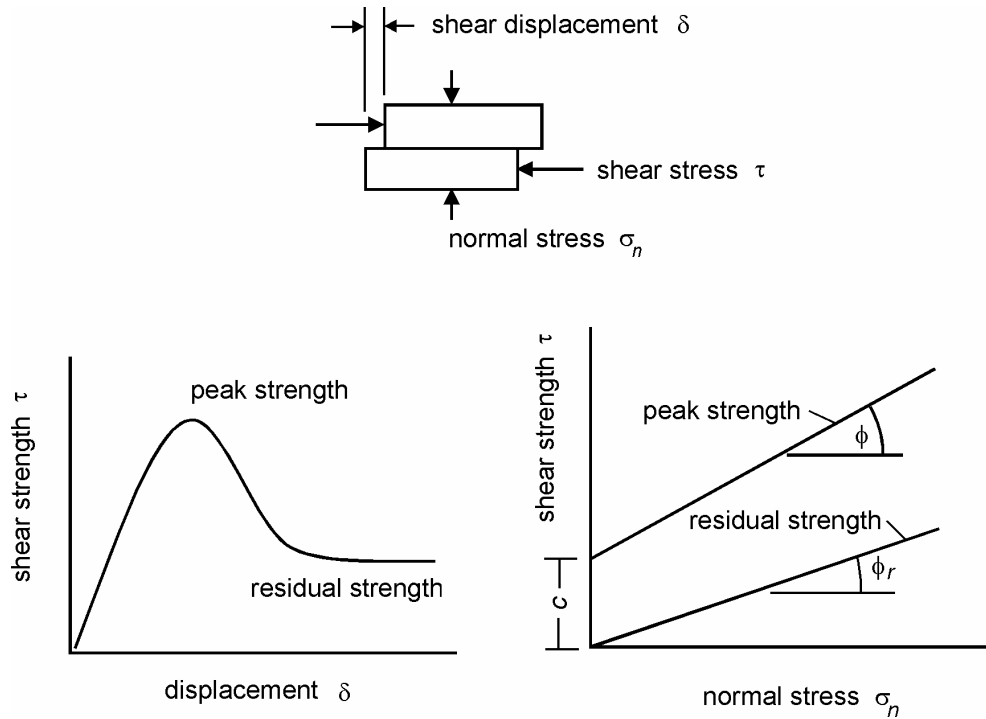


Figure 1: Shear testing of discontinuities

In the case of the residual strength, the cohesion c has dropped to zero and the relationship between ϕ_r and σ_n can be represented by:

$$\tau_r = \sigma_n \tan \phi_r \quad (2)$$

where ϕ_r is the residual angle of friction.

This example has been discussed in order to illustrate the physical meaning of the term cohesion, a soil mechanics term, which has been adopted by the rock mechanics community. In shear tests on soils, the stress levels are generally an order of magnitude lower than those involved in rock testing and the cohesive strength of a soil is a result of the adhesion of the soil particles. In rock mechanics, true cohesion occurs when cemented surfaces are sheared. However, in many practical applications, the term cohesion is used for convenience and it refers to a mathematical quantity related to surface roughness, as discussed in a later section. Cohesion is simply the intercept on the τ axis at zero normal stress.

The basic friction angle ϕ_b is a quantity that is fundamental to the understanding of the shear strength of discontinuity surfaces. This is approximately equal to the residual friction angle ϕ_r but it is generally measured by testing sawn or ground rock surfaces. These tests, which can be carried out on surfaces as small as 50 mm \times 50 mm, will produce a straight line plot defined by the equation:

$$\tau_r = \sigma_n \tan \phi_b \quad (3)$$

Shear strength of rock discontinuities

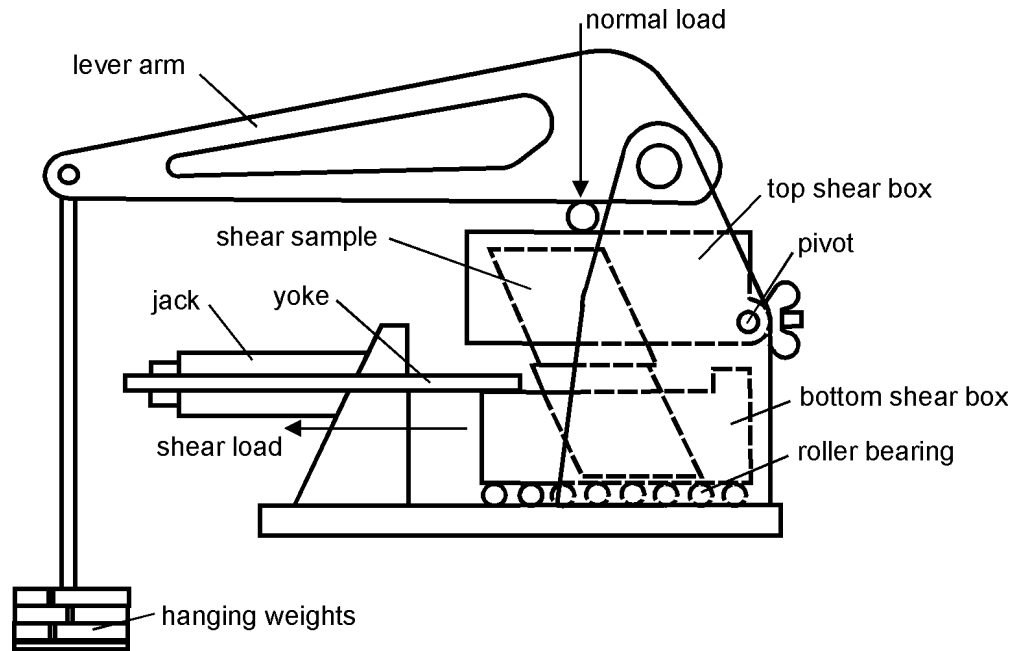


Figure 2: Diagrammatic section through shear machine used by Hencher and Richards (1982).

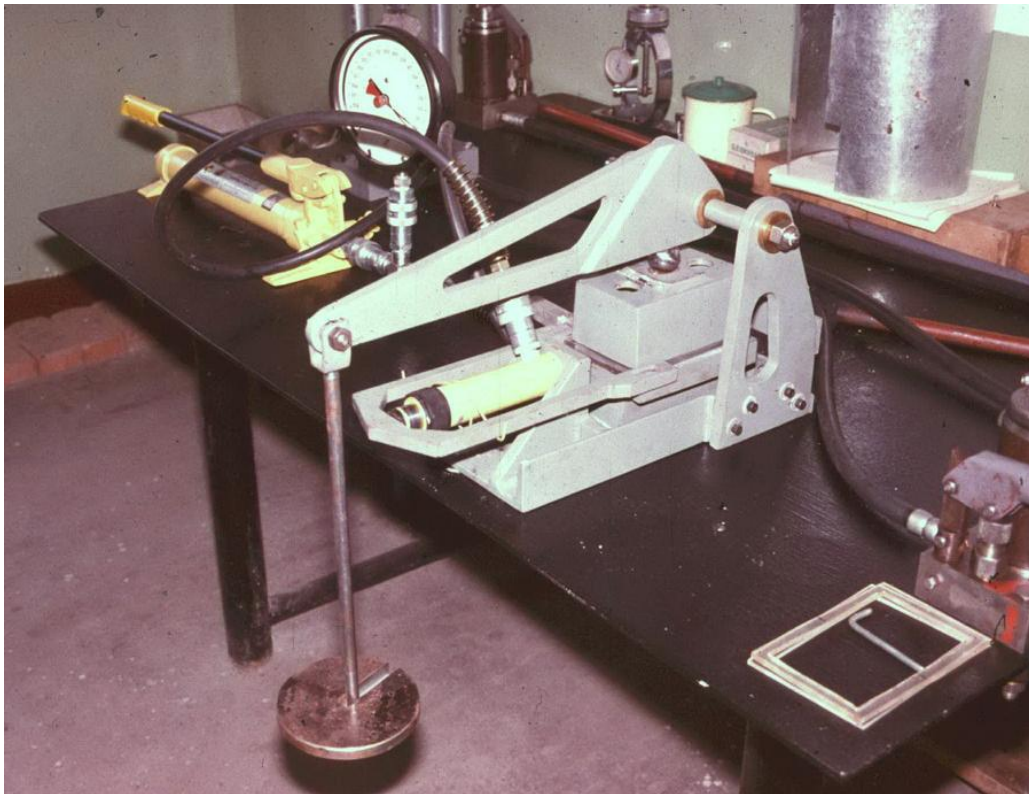


Figure 3: Shear machine of the type used by Hencher and Richards (1982) for measurement of the shear strength of sheet joints in Hong Kong granite.

A typical shear testing machine, which can be used to determine the basic friction angle ϕ_b is illustrated in Figures 2 and 3. This is a very simple machine and the use of a mechanical lever arm ensures that the normal load on the specimen remains constant throughout the test. This is an important practical consideration since it is difficult to maintain a constant normal load in hydraulically or pneumatically controlled systems and this makes it difficult to interpret test data. Note that it is important that, in setting up the specimen, great care has to be taken to ensure that the shear surface is aligned accurately in order to avoid the need for an additional angle correction.

Most shear strength determinations today are carried out by determining the basic friction angle, as described above, and then making corrections for surface roughness as discussed in the following sections of this chapter. In the past there was more emphasis on testing full scale discontinuity surfaces, either in the laboratory or in the field. There are a significant number of papers in the literature of the 1960s and 1970s describing large and elaborate in situ shear tests, many of which were carried out to determine the shear strength of weak layers in dam foundations. However, the high cost of these tests together with the difficulty of interpreting the results has resulted in a decline in the use of these large scale tests and they are seldom seen today.

The author's opinion is that it makes both economical and practical sense to carry out a number of small scale laboratory shear tests, using equipment such as that illustrated in Figures 2 and 3, to determine the basic friction angle. The roughness component which is then added to this basic friction angle to give the effective friction angle is a number which is site specific and scale dependent and is best obtained by visual estimates in the field. Practical techniques for making these roughness angle estimates are described on the following pages.

Shear strength of rough surfaces

A natural discontinuity surface in hard rock is never as smooth as a sawn or ground surface of the type used for determining the basic friction angle. The undulations and asperities on a natural joint surface have a significant influence on its shear behaviour. Generally, this surface roughness increases the shear strength of the surface, and this strength increase is extremely important in terms of the stability of excavations in rock.

Patton (1966) demonstrated this influence by means of an experiment in which he carried out shear tests on 'saw-tooth' specimens such as the one illustrated in Figure 4. Shear displacement in these specimens occurs as a result of the surfaces moving up the inclined faces, causing dilation (an increase in volume) of the specimen.

The shear strength of Patton's saw-tooth specimens can be represented by:

$$\tau = \sigma_n \tan(\phi_b + i) \quad (4)$$

where ϕ_b is the basic friction angle of the surface and
 i is the angle of the saw-tooth face.

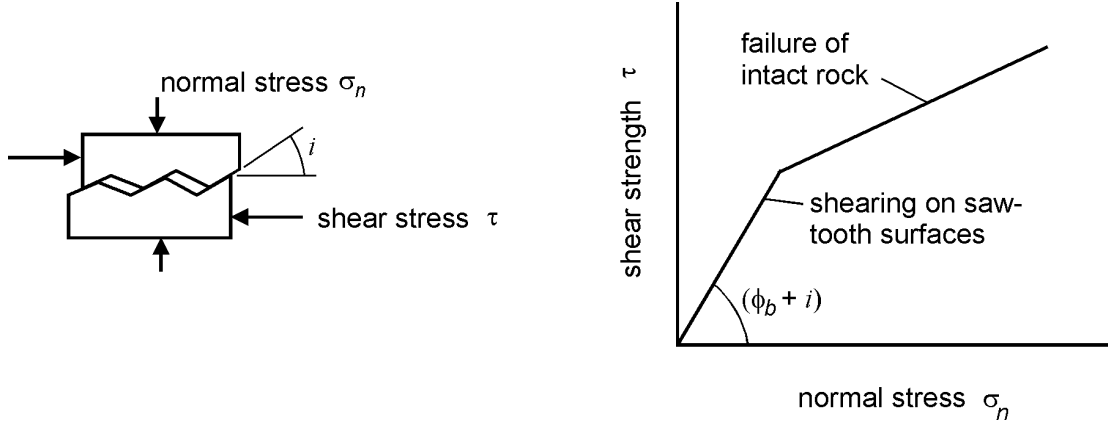


Figure 4: Patton's experiment on the shear strength of saw-tooth specimens.

Barton's estimate of shear strength

Equation (4) is valid at low normal stresses where shear displacement is due to sliding along the inclined surfaces. At higher normal stresses, the strength of the intact material will be exceeded and the teeth will tend to break off, resulting in a shear strength behaviour which is more closely related to the intact material strength than to the frictional characteristics of the surfaces.

While Patton's approach has the merit of being very simple, it does not reflect the reality that changes in shear strength with increasing normal stress are gradual rather than abrupt. Barton (1973, 1976) studied the behaviour of natural rock joints and proposed that equation (4) could be re-written as:

$$\tau = \sigma_n \tan \left(\phi_b + JRC \log_{10} \left(\frac{JCS}{\sigma_n} \right) \right) \quad (5)$$

where JRC is the joint roughness coefficient and JCS is the joint wall compressive strength .

Barton developed his first non-linear strength criterion for rock joints (using the basic friction angle ϕ_b) from analysis of joint strength data reported in the literature. Barton and Choubey (1977), on the basis of their direct shear test results for 130 samples of variably weathered rock joints, revised this equation to

$$\tau = \sigma_n \tan \left(\phi_r + JRC \log_{10} \left(\frac{JCS}{\sigma_n} \right) \right) \quad (6)$$

Where ϕ_r is the residual friction angle
Barton and Choubey suggest that ϕ_r can be estimated from

$$\phi_r = (\phi_b - 20) + 20(r/R) \quad (7)$$

where r is the Schmidt rebound number wet and weathered fracture surfaces and R is the Schmidt rebound number on dry unweathered sawn surfaces.

Equations 6 and 7 have become part of the Barton-Bandis criterion for rock joint strength and deformability (Barton and Bandis, 1990).

Field estimates of *JRC*

The joint roughness coefficient *JRC* is a number that can be estimated by comparing the appearance of a discontinuity surface with standard profiles published by Barton and others. One of the most useful of these profile sets was published by Barton and Choubey (1977) and is reproduced in Figure 5.

The appearance of the discontinuity surface is compared visually with the profiles shown and the *JRC* value corresponding to the profile which most closely matches that of the discontinuity surface is chosen. In the case of small scale laboratory specimens, the scale of the surface roughness will be approximately the same as that of the profiles illustrated. However, in the field the length of the surface of interest may be several metres or even tens of metres and the *JRC* value must be estimated for the full scale surface.

An alternative method for estimating *JRC* is presented in Figure 6.

Field estimates of *JCS*

Suggested methods for estimating the joint wall compressive strength were published by the ISRM (1978). The use of the Schmidt rebound hammer for estimating joint wall compressive strength was proposed by Deere and Miller (1966), as illustrated in Figure 7.

Influence of scale on *JRC* and *JCS*

On the basis of extensive testing of joints, joint replicas, and a review of literature, Barton and Bandis (1982) proposed the scale corrections for *JRC* defined by the following relationship:

$$JRC_n = JRC_o \left(\frac{L_n}{L_o} \right)^{-0.02JRC_o} \quad (8)$$

where *JRC_o*, and *L_o* (length) refer to 100 mm laboratory scale samples and *JRC_n*, and *L_n* refer to in situ block sizes.

Because of the greater possibility of weaknesses in a large surface, it is likely that the average joint wall compressive strength (*JCS*) decreases with increasing scale. Barton and Bandis (1982) proposed the scale corrections for *JCS* defined by the following relationship:

$$JCS_n = JCS_o \left(\frac{L_n}{L_o} \right)^{-0.03JRC_o} \quad (9)$$

where *JCS_o* and *L_o* (length) refer to 100 mm laboratory scale samples and *JCS_n* and *L_n* refer to in situ block sizes.

Shear strength of rock discontinuities

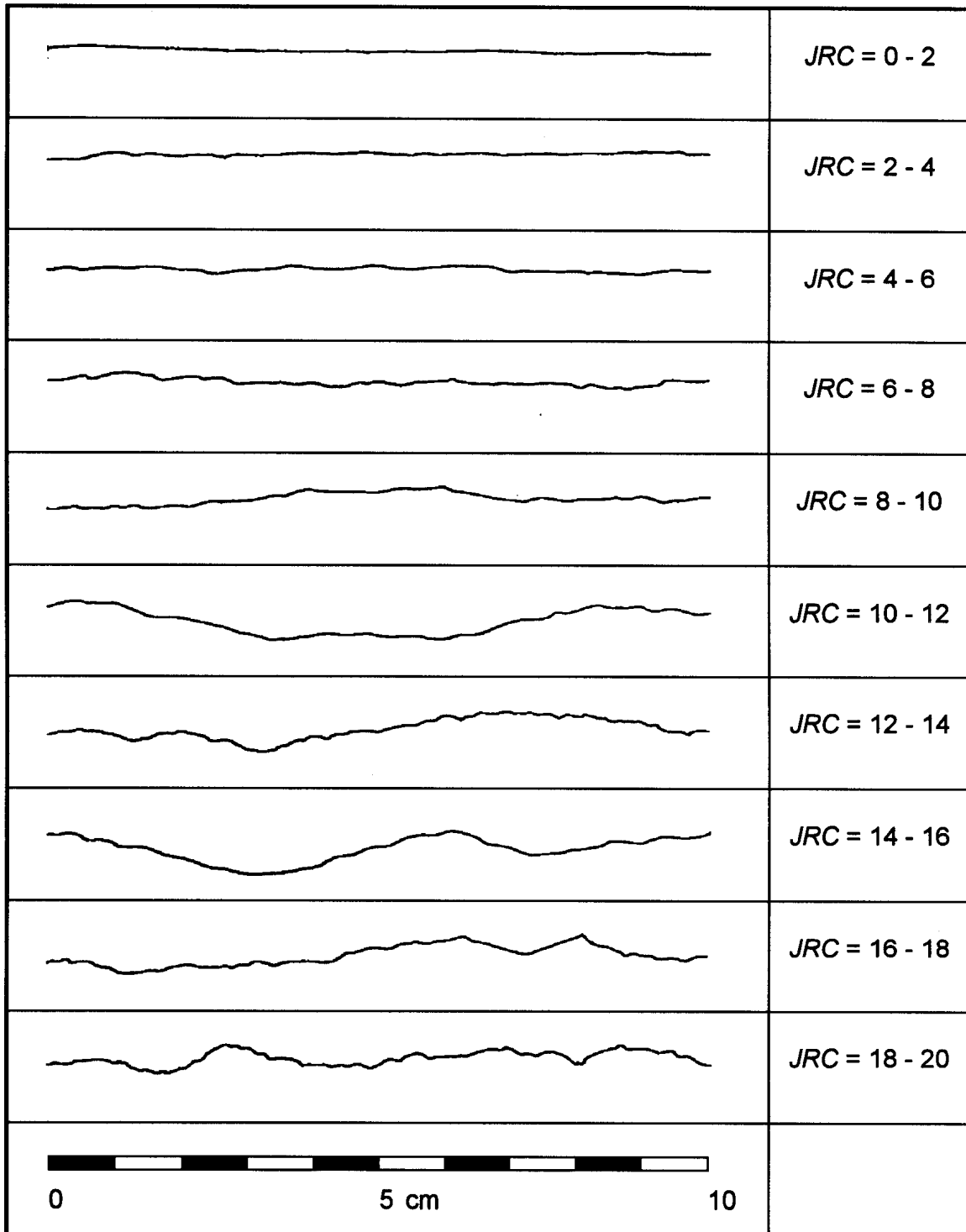


Figure 5: Roughness profiles and corresponding JRC values (After Barton and Choubey 1977).

Shear strength of rock discontinuities

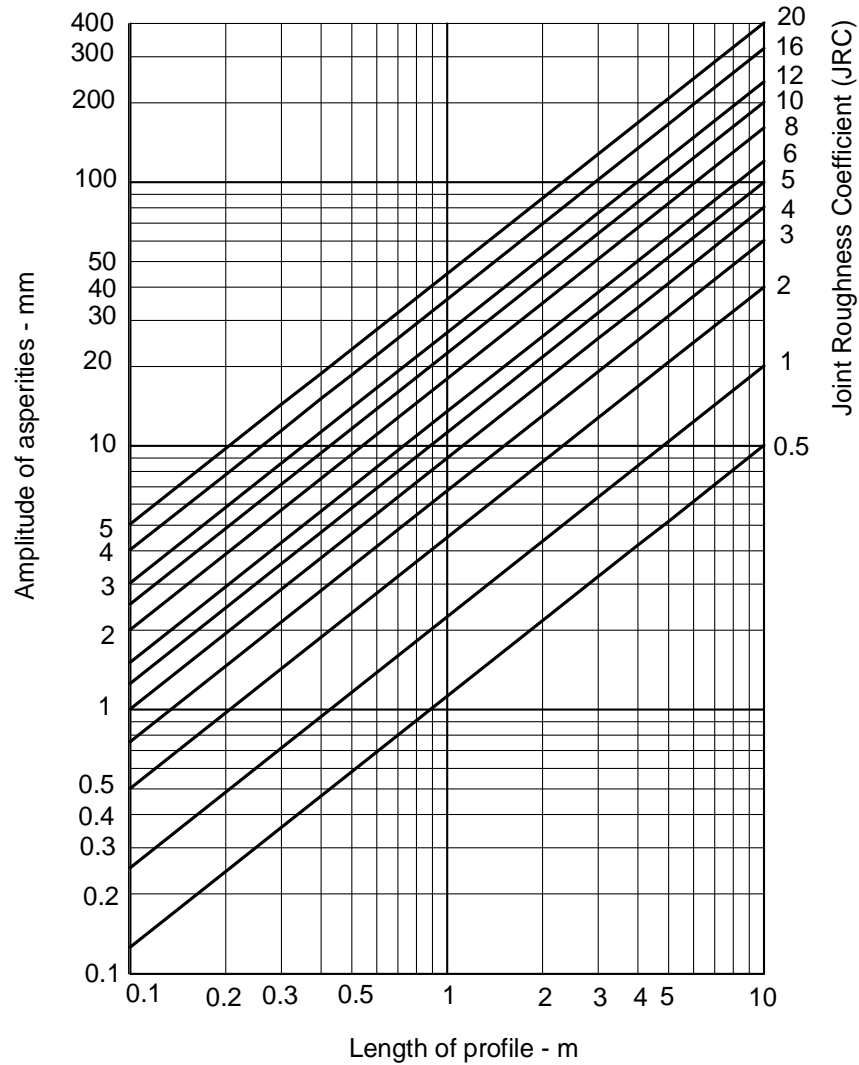
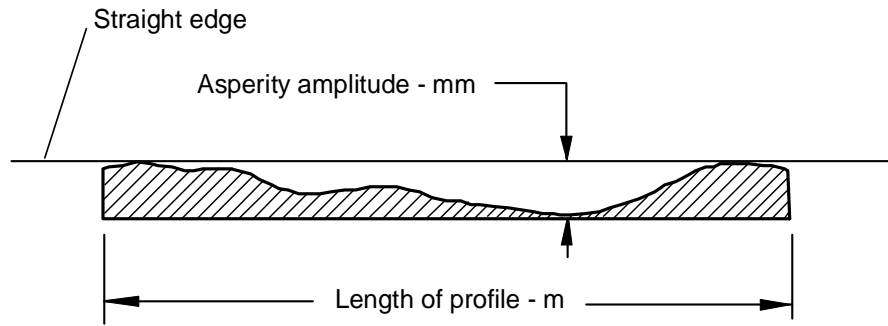


Figure 6: Alternative method for estimating *JRC* from measurements of surface roughness amplitude from a straight edge (Barton 1982).

Shear strength of rock discontinuities

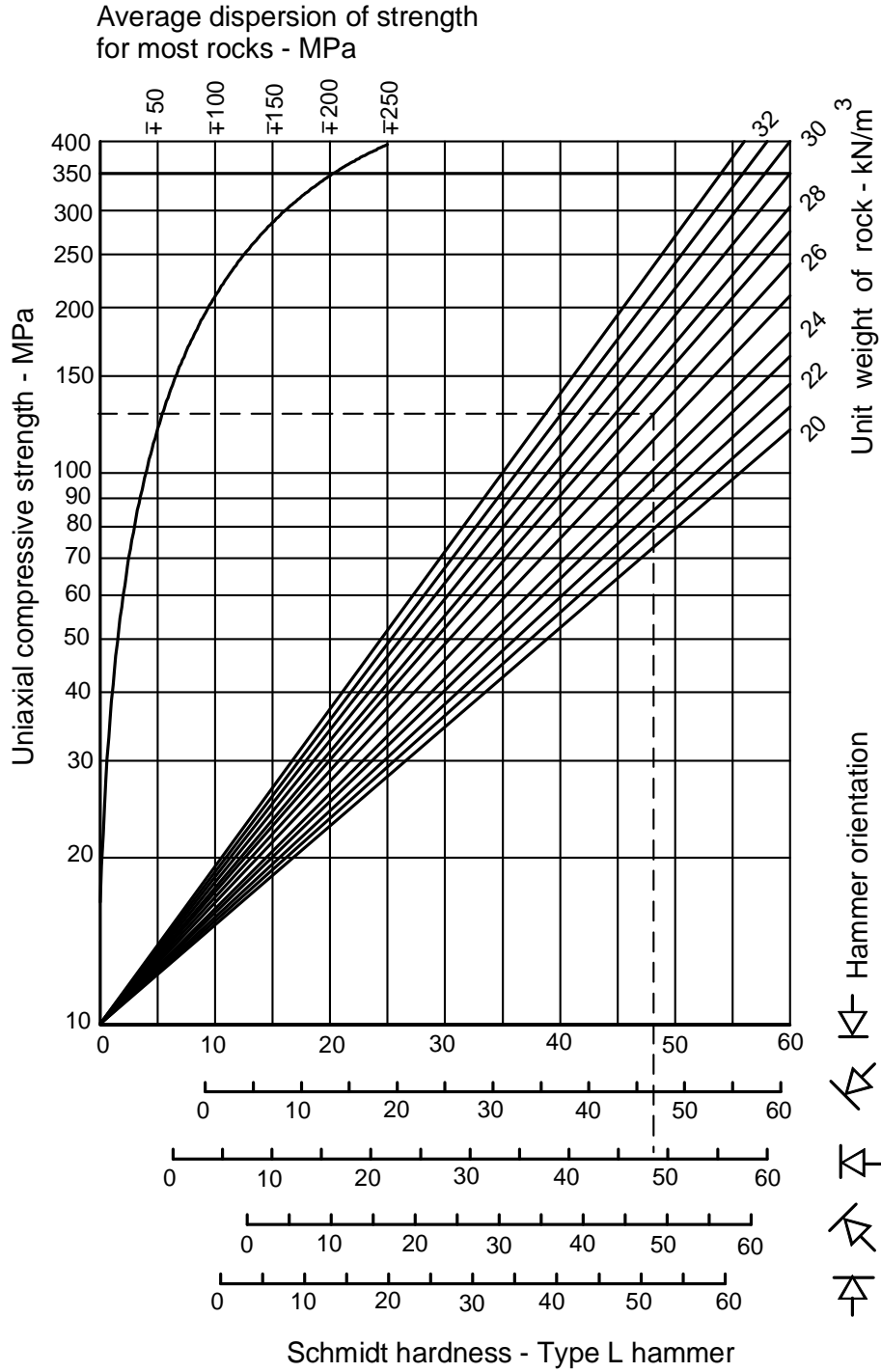


Figure 7: Estimate of joint wall compressive strength from Schmidt hardness.

Shear strength of filled discontinuities

The discussion presented in the previous sections has dealt with the shear strength of discontinuities in which rock wall contact occurs over the entire length of the surface under consideration. This shear strength can be reduced drastically when part or all of the surface is not in intimate contact, but covered by soft filling material such as clay gouge. For planar surfaces, such as bedding planes in sedimentary rock, a thin clay coating will result in a significant shear strength reduction. For a rough or undulating joint, the filling thickness has to be greater than the amplitude of the undulations before the shear strength is reduced to that of the filling material.

A comprehensive review of the shear strength of filled discontinuities was prepared by Barton (1974) and a summary of the shear strengths of typical discontinuity fillings, based on Barton's review, is given in Table 1.

Where a significant thickness of clay or gouge fillings occurs in rock masses and where the shear strength of the filled discontinuities is likely to play an important role in the stability of the rock mass, it is strongly recommended that samples of the filling be sent to a soil mechanics laboratory for testing.

Influence of water pressure

When water pressure is present in a rock mass, the surfaces of the discontinuities are forced apart and the normal stress σ_n is reduced. Under steady state conditions, where there is sufficient time for the water pressures in the rock mass to reach equilibrium, the reduced normal stress is defined by $\sigma_n' = (\sigma_n - u)$, where u is the water pressure. The reduced normal stress σ_n' is usually called the effective normal stress, and it can be used in place of the normal stress term σ_n in all of the equations presented above.

Instantaneous cohesion and friction

Due to the historical development of the subject of rock mechanics, many of the analyses, used to calculate factors of safety against sliding, are expressed in terms of the Mohr-Coulomb cohesion (c) and friction angle (ϕ), defined in Equation 1. Since the 1970s it has been recognised that the relationship between shear strength and normal stress is more accurately represented by a non-linear relationship such as that proposed by Barton and Bandis (1990). However, because this relationship (e.g. is not expressed in terms of c and ϕ , it is necessary to devise some means for estimating the equivalent cohesive strengths and angles of friction from relationships such as those proposed by Barton and Bandis.

Figure 8 gives definitions of the *instantaneous cohesion* c_i and the *instantaneous friction* angle ϕ_i for a normal stress of σ_n . These quantities are given by the intercept and the inclination, respectively, of the tangent to the non-linear relationship between shear strength and normal stress. These quantities may be used for stability analyses in which the Mohr-Coulomb failure criterion (Equation 1) is applied, provided that the normal stress σ_n is reasonably close to the value used to define the tangent point.

Shear strength of rock discontinuities

Table 1: Shear strength of filled discontinuities and filling materials (After Barton 1974)

Rock	Description	Peak c' (MPa)	Peak ϕ°	Residual c' (MPa)	Residual ϕ°
Basalt	Clayey basaltic breccia, wide variation from clay to basalt content	0.24	42		
Bentonite	Bentonite seam in chalk	0.015	7.5		
	Thin layers	0.09-0.12	12-17		
	Triaxial tests	0.06-0.1	9-13		
Bentonitic shale	Triaxial tests	0-0.27	8.5-29		
	Direct shear tests			0.03	8.5
Clays	Over-consolidated, slips, joints and minor shears	0-0.18	12-18.5	0-0.003	10.5-16
Clay shale	Triaxial tests	0.06	32		
	Stratification surfaces			0	19-25
Coal measure rocks	Clay mylonite seams, 10 to 25 mm	0.012	16	0	11-11.5
Dolomite	Altered shale bed, \pm 150 mm thick	0.04	1(5)	0.02	17
Diorite, granodiorite and porphyry	Clay gouge (2% clay, PI = 17%)	0	26.5		
Granite	Clay filled faults	0-0.1	24-45		
	Sandy loam fault filling	0.05	40		
	Tectonic shear zone, schistose and broken granites, disintegrated rock and gouge	0.24	42		
Greywacke	1-2 mm clay in bedding planes			0	21
Limestone	6 mm clay layer			0	13
	10-20 mm clay fillings	0.1	13-14		
	<1 mm clay filling	0.05-0.2	17-21		
Limestone, marl and lignites	Interbedded lignite layers	0.08	38		
	Lignite/marl contact	0.1	10		
Limestone	Marlaceous joints, 20 mm thick	0	25	0	15-24
Lignite	Layer between lignite and clay	0.014-0.03	15-17.5		
Montmorillonite Bentonite clay	80 mm seams of bentonite (montmorillonite) clay in chalk	0.36 0.016-0.02	14 7.5-11.5	0.08	11
Schists, quartzites and siliceous schists	100-15- mm thick clay filling	0.03-0.08	32		
	Stratification with thin clay	0.61-0.74	41		
	Stratification with thick clay	0.38	31		
Slates	Finely laminated and altered	0.05	33		
Quartz / kaolin / pyrolusite	Remoulded triaxial tests	0.042-0.09	36-38		

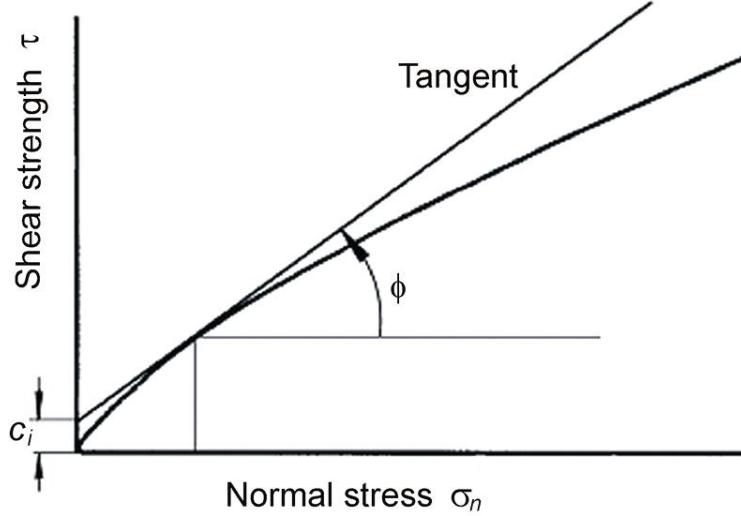


Figure 8: Definition of instantaneous cohesion c_i and instantaneous friction angle ϕ_i for a non-linear failure criterion.

Note that equation 6 is not valid for $\sigma_n = 0$ and it ceases to have any practical meaning for $\phi_r + JRC \log_{10}(JCS / \sigma_n) > 70^\circ$. This limit can be used to determine a minimum value for σ_n . An upper limit for σ_n is given by $\sigma_n = JCS$.

In a typical practical application, a spreadsheet program can be used to solve Equation 6 and to calculate the instantaneous cohesion and friction values for a range of normal stress values. A portion of such a spreadsheet is illustrated in Figure 9. In this spreadsheet the instantaneous friction angle ϕ_i , for a normal stress of σ_n , has been calculated from the relationship

$$\phi_i = \arctan\left(\frac{\partial\tau}{\partial\sigma_n}\right) \quad (10)$$

$$\frac{\partial\tau}{\partial\sigma_n} = \tan\left(JRC \log_{10} \frac{JCS}{\sigma_n} + \phi_r\right) - \frac{\pi JRC}{180 \ln 10} \left[\tan^2\left(JRC \log_{10} \frac{JCS}{\sigma_n} + \phi_r\right) + 1 \right] \quad (11)$$

The instantaneous cohesion c_i is calculated from:

$$c_i = \tau - \sigma_n \tan \phi_i \quad (12)$$

In choosing the values of c_i and ϕ_i for use in a particular application, the average normal stress σ_n acting on the discontinuity planes should be estimated and used to determine the appropriate row in the spreadsheet. For many practical problems in the field, a single average value of σ_n will suffice but, where critical stability problems are being considered, this selection should be made for each important discontinuity surface.

Shear strength of rock discontinuities

Barton shear failure criterion

Input parameters:

Residual friction angle (PHIR) - degrees	29
Joint roughness coefficient (JRC)	16.9
Joint compressive strength (JCS)	96
Minimum normal stress (SIGNMIN)	0.360

Normal stress (SIGN) MPa	Shear strength (TAU) MPa	$\frac{dTAU}{dSIGN}$ (DTDS)	Friction angle (PHI) degrees	Cohesive strength (COH) MPa
0.360	0.989	1.652	58.82	0.394
0.720	1.538	1.423	54.91	0.513
1.440	2.476	1.213	50.49	0.730
2.880	4.073	1.030	45.85	1.107
5.759	6.779	0.872	41.07	1.760
11.518	11.344	0.733	36.22	2.907
23.036	18.973	0.609	31.33	4.953
46.073	31.533	0.496	26.40	8.666

Cell formulae:

$$SIGNMIN = 10^{((70 - PHIR) / JRC)}$$

$$TAU = SIGN * \tan\left(\left(\frac{PHIR + JRC * \log(JCS / SIGN)}{180}\right) * \pi\right)$$

$$DTDS = \frac{\tan\left(\left(\frac{JRC * \log(JCS / SIGN) + PHIR}{180}\right) * \pi\right) - (JRC / \ln(10))}{\left(\tan\left(\left(\frac{JRC * \log(JCS / SIGN) + PHIR}{180}\right) * \pi\right)\right)^2 + 1} * \pi / 180$$

$$PHI = \text{ATAN}(DTDS) * 180 / \pi$$

$$COH = TAU - SIGN * DTDS$$

Figure 9 Printout of spreadsheet cells and formulae used to calculate shear strength, instantaneous friction angle and instantaneous cohesion for a range of normal stresses.

References

- Barton, N. 1976. The shear strength of rock and rock joints. *Int. J. Rock Mech. Min. Sci. & Geomech. Abstr.* **13**, 1-24.
- Barton, N.R. 1973. Review of a new shear strength criterion for rock joints. *Eng. Geol.* **7**, 287-332.
- Barton, N.R. 1974. *A review of the shear strength of filled discontinuities in rock.* Norwegian Geotech. Inst. Publ. No. 105. Oslo: Norwegian Geotech. Inst.
- Barton, N.R. 1976. The shear strength of rock and rock joints. *Int. J. Mech. Min. Sci. & Geomech. Abstr.* **13**(10), 1-24.
- Barton, N.R. and Bandis, S.C. 1982. Effects of block size on the the shear behaviour of jointed rock. *23rd U.S. symp. on rock mechanics*, Berkeley, 739-760.
- Barton, N.R. and Bandis, S.C. 1990. Review of predictive capabilities of JRC-JCS model in engineering practice. In *Rock joints, proc. int. symp. on rock joints*, Loen, Norway, (eds N. Barton and O. Stephansson), 603-610. Rotterdam: Balkema.
- Barton, N.R. and Choubey, V. 1977. The shear strength of rock joints in theory and practice. *Rock Mech.* **10**(1-2), 1-54.
- Deere, D.U. and Miller, R.P. 1966. *Engineering classification and index properties of rock.* Technical Report No. AFNL-TR-65-116. Albuquerque, NM: Air Force Weapons Laboratory
- Hencher, S.R. & Richards, L.R. (1982). The basic frictional resistance of sheeting joints in Hong Kong granite *Hong Kong Engineer*, Feb., 21-25.
- International Society for Rock Mechanics Commission on Standardisation of Laboratory and Field Tests. 1978. Suggested methods for the quantitative description of discontinuities in rock masses. *Int. J. Rock Mech. Min. Sci. & Geomech. Abstr.* **15**, 319-368.
- Patton, F.D. 1966. Multiple modes of shear failure in rock. *Proc. 1st Congr. Int. Soc. Rock Mech.*, Lisbon **1**, 509-513.